

Utah State University

DigitalCommons@USU

All Graduate Theses and Dissertations

Graduate Studies

5-2009

Modeling the Evolution of Insect Phenology with Particular Reference to Mountain Pine Beetle

Brian P. Yurk
Utah State University

Follow this and additional works at: <https://digitalcommons.usu.edu/etd>

 Part of the [Mathematics Commons](#)

Recommended Citation

Yurk, Brian P., "Modeling the Evolution of Insect Phenology with Particular Reference to Mountain Pine Beetle" (2009). *All Graduate Theses and Dissertations*. 385.
<https://digitalcommons.usu.edu/etd/385>

This Dissertation is brought to you for free and open access by the Graduate Studies at DigitalCommons@USU. It has been accepted for inclusion in All Graduate Theses and Dissertations by an authorized administrator of DigitalCommons@USU. For more information, please contact digitalcommons@usu.edu.



MODELING THE EVOLUTION OF INSECT PHENOLOGY WITH
PARTICULAR REFERENCE TO MOUNTAIN PINE BEETLE

by

Brian P. Yurk

A dissertation submitted in partial fulfillment
of the requirements for the degree

of

DOCTOR OF PHILOSOPHY

in

Mathematical Sciences

Approved:

Dr. James Powell
Major Professor

Dr. Barbara J. Bentz
Committee Member

Dr. James W. Haefner
Committee Member

Dr. Peg Howland
Committee Member

Dr. Joseph V. Koebbe
Committee Member

Dr. Byron R. Burnham
Dean of Graduate Studies

UTAH STATE UNIVERSITY
Logan, Utah

2009

Copyright © Brian P. Yurk 2009

All Rights Reserved

ABSTRACT

Modeling the Evolution of Insect Phenology with Particular Reference to Mountain
Pine Beetle

by

Brian P. Yurk, Doctor of Philosophy

Utah State University, 2009

Major Professor: Dr. James Powell
Department: Mathematics and Statistics

Climate change is likely to disrupt the timing of developmental events (phenology) in insect populations in which development time is largely determined by temperature. Shifting phenology puts insects at risk of being exposed to seasonal weather extremes during sensitive life stages and losing synchrony with biotic resources. Additionally, warming may result in loss of developmental synchronization within a population, making it difficult to find mates or mount mass attacks against well-defended resources at low population densities. It is unknown whether genetic evolution of development time can occur rapidly enough to moderate these effects.

The work presented here is largely motivated by the need to understand how mountain pine beetle (MPB) populations will respond to climate change. MPB is an important forest pest from both an economic and ecological perspective, because MPB outbreaks often result in massive timber loss. Recent MPB range expansion and increased outbreak frequency have been linked to warming temperatures.

We present a novel approach to modeling the evolution of phenology by allowing the parameters of a phenology model to evolve in response to selection on emergence time and density. We also develop a temperature-dependent phenology model for MPB that accounts for multiple types of developmental variation: variation that persists throughout a life stage, random variation, and variation due to the MPB oviposition mechanism. This model is parameterized using MPB development time data from constant temperature laboratory experiments.

We use Laplace's method to approximate steady distributions of the evolution model under stable temperatures. Here the mean phenotype allows for parents and offspring to be oviposited at exactly the same time of year in consecutive generations. These results are verified numerically for both MPB and a two-stage model insect.

The evolution model is also applied to investigate the evolution of phenology for MPB and the two-stage model insect under warming temperatures. The model predicts that local populations can only adapt to climate change if development time can adapt so that individuals can complete exactly one generation per year and if the rate of temperature change is moderate.

(166 pages)

For Michelle and Porter.

ACKNOWLEDGMENTS

I would like to thank my advisor, James Powell, for many hours of fruitful discussion and invaluable guidance. I also thank the members of my committee, Barbara Bentz, James Haefner, Peg Howland, and Joseph Koebbe, for taking the time to read my dissertation and for providing comments. In addition, I would like to thank Barbara Bentz and Martha Garlick for insightful feedback on early versions of the papers that compose this dissertation. I also thank Barbara Bentz for providing development time data for mountain pine beetle and Amy Adams, Jason Barker, Leslie Brown, Amanda Cangelosi, Rebecca Gerhart, Estella Gilbert, Matt Hansen, Justin Heavilin, Jeff Leek, Lynn Rasmussen, Jackie Redmer, Greta Schen, and Jim Vandygriff for assistance with data collection. Finally, I thank my wife, Michelle, for her boundless support and patience.

This work was supported by a Willard L. Eccles Foundation Graduate Fellowship and by the National Science Foundation under grant number DMS-0077663.

Brian P. Yurk

CONTENTS

	Page
ABSTRACT	iii
ACKNOWLEDGMENTS	vi
LIST OF TABLES	x
LIST OF FIGURES	xi
1 INTRODUCTION	1
2 MODELING THE EVOLUTION OF INSECT PHENOLOGY . .	15
2.1 Introduction	15
2.2 Model development	20
2.2.1 Temperature-dependent phenology model	20
2.2.2 Development time as a quantitative trait	23
2.2.3 Evolution map	25
2.2.4 Natural selection	27
2.2.5 Sexual reproduction	28
2.2.6 Characterization of the evolution map	30
2.3 Analytical results	32
2.3.1 Approximation of the development map	32
2.3.2 Steady distributions of the evolution map	34
2.4 Numerical simulations	40
2.4.1 Two-stage model insect	40
2.4.2 Simulations: periodic temperature	42
2.4.3 Simulation: increasing temperature and advancing resource phenology	46
2.5 Summary and future directions	50

3	DEVELOPMENTAL VARIATION AND INSECT PHENOLOGY	52
3.1	Introduction	52
3.2	Model development	58
3.2.1	Temperature-dependent individual phenology	58
3.2.2	Population phenology (no variation in development time)	59
3.2.3	Persistent variation	61
3.2.4	Random variation	62
3.2.5	Summary of phenology models	65
3.3	Constant temperature solution	66
3.4	Mountain pine beetle parameter estimation	68
3.5	Simulation of MPB phenology and comparison to field data	74
3.5.1	Field data	74
3.5.2	Simulations	77
3.6	Discussion and conclusion	79
4	EVOLUTION OF MOUNTAIN PINE BEETLE PHENOLOGY	84
4.1	Introduction	84
4.2	Model development	91
4.2.1	Temperature-dependent development time curves	91
4.2.2	Simple individual phenology model	94
4.2.3	The G-function	95
4.2.4	Population phenology model	97
4.2.5	Development time as a quantitative trait	98
4.2.6	Evolution map	102
4.2.7	Natural selection	103
4.2.8	Sexual reproduction	106
4.2.9	Summary of the evolution map	110
4.3	Numerical results	112
4.3.1	Simulations: stable temperatures	112
4.3.2	Simulations: increasing temperatures and rate of adaptation	117
4.3.3	Regions of stable fixed points and evolutionary consequences	119
4.4	Summary and conclusion	123

5 SUMMARY AND CONCLUSION	126
REFERENCES	130
APPENDIX	136
VITA	143

LIST OF TABLES

Table	Page
2.1 Development time curve parameters for 2-stage model insect used in numerical simulations.	41
2.2 Parameters for the selection functions in the periodic temperature simulations. In simulation 1 there is emergence time dependent truncation selection. In simulation 2 there is emergence time dependent truncation selection and density dependent selection with an Allee effect. The values listed for t_{early} and t_{late} are for generation n	43
2.3 Parameters for the selection functions in the warming temperature simulations. There is truncation selection on emergence time with a shifting emergence window. There is also density dependent selection with an Allee effect. The values listed for t_{early} and t_{late} are for generation n	47
3.1 Parameterization for MPB development time curves and variance parameters for each life stage (egg-teneral adult(TA)). $L1 - L4$ indicate larval instars 1-4. These parameters were fit to data from constant-temperature laboratory experiments. The parameterization for MPB burrowing time curve is also shown (OA). These parameters were also fit to data from constant-temperature laboratory experiments. The negative log-likelihood (LL) is shown for the best fit parameters. In the cases that 5 development time parameters (c_i) are listed, the development time curve was the sum of decreasing and increasing exponential functions. In the cases that 3 development time parameters are listed, the development time curve was a decreasing exponential function. Note that in all developmental stages but the fourth larval instar, incorporating a diffusion term (random variation) did not improve the fit.	73
4.1 Parameterization for MPB development time curves for each life stage (egg-teneral adult). The parameterization for MPB burrowing time curve is also shown (ovi. adult). $L1 - L4$ indicate larval instars 1-4. These parameters were fit to data from constant-temperature laboratory experiments. In cases that five parameters (c_i) are listed, the development time curve was the sum of decreasing and increasing exponential functions. In the cases that three parameters are listed, the development time curve was a decreasing exponential function.	92

LIST OF FIGURES

Figure	Page	
2.1	An example of a development time curve. An insect's development time is the duration of a life stage at a certain temperature.	21
2.2	a. An example of a G function. Given the oviposition time t of an insect, its emergence time is $G(t)$. $G(t) - 365$ is plotted to show the time of year of emergence relative to the time of year of oviposition. b. A developmental circle map and its fixed point dynamics. The circle map is the solid curve, and the fixed point line $G(t_o^n) = t_o^n$ is dashed. As the map is iterated oviposition time converges (arrows) to stable fixed points that occur at intersections of the two curves intersect where the slope of the circle map curve is less than one.	22
2.3	a. The G_α function for various values of α . Given the oviposition time t of an individual with phenotype α , the individual's emergence time is $G_\alpha(t)$. Although α varies continuously within a population, this plot shows only a few representative curves. b. Given an oviposition time t , α_t is the unique phenotype that results in a univoltine fixed point for the G_α function at time t , i.e. $G_{\alpha_t}(t) = t + 365$. These fixed points are stable ($\frac{\partial}{\partial t}[G_{\alpha_t}(t)] < 1$) where α_t is increasing and unstable where α_t is decreasing (see text). The arrows point to the same unstable (solid) and stable (dotted) univoltine fixed points in both parts of the figure for individuals with phenotype $\alpha = 1.4$	25
2.4	A diagram of the evolution map. Development (D) maps the oviposition distribution to the emergence distribution for generation n . Selection/reproduction (S,R) maps the emergence distribution for generation n to the oviposition distribution for generation $n + 1$	26
2.5	Development time curves for the two-stage model insect. These curves are scaled mountain pine beetle development time curves.	41

- 2.6 Results after 1000 generations of the first periodic temperature simulation with truncation selection on emergence time. The time of year of oviposition is shown on the horizontal axes. **a.** Oviposition density. Most mass occurs at stable fixed points (between arrows). **b.** Mean phenotype (solid) and α_t (dashed), the phenotype that makes t a univoltine fixed point of G_α . Consistent with analytical results, $\mu_o^n(t) \approx \alpha_t$ at stable fixed points. The prediction fails at unstable fixed points, where there is little mass and the population structure is mainly determined by the phenotypes of individuals leaked from nearby stable fixed points. **c.** Rescaled phenotypic variance (solid) and $v_p(t)$ (dashed), the predicted rescaled variance at a steady distribution where $\mu_o^n(t) = \alpha_t$. Numerical rescaled variance results also agree with analytical predictions at all but the earliest and latest stable fixed points. The prediction does not hold at unstable fixed points where there is little mass. 44
- 2.7 Results after 1000 generations of the second periodic temperature simulation with selection on emergence time and emergence density. The time of year of oviposition is shown on the horizontal axes. **a.** Oviposition density (solid) and the predicted density (dash-dot) at a steady state where $\mu_o^n(t) = \alpha_t$ (40,000 is the non-trivial fixed point of $H(N)$). Most mass occurs at stable fixed points (between arrows). More mass is leaked to the unstable fixed points in this experiment than in the first periodic temperature experiment. This mass persists due to positive pressure from density dependent selection. **b.** Mean phenotype (solid) and α_t (dashed), the phenotype that makes t a univoltine fixed point of G_α . Consistent with analytical results, $\mu_o^n(t) \approx \alpha_t$ at stable fixed points. The prediction fails at unstable fixed points, where the population structure is mainly determined by the phenotypes of individuals leaked from nearby stable fixed points. **c.** Rescaled phenotypic variance (solid) and $v_p(t)$ (dashed), the predicted rescaled variance at a steady distribution where $\mu_o^n(t) = \alpha_t$. Numerical rescaled variance results also agree with analytical predictions at stable fixed points, but not at unstable fixed points. 45
- 2.8 Number of eggs laid per generation in the increasing temperature simulation. The generation number appears along the bottom horizontal axis, and the corresponding temperature shift appears along the top horizontal axis. In this simulation, mean annual temperature increases by 6°C over 100 years, and a 20 day long emergence window advances 24 days over 100 years. Density dependent selection is also imposed. The steep population decline between generations 60 and 73 corresponds to a loss of stable fixed points inside of the emergence time window. 48

- 2.9 A diagram of the stability of univoltine fixed points of the G_α function under different shifts of the temperature series $T(t) = 8 - 18 \cos(2\pi t/365)$ and the emergence time window for the increasing temperature simulation (between thick black lines). For the two-stage model insect there is a phenotype α that makes each emergence time a univoltine fixed point of the G_α map. The stability of these fixed points is indicated in the diagram, with stable fixed points occurring in white regions and unstable fixed points occurring in gray regions. Note that after the temperature shift reaches 4.1°C there are no stable fixed points within the emergence time window. The loss of stable fixed points coincides with population collapse in the increasing temperature simulation. 49
- 3.1 Mean MPB egg development times measured at various constant temperatures. Error bars indicate \pm one standard deviation. Notice that the standard deviation of development time generally increases with development time. 69
- 3.2 Base development time curve fit to MPB egg development times measured at various constant temperatures (solid curve). Base development time \pm the predicted standard deviation of development time (sdp) is also plotted (dotted curves). Observed mean development times are plotted (dots), as well as error bars indicating \pm one standard deviation about the sample mean. Note that the likelihood fitting procedure employed here does not fit curves directly to mean development times (see text). 74
- 3.3 Base development time curves fit to MPB development times for each developmental stage. Two means were plotted when there were two separate development experiments performed at the same temperature. Note that the likelihood fitting procedure employed here does not fit curves directly to mean development times (see text). The means are not equally weighted by the fitting algorithm. For example, the mean development time for the third larval instar at 10°C has relatively little weight in the fit, because four beetles were observed at that temperature, whereas 29 and 42 beetles were observed at 16°C and 20°C 75
- 3.4 Burrowing time curve $\rho(T)$ for MPB ovipositional adult (solid curve) fit to burrowing times measured in constant-temperature laboratory experiments (dots). Burrowing time is the time necessary for a MPB female to construct one centimeter of gallery at a given temperature. 76
- 3.5 Average of north and south side temperatures measured hourly in the phloem of tree 1 at site V from 2001 until 2002. 77

3.6	Plots of predicted (solid) and observed (dotted) emergence distributions for seven trees from central Idaho in 2002 and 2003, along with R^2 values. Data was collected at 2 sites, V and NP, where hourly phloem temperatures, attack time distributions and emergence time distributions were measured. Predicted emergence time distributions were obtained using the phenotype-dependent advection model. Note that the position of the median egg in the egg gallery was chosen to fit the mean emergence time predictions to the observed means.	80
4.1	Base development time curves fit to MPB development times for each developmental stage. Two means are plotted at the same temperature if there were two separate development experiments performed at that temperature.	93
4.2	Burrowing time curve $\rho(T)$ for MPB ovipositional adult (solid curve) fit to burrowing times measured in constant-temperature laboratory experiments (dots). Burrowing time is the time necessary for a MPB female to construct on centimeter of gallery at a given temperature.	94
4.3	a. An example of a G function (solid) for MPB. Given the oviposition time t of an insect in generation n , the oviposition time of its median egg in generation $n + 1$ is $G(t)$. $G(t) - 365$ is plotted to show the time of year of emergence relative to the time of year of oviposition. Also plotted is the fixed point line (dashed); times at which the G function intersects the fixed point line (fixed points) correspond to times of year where oviposition occurs at exactly the same time of year in successive generations. b. A developmental circle map for MPB and its fixed point dynamics. The circle map is the solid curve, and the fixed point line $G(t_o^n) = t_o^n$ is dashed. The circle map corresponds to the G function in the left panel. As the map is iterated, oviposition times converge (arrows) to stable fixed points (fixed points that occur where slope of the circle map curve is less than one).	96

- 4.4 **a.** The G_α function for MPB for various values of α . An individual with phenotype α that was oviposited at time t in generation n will lay its median egg at time $G_\alpha(t)$ in the next generation. Although α is assumed to vary continuously within a population, this plot shows only a few representative curves. Also plotted is the fixed point line. Note that individuals with different phenotypes have different fixed points. **b.** Given an oviposition time t , α_t is the unique phenotype that results in a fixed point for the G_α function at time t , i.e. $G_{\alpha_t}(t) = t + 365$. These fixed points are stable ($\frac{\partial}{\partial t}[G_{\alpha_t}(t)] < 1$) where α_t is increasing and unstable where α_t is decreasing (see text). The arrows point to the same unstable (solid) and stable (dotted) univoltine fixed points in both parts of the figure for individuals with phenotype $\alpha = 1.0$ 101
- 4.5 An example of the effects of the development map on an oviposition distribution. Development maps an oviposition distribution to an emergence distribution for the same generation according to the phenotype-dependent phenology model. Note that although the oviposition and emergence distributions depend on phenotype, only the phenotype-independent distributions are shown for clarity. 104
- 4.6 An example of the effect of natural selection on emergence time and density ($N_e^n(t)$). Beetles that do not emerge at densities greater than the attack threshold (A') or within the emergence time window (i.e. beetles that emerge within the gray regions in the left panel) do not reproduce successfully. The post-selection density ($N_s^n(t)$) is shown in the right panel. The post-selection density is the density of females in generation $n + 1$ produced by females emerging in generation n at time t 105
- 4.7 An example of the effect of the distributed oviposition map on a post-selection distribution. The post-selection density $N_s^n(t)$ is shown in the left panel). Oviposition densities are shown for eggs 1 (dashed), 10 (dash-dotted), and 20 (dotted) in the left panel. The composite oviposition distribution (solid) is also shown (the entire oviposition distribution accounting for all 20 eggs, $N_o^{n+1}(t)$). Note that the dependence of post-selection and oviposition densities on phenotype is suppressed for clarity. 111
- 4.8 Minimum daily phloem temperatures observed at two MPB infestation sites: the Sawtooth National Recreation Area (SNRA, left) in central Idaho and Panguitch Lake, Utah (PAN, right). The hourly temperature series from which these figures were generated is composed of the average of north- and south-side phloem temperature measurements made at a single tree at each site. 112

- 4.9 Post-selection density (top) and mean phenotype (bottom) for the SNRA steady distribution. The evolution map was numerically implemented for 1000 generations with stable temperatures. The temperature series consisted of the average of north- and south-side hourly phloem temperatures measured at a tree in the Sawtooth National Recreation Area in central Idaho. The mean phenotype for the steady population is 0.5463. 114
- 4.10 Post-selection density (top) and mean phenotype (bottom) for the PAN steady distribution. The evolution map was numerically implemented for 1000 generations with stable temperatures. The temperature series consisted of the average of north- and south-side hourly phloem temperatures measured at a tree in Panguitch Lake, Utah. The mean phenotype for the steady population is 1.4309. 115
- 4.11 Mean phenotype for the SNRA steady distribution (Steady Mean, black) and α_t for eggs 1, 10, and 20 (gray). α_t is the phenotype that results in a fixed point at time t . Fixed points are stable where α_t is increasing and unstable where α_t is decreasing. 116
- 4.12 Mean phenotype for the PAN steady distribution (Steady Mean, black) and α_t for eggs 1, 10, and 20 (gray). 116
- 4.13 Number of generations before extinction under different rates of temperature change. The initial population distribution for each simulation was well-adapted to SNRA 2001-2001 temperatures. Temperatures were ramped from hourly phloem temperatures measured during 2001-2002 in the Sawtooth National Recreation Area (SNRA) in central Idaho to hourly phloem temperatures measured during 1996-1997 at Panguitch Lake, Utah (PAN). Then temperatures were held at the Panguitch Lake values. Measured hourly phloem temperatures average $2.56^\circ C$ warmer at the Panguitch Lake site than at the central Idaho site. In successive simulations, the temperature was ramped up over increasing numbers of generations (see text). The population was able to adapt to Panguitch Lake temperatures if the ramp occurred over eight or more generations. 118

- 4.14 Diagram of stable univoltine fixed points of the G_α function for egg 10 under different shifts of the SNRA 2001-2002 phloem temperature series. Only emergence time that are adaptive are shown (i.e. inside of the MPB emergence window). For each shifted temperature series, there may be a phenotype α that makes a particular emergence day a fixed point of the G_α map. If so, that fixed point is either stable or unstable. Note that at high and low temperatures there are no fixed points—at these temperatures reasonable adaptation in the teneral stage cannot result in strict univoltinism. 121
- 4.15 The G_3 function for egg 10 under two different shifts of the SNRA temperature series ($T_{shift} = 4.0^\circ C$ and $T_{shift} = 4.3^\circ C$). Note that there are fixed points for $T_{shift} = 4.0^\circ C$, but there are no fixed points for $T_{shift} = 4.3^\circ C$ 122

CHAPTER 1

INTRODUCTION

Understanding the evolution of insect phenology (the timing of developmental events, such as oviposition or adult emergence) is a crucial step toward predicting how insect populations will respond to climate change. It is particularly important to understand how climate change will affect pollinators and eruptive insects due to their economic and ecological importance. One such eruptive insect that will be considered in detail here is the mountain pine beetle (*Dendroctonus ponderosae* Hopkins). There are strong selective pressures on insects to maintain appropriate phenology, including synchrony with resources and within populations. Insect phenology changes as yearly temperature changes, because the time necessary for an insect to complete its life cycle is largely dependent on temperature [47]. This link has been observed in populations around the globe; recent phenology shifts [31] and range expansions [10] have been linked to changing temperatures in multiple populations including mountain pine beetle populations. The response of development time to temperature varies within and between populations and has been shown to be heritable [5]. Describing this variation is critical in developing a model of the evolution of phenology since natural selection acts on heritable variation. In this work we present novel approaches to modeling variation in insect phenology and its evolution in response to selection on phenology—a response that previously was not well understood. This work is largely motivated by the need to understand how mountain pine beetle populations will respond to global warming, and the phenology models developed are parameterized using mountain pine beetle development data.

An individual's fitness is highly dependent on its phenology relative to the timing

of abiotic factors and the phenology of other organisms. In order to be successful, development must be timed to avoid extreme weather during sensitive life stages, lessening the risk of desiccation in the summer and cold-induced mortality in the winter [27]. For example, the northern extent of the mountain pine beetle range is thought to be largely determined by exposure to cold temperatures [6]. An individual's fitness may also be highly dependent on synchrony between its phenology and that of its biotic resources. This is apparent in plant-pollinator systems, where the timing of pollinator flight activity must coincide with the timing of flower production [29], and in plant-herbivore systems, where the timing of certain developmental stages must coincide with resource availability. For example, winter moth (*Operophtera brumata*) fitness is highly dependent on the coincidence of egg hatching with oak (*Quercus robur*) bud break [46].

Developmental synchrony within a population can also be an important determinant of fitness, especially at low population densities. Finding mates can be difficult when there are few individuals within a population with overlapping reproductive periods [9]. Developmental synchrony within a population of herbivorous insects may also be necessary at low population densities to overwhelm resource defenses. For example, mountain pine beetles have short periods of flight activity during which they must attack pine trees in large enough numbers to result in tree mortality [7]. Both the need for reproductive synchrony to find mates and the need for developmental synchrony to mount mass attacks result in Allee effects [1], where the fitness of an emerging individual at low population densities increases with emergence density. However, interspecific competition for resources becomes the dominant effect at high emergence densities, and increasing emergence density reduces fitness [7].

Temperature plays a major role in determining the phenology of poikilothermic organisms such as insects. Although some insects possess physiological mechanisms

using cues other than temperature to control phenology (e.g. diapause or photoperiod sensitivity) [47], for others, phenology is directly controlled by the dependence of development time on temperature [13]. The body temperature of poikilotherms is not internally regulated; instead their body temperatures, and consequently their metabolic rates, depend on ambient temperature, causing them to develop at different rates at different temperatures [15, 41]. Increasing temperature speeds metabolism at low to moderate temperatures, resulting in a shorter time period required for development. However, increasing temperature can be counterproductive at high temperatures, resulting in longer development time [4]. Consequently, the response of phenology to temperature is a highly plastic trait, i.e. phenology can change in response to yearly temperature change with no underlying molecular evolution. The dependence of development time on temperature varies between developmental stages. This can have a strong synchronizing effect on a population; at low temperatures development can effectively halt for individuals in one stage allowing individuals in earlier stages to catch up [19].

Laboratory experiments have measured development time at various constant temperatures for many insect species (e.g. [4, 15, 17, 28, 41]). We are careful to make the distinction between development time, the time it takes for an insect to develop through a life stage or life cycle, and phenology, the timing (i.e. time of year) of developmental milestones. In laboratory experiments, insects are held at a constant temperature and allowed to develop through a life stage. The time it takes to complete the stage (development time) is recorded. These experiments are carried out at many different temperatures for each life stage. Empirical models (discussed in detail later) are then developed to describe the dependence of development time on temperature in each stage. These models are used to predict development time

under both constant temperatures and varying temperatures in the laboratory and in the field.

The work presented here is largely motivated by the need to understand how mountain pine beetle phenology depends on temperature, how that dependence varies within a population, and how it might adapt to climate change. The mountain pine beetle (MPB) is an eruptive bark beetle found in western North America that spends most of its life cycle beneath the bark of host pine trees. Development from egg to adult occurs within host trees, after which the beetles emerge to mate and attack new hosts where they lay the next generation of eggs (see [39] for a review of mountain pine beetle biology). These attacks have resulted in massive timber loss (see, for example, www.for.gov.bc.ca), making mountain pine beetle an important insect from both an ecological and economic perspective. Mountain pine beetle fitness is highly dependent on phenology [26]; they are found in areas where temperatures can be lethal to certain life stages, so developmental timing is an important factor in population viability [6, 27]. In fact, exposure to cold temperatures is likely the most important mortality factor for mountain pine beetle [12]. Furthermore, recruitment depends on the beetles' ability to overwhelm tree defenses and kill at least a portion of the host tree, necessitating a sufficient density of simultaneously emerging attackers [7]. At low population densities this can only occur if emergence is highly synchronized within the population.

The response of insect populations (including mountain pine beetles) to global warming has been the focus of many recent studies, e.g. [10, 27, 29, 31, 46]. Shifting phenology (e.g. [31]) and range expansion (e.g. [10]) have been linked to temperature change in several natural populations. Since changing temperature shifts phenology and insect fitness is highly dependent on phenology, it follows that global warming will result in strong selection on development time. Predicting how populations might

evolve to cope with global warming requires a mechanistic understanding of how phenology depends on temperature before the evolution of that dependence can be modeled.

One approach to understanding phenology is to use developmental rate curves to describe the development of the median individual in a population. Previous phenology models (e.g. [4, 27, 34]) use temperature-dependent developmental rate curves to predict development time of the median individual (developmental rate is the reciprocal of development time). These rate curves are typically fit to the reciprocal of development time data from constant temperature laboratory experiments (e.g. [27, 34]). The curves are then integrated to determine development time under either constant or variable temperatures.

Our approach to modeling phenology is based on fitting curves to development time rather than developmental rate. Bentz et al. [4] showed that fitting developmental rate curves to the reciprocal of laboratory development time data results in large errors when the curves are used to predict development time, especially at low temperatures. This error is due to transformation of the error variance that results from using the reciprocal of the laboratory data and does not occur when curves are fit directly to development time data. Within populations of insects whose phenology is under direct temperature control, developmental synchronization is attributed to long development times at cold temperatures [19]. Since developmental synchrony can be an important determinant of fitness, it is critical to accurately predict development time at low temperatures in these populations. Phenology models fit to laboratory development times rather than rates offer a clear advantage in this case due to greater accuracy at low temperatures.

In addition to fitting development time curves to laboratory development time data, our approach to modeling phenology is unique in that it is directly based on de-

velopment time curves rather than developmental rate curves. Although curves were fit to development time data in [4] and subsequent studies (e.g. [27]), the phenology models developed in those papers were based on reciprocal curves (developmental rate curves), largely because rates fit more naturally into previous phenology modeling frameworks. In addition to necessitating transformation of laboratory data to parameterize the model, these rate-oriented phenology models require transformation of field data to obtain boundary conditions for simulations (e.g. [17]). In contrast, our parameters and initial conditions are directly related to laboratory and field measurements.

The mountain pine beetle development time data that we use for model parameterization incorporate previously published data [4, 25, 27] as well as previously unpublished data that include development times at temperatures not observed in previous experiments. We expect that inclusion of these new data will result in more accurate phenology predictions at these temperatures, especially in the teneral adult stage. Previous phenology models for MPB have assumed that development halts in this stage at temperatures below $17^{\circ}C$ [27, 35]. The new data show that development occurs at temperatures as low as $8^{\circ}C$ in the teneral adult stage. This has important implications for mountain pine beetle phenology. In particular, the warm developmental threshold in the teneral adult stage that was imposed in previous models may result in predictions of later emergence and more developmental synchrony than a model without this threshold.

Previous models of mountain pine beetle phenology give useful predictions of how populations will respond to climate change. However, since these models do not account for evolution of development time, their predictions are only valid in the absence of evolution. These models predict that developmental synchrony within a population can only be maintained within a narrow range of mean annual temper-

atures; this range spans approximately 2.5°C for mountain pine beetle, and a 2°C increase in mean annual temperature (well within current estimates of climate warming within the mountain pine beetle range [11]) would push temperatures outside of this range [27]. In addition to losing developmental synchrony outside of this range of temperatures, populations that do not evolve cease to be strictly univoltine (one generation per year), which is likely to result in maladaptive developmental timing relative to weather extremes [27]. On the other hand, even if temperatures do allow developmental synchrony within the population, there is no guarantee that the timing of developmental events will be adaptive. For example, over the 2.5°C range that mountain pine beetle is predicted to maintain developmental synchrony, its emergence time is predicted to advance by 60 days [27]. It is unlikely that such a large degree of phenology advancement could be adaptive, especially since fitness is highly dependent on developmental timing relative to weather extremes. These predictions reinforce the idea that evolution of the temperature-dependence of development time will be necessary for populations to successfully adapt to changing climate, and indicate the need to develop a mechanistic understanding of the evolution of phenology.

The dependence of development time on temperature varies within and between populations of insects [5]. This variation arises due to genetic variation in traits that affect development time (e.g. size at maturity), maternal effects (e.g. egg size), and environmental variation (e.g. resource quality at the oviposition site or variation in micro-habitat). Variation is expressed in both the laboratory and the field. In the laboratory, variation may also arise due to fluctuations in experimental conditions (e.g. small temperature oscillations in the thermal cabinet). Since variation affects timing and synchrony, it must be accounted for if we are to predict how climate change will affect insect populations. Furthermore, understanding variation in development time is essential to modeling the evolution of insect phenology; in order for natural

selection to cause evolution of development time within a population there must be heritable variation in that trait within the population [18]. An interesting consequence of variability in development time is the potential for reproductive isolation within a population. In particular, insects with short development times will emerge before insects with long development times, and since reproduction occurs shortly after emergence, individuals with similar phenotypes may be more likely to mate than individuals with very different phenotypes.

Variability in the dependence of development time on temperature has been observed in mountain pine beetles both within a single population [17] and between distinct populations that are adapted to different local environments [5]. One study by Bentz et al. [5] showed this variability to be heritable in mountain pine beetles; this study revealed a similar pattern of variation in body size between mountain pine beetle populations, although variation in body size between populations exceeds variation within populations. Since smaller insects generally complete development faster than larger insects under the same environmental conditions [38], variation in body size may provide a more easily measured surrogate for variation in development time (at least between populations) in the future.

Some previous phenology models have accounted for variation in phenology [17, 25, 40, 44]; Several of these models are discussed in [17]. The models describe variation in developmental rates and predict temporal variation in developmental milestones by solving a partial differential equation [17] or by direct application of a distributional model that results from assumptions about developmental rate distributions [25, 40, 44]. The partial differential equation model developed by Gilbert et al. [17], which they call the Extended von Foerster model, is an advection-diffusion equation in which the drift coefficient is the median development rate in a population and the diffusion coefficient is related to the variance in development rates.

The shape of the distribution of developmental rates is irrelevant in the Extended von Foerster model. This simplifies efforts to describe developing insect populations, because less information is required to parameterize the model. However, the ability to adapt the shape of phenology distributions to reflect laboratory or field data is lost. Fortunately, the Extended von Foerster model does a good job at predicting the shape of mountain pine beetle emergence distributions observed in the laboratory at constant temperatures [17]. In implementing the Extended von Foerster model, Gilbert et al. assume that variation in developmental rate is constant [17], though this is not essential to the model formulation.

The distributional model developed by Sharpe et al. [40] assumes that variation in developmental rates at constant temperature is the result of variability in the concentration of rate controlling enzymes. To extend their model to varying temperatures, Sharpe et al. assume that developmental rate variance is proportional to the mean developmental rate [40]. The shape of phenology distributions predicted by the Sharpe et al. are dependent on the shape of the distribution of developmental rates, so more information is required to parameterize this model than the Extended von Foerster model. However, this model affords more flexibility in specifying the shape of phenology distributions.

Neither the Extended von Foerster model nor the Sharpe et al. model provide a natural framework for studying the evolution of development time in response to natural selection on phenology. In particular, there is no clear way to identify and track individual developmental phenotypes in either model, so it is impossible to identify how selection impacts individual developmental phenotypes. Since they consider populations in aggregate, neither the Extended von Foerster model nor the Sharpe et al. model will reveal temporal structure in the distribution of phenotypes. For example, neither model would be able to predict that individuals that develop slowly

due to their genotypes will emerge later than individuals that develop quickly. The ability to predict such patterns is important in modeling the evolution of development time, because individuals that emerge at different times will be exposed to different selective pressures.

We develop a phenology modeling framework that explicitly accounts for variation in development time while allowing phenology distributions of individual phenotypes to be tracked. This is achieved by introducing a developmental phenotype that scales some base temperature-dependent development time curve. This phenotype is assumed to vary within a population, and development is simulated separately for insects with different phenotypes. Hence, temporal structure in developmental phenotype and the effects of phenology selection on different phenotypes can be accounted for explicitly. This model also differs from the models of Gilbert et al. and Sharpe et al. in that it directly describes variation in development time rather than developmental rates. As a consequence of our approach, variation in development time is proportional to mean development time—a simple pattern that is supported by laboratory observations, but is not achieved by either the Sharpe et al. model or the Extended von Foerster model because they are formulated in terms of developmental rates. Like the Extended von Foerster model, our approach is based on a partial differential equation formulation and allows random variation in development time (due to environmental noise) to be incorporated into a diffusion term. However, our approach retains the flexibility of the Sharpe et al. model to specify the shape of developmental distributions.

We take a maximum likelihood approach to determine phenology model parameters using constant temperature laboratory development time data for mountain pine beetle. This is different than previous developmental parameterizations for mountain pine beetle, in which a curve was fit directly to the median development rates or times

at each constant temperature (e.g. [4, 27]). The maximum likelihood approach has two major advantages when fitting phenology models to laboratory development time data. First, temperatures at which fewer observations were made have less weight in fitting development time curve parameters. This is especially important if few observations are made at some temperatures, since fitting a development time curve directly to the median development times would give equal weight to these temperatures. Second, the maximum likelihood approach allows us to explicitly incorporate variation in development time and to simultaneously fit development time curve and variance parameters.

Our phenology model, which incorporates phenotypic variation in development time, is easily extended to study the evolution of development time in response to selection on phenology. Our approach inherently assumes that development time is a continuous trait (also known as a quantitative or multifactorial trait) as opposed to a discrete trait (see [21, 23]). This is justified, because development time is affected by many aspects of physiology and environment and is likely influenced by many genes, whereas a discrete trait is controlled by few genes. Consequently, development time varies continuously within a population. We are unaware of any published quantitative genetic model that explicitly describes the evolution of phenology.

Quantitative genetic models describe how selection affects variation in quantitative traits and how that variation is inherited by successive generations [20, 42, 43]. Selection acts on heritable traits through differential fitness, so that phenotypes associated with higher fitness are better represented in the next generation. The simplest quantitative genetic model is the Breeder's Equation. This model states that the change in mean phenotype in successive generations is equal to the product of the change in the mean of the earlier generation following selection and the heritability of the trait. This model is insufficient for studying the evolution of development

time, because it is restricted to describing the change in the mean phenotype. The Breeder's equation does not allow for phenotypic mating structure (e.g. temporal structure in the case of development time), as there is the inherent assumption that every individual in the population is capable of breeding with every other individual. This assumption is violated for development time, since individuals with similar phenotypes are more likely to mate than individuals with dissimilar phenotypes. For example, slow developers are more likely to mate with other slow developers, because they are more likely to be in their reproductive phases at the same time (late in the reproductive season). In other quantitative genetic models assumptions are typically made about the shape of the phenotype distribution within a population (e.g. normality [21]), and the models describe how selection and reproduction affects the mean and variance of the phenotype distribution for the next generation [42].

We take a direct approach to modeling the evolution of insect development time in response to selection on emergence time. Development is tracked and the emergence time distribution is predicted for each phenotype. A selection function is then applied that assigns fitness based on emergence time and density (individuals emerging on the same day have the same fitness regardless of phenotype). The phenotypes of offspring laid as eggs on a particular day are assumed to be normally distributed with the same mean as their parents and variance related to their parents' phenotypic variance, consistent with [42]. A clear benefit of this approach is that it allows a fairly complex evolutionary scenario (indirect, density-dependent selection on a highly plastic, temporally structured quantitative trait) to be represented in a fairly simple way. Additionally, the simplicity of this approach admits analysis using classical tools of applied mathematics. The model can also be easily extended to study even more realistic (more complicated) scenarios. For example, it could be extended to account for direct correlations between development time and fitness (larger insects

take longer to develop but are capable of producing more offspring). The major drawback of our approach is that it is computationally complex, development must be tracked for many phenotypes, potentially over many generations.

In this manuscript we begin by developing and analyzing a general mathematical model of the evolution of phenology that is under direct temperature control. Variation in development time is accounted for by a parameter that scales temperature-dependent development time curves, and a well-established phenology model [34] is used to describe the effect of this variation on phenology (emergence time) within a population. We model natural selection on emergence time and emergence density with an Allee effect. These selection pressures indirectly affect the variation in the dependence of development time on temperature (i.e. an individual's phenotype). Inheritance of this variation through sexual reproduction is represented by assuming that offspring inherit the mean parent phenotype plus some small random deviation. Our evolution model is made up of phenotype-dependent development, selection, and reproduction mappings composed. We characterize this seemingly complex map by its effect on a few simple population characteristics: the density, mean phenotype, and phenotypic variance of insects that are oviposited at each time of year. We use this characterization to find an asymptotic approximation for the evolution model using Laplace's method, which is employed to demonstrate the existence of steady phenotype distributions. These distributions have means approximately equal to the phenotypes that allow for parents and offspring to be oviposited at the same time of year and predictable variances. We numerically validate the approximation results and demonstrate other dynamics of the evolution map for a model insect whose phenology is qualitatively similar to a large class of insect species.

Next we extend the phenology model to describe different sources of developmental variation and parameterize the model using constant temperature laboratory

data for mountain pine beetles. Additional random variation in development time is incorporated into the model by adding a diffusion term, resulting in a Fokker-Planck development equation. The Fokker-Planck development equation is solved under constant temperatures and fit to development time data. The models are then used to simulate mountain pine beetle phenology using phloem temperatures measured in the field and field counts of beetle attacks on successfully colonized lodgepole pine trees; the emergence distributions predicted by the phenology models are compared to emergence measured in the field.

Finally, we investigate the evolutionary dynamics of mountain pine beetle phenology under selection on emergence time. The evolution model is implemented using developmental parameters for mountain pine beetle, and the selection scheme is based on a model that links phenology and demography for MPB developed by Powell and Bentz [33]. We verify that the steady distribution results hold for mountain pine beetle populations under stable climate conditions, even with additional phenology variation due to distributed oviposition. We also simulate warming by shifting temperatures from a phloem temperature series measured in central Idaho to a phloem temperature series measured in southern Utah. We show that populations can adapt to warming only if they retain the ability to complete one generation per year and if the warming rate is moderate.

CHAPTER 2

MODELING THE EVOLUTION OF INSECT PHENOLOGY¹

2.1 Introduction

Can evolution moderate the disruptive effects of global warming on phenology, the timing of developmental milestones such as emergence or oviposition, in insect populations? There are strong selective pressures on insects to maintain appropriate phenology, including developmental synchrony with resources and within populations. Insect phenology changes as yearly temperature changes, because the time necessary for an insect to complete its life cycle is largely dependent on temperature [47]. This link has been observed in populations around the globe; recent temperature change has been linked to shifting phenology [31] and range expansion [10] in multiple populations. It is not well understood how evolution of temperature-dependent development time may moderate the effects of increasing temperature on phenology. In this paper we present a novel approach to modeling the evolution of temperature-dependent development time in response to selection on phenology.

An individual's phenology relative to the timing of abiotic factors and the phenology of other organisms has a major effect on its fitness. It is essential that development is timed to avoid the coincidence of sensitive life stages with extreme weather to lessen the risk of desiccation in the summer or cold-induced mortality in the winter [27]. An individual's fitness may also be highly dependent on synchrony between its phenology and the phenology of its biotic resources. This is apparent in plant-pollinator systems, where the timing of pollinator flight activity must coincide with the timing

¹This chapter is reprinted from Brian Yurk and James Powell, *Modeling the evolution of insect phenology*, Bulletin of Mathematical Biology **71** (2009), 952-979.

of flower production [29], and in plant-herbivore systems, where the timing of certain developmental stages must coincide with resource availability. For example, winter moth (*Operophtera brumata*) fitness is highly dependent on the coincidence of egg hatching with oak (*Quercus robur*) bud break [46].

Developmental synchrony within a population can also be an important determinant of fitness, especially at low population densities. Finding mates can be difficult when there are few individuals within a population with overlapping reproductive periods [9]. Developmental synchrony within a population of herbivorous insects may also be a necessity at low population densities to overwhelm resource defenses. For example, mountain pine beetles (*Dendroctonus ponderosae* Hopkins) have short periods of flight activity during which they must attack pine trees in large enough numbers to result in tree mortality [7]. Both the need for reproductive synchrony, and the need for developmental synchrony for mass attack result in an Allee effect, in which the fitness of an emerging individual at low population densities increases with the emergence density [1]. However, interspecific competition for resources becomes the dominant effect at high emergence densities, and increasing emergence density reduces fitness.

Temperature plays a major role in determining the phenology (and hence the fitness) of poikilothermic organisms such as insects. The body temperature of poikilotherms is not internally regulated; instead their body temperature and consequently their metabolic rate depend on ambient temperature, causing them to develop at different rates at different temperatures [15, 41]. At low to moderate temperatures increasing temperature speeds metabolism resulting in a shorter time period required for development. At high temperatures, however, increasing temperature can be counterproductive, resulting in longer development time [4]. We make the distinction between development time, the time it takes for an insect to develop through a life

stage or life cycle, and phenology, the timing (i.e. time of year) of developmental milestones. Many insects possess physiological mechanisms using cues other than temperature to control phenology, such as diapause or photoperiod sensitivity [47]. However, for some insects phenology is directly controlled by the dependence of development time on temperature [13]. For these insects, the response of phenology to temperature is a highly plastic trait, i.e. phenology can change in response to yearly temperature change with no underlying molecular evolution.

Previous phenology models describe the plastic response of phenology to temperature for systems in which phenology is under direct temperature control (e.g. [13]). This response is particularly well-understood for mountain pine beetle. Although presented in a general context, our evolution model is based on generalizing models of mountain pine beetle phenology (see for example [19]). These models, described in detail in §2.2.1, predict that developmental synchrony within a population can only be maintained within a narrow range of mean annual temperatures; this range spans approximately 2.5°C for mountain pine beetle, and a 2°C increase in mean annual temperature (well within current estimates of climate warming within the mountain pine beetle range [11]) would push temperatures outside of this range [27]. In addition to losing developmental synchrony outside of this range of temperatures, populations that do not evolve cease to be strictly univoltine (one generation per year), which is likely to result in maladaptive developmental timing relative to weather extremes [27]. On the other hand, even if temperatures do allow developmental synchrony within the population, there is no guarantee that the timing of developmental events will be adaptive. For example, over the 2.5°C range that mountain pine beetle is predicted to maintain developmental synchrony its emergence time is predicted to advance by 60 days [27]. It is unlikely that such a large degree of phenology advancement could

be adaptive, especially if it occurs in a population in which fitness is highly dependent on synchronization with the phenology of a biotic resource.

Genetic evolution may allow insect phenology to adapt to changing selective pressures as temperatures increase. In order for natural selection to cause evolution of a trait within a population there must be heritable variation in that trait within the population [18]. Variability in the dependence of development time on temperature has been observed in mountain pine beetle both within a single population [17] and between distinct populations that are adapted to different local environments [5]. Laboratory experiments have shown this variability to be heritable [5]. The same study revealed a similar pattern of variation in body size between populations; generally, smaller insects complete development faster than larger insects under the same environmental conditions [38]. In the future, variation in body size may provide a more easily measured surrogate for variation in development time (at least between populations). An interesting consequence of variability in development time is the potential for reproductive isolation within a population. In particular, insects with short development times will emerge before insects with long development times, and since reproduction occurs after emergence, individuals with similar phenotypes may be more likely to mate than individuals with very different phenotypes.

The dependence of insect development time on temperature varies continuously within a population. It is affected by many aspects of physiology and environment and is likely influenced by many genes. Hence, it is best regarded as a quantitative (multifactorial) trait [21, 23], as opposed to a discrete trait that is controlled by few genes and varies in a discrete manner. Quantitative genetic models describe how selection affects variation in quantitative traits and how that variation is inherited by successive generations [20, 42, 43]. Typically some assumption is made about the shape of the phenotype distribution within a population (e.g. normality [21]), and

the quantitative genetic model describes how selection and reproduction affects the mean and variance of the phenotype distribution for the next generation [42]. We are unaware of any published quantitative genetic model that explicitly describes the evolution of phenology.

In this paper we develop and analyze a general mathematical model of the evolution of phenology that is under direct temperature control. Variation in development time is accounted for by a parameter that scales temperature-dependent development time curves, and a well-established phenology model [34] is used to describe the effect of this variation on phenology (emergence time) within a population. We then model natural selection on emergence time and emergence density with an Allee effect. These selection pressures indirectly affect the variation in the dependence of development time on temperature (i.e. an individual's phenotype). Inheritance of this variation through sexual reproduction is represented by assuming that offspring inherit the mean parent phenotype plus some small random deviation. Our evolution model is made up of phenotype-dependent development, selection, and reproduction mappings composed. We characterize this seemingly complex map by its effect on a few simple population characteristics: the density, mean phenotype, and phenotypic variance of insects that are oviposited at each time of year. We use this characterization to find an asymptotic approximation for the evolution model using Laplace's method, which is employed to demonstrate the existence of steady phenotype distributions. These distributions have means approximately equal to the phenotypes that allow for parents and offspring to be oviposited at the same time of year and predictable variances. Finally, we numerically validate the approximation results and demonstrate other dynamics of the evolution map for a model insect whose phenology is qualitatively similar to a large class of insect species.

2.2 Model development

2.2.1 Temperature-dependent phenology model

The temperature-dependent phenology model that forms the foundation of our evolution model was originally developed to predict mountain pine beetle phenology [34], but is easily adapted to describe any insect whose development time depends directly on temperature. For such insects, let $\rho_i(T)$ be the time required for an individual to complete development through its i th life stage at constant temperature T . These development time curves are typically U-shaped [45]. Development time is minimized at some optimal temperature (often approximately 20°C) and increases as temperature get cooler or warmer [41]. In practice, $\tau_i(T)$ is approximated by measuring development time at constant temperatures in a laboratory, then fitting an appropriate curve to the data [4]. A piecewise exponential curve captures the U-shaped dependence of development time on temperature:

$$\tau_i(T) = \begin{cases} a + \exp[b - cT], & T < \theta, \\ a + \exp[b - \theta(d + c) + dT], & T \geq \theta. \end{cases} \quad (2.1)$$

To maintain the appropriate U-shape and to avoid zero and negative development times, the parameters a, c, d are positive. An example of a development time curve with this formulation is shown in Figure 2.1.

These curves are used to predict phenology for insects under variable temperatures. Define $T(t)$ to be the temperature at time t and $a(t)$ to be the proportion of a life stage that an insect has completed at that time, a dimensionless quantity taking values between 0 and 1. Since an insect takes $\tau_i(T)$ days to develop through the entire life stage at constant temperature T , the simplest developmental model

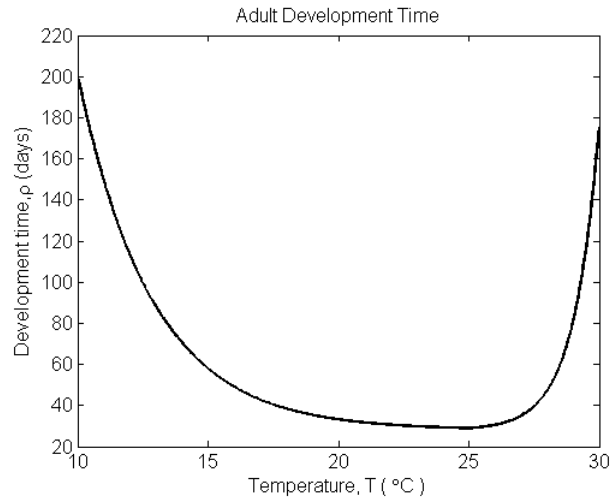


Fig. 2.1: An example of a development time curve. An insect's development time is the duration of a life stage at a certain temperature.

predicts it will take $\Delta t = \tau_i(T)\Delta a$ days to develop through a fraction Δa of the life stage at that temperature. If the relationship $\Delta a/\Delta t = 1/\tau_i(T)$ holds for arbitrarily small values of Δt , i.e. $da/dt = 1/\tau_i(T(t))$, then development through stage i for an insect that began at time t_0 is described by the initial value problem

$$\frac{da}{dt} = \frac{1}{\tau_i(t)}, \quad a(t_0) = 0, \quad (2.2)$$

where $\tau_i(t) = \tau_i(T(t))$. The differential equation (2.2) is integrated to determine the insect's age at time t ,

$$a(t) = \int_{t_0}^t \frac{ds}{\tau_i(s)}.$$

In particular, the time that an insect will complete stage i if it began at time t , $g_i(t)$, satisfies

$$1 = \int_t^{g_i(t)} \frac{ds}{\tau_i(s)}. \quad (2.3)$$

When an insect completes a stage it begins the next stage; for example, an insect that enters stage 1 at time t will complete that stage and enter stage 2 at time $g_1(t)$. The same insect will complete stage 2 at time $g_2(g_1(t)) = (g_2 \circ g_1)(t)$. If $G(t)$ is the time that an insect completes its life cycle when it began at time t , then for an insect with an m -stage life cycle

$$G(t) = (g_m \circ g_{m-1} \circ \dots \circ g_2 \circ g_1)(t); \quad (2.4)$$

a typical G function is shown in Figure 2.2.

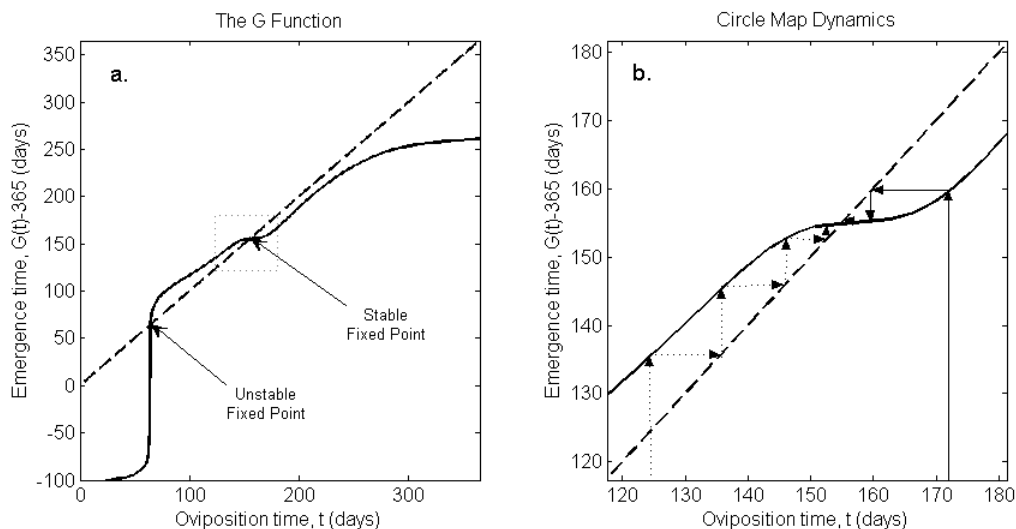


Fig. 2.2: **a.** An example of a G function. Given the oviposition time t of an insect, its emergence time is $G(t)$. $G(t) - 365$ is plotted to show the time of year of emergence relative to the time of year of oviposition. **b.** A developmental circle map and its fixed point dynamics. The circle map is the solid curve, and the fixed point line $G(t_o^n) = t_o^n$ is dashed. As the map is iterated oviposition time converges (arrows) to stable fixed points that occur at intersections of the two curves intersect where the slope of the circle map curve is less than one.

Previous work has focused on the G function to understand the plastic response of phenology to temperature [27, 35]. If temperatures are periodic with the same variation each year (which is roughly true in natural systems), then the G function

viewed modulo 365 days results in a periodic circle map between t_o^n , the time of year that an individual in generation n is oviposited, and t_o^{n+1} , the time of year that its offspring are oviposited in generation $n + 1$. Univoltine (one generation per year) fixed points of the circle map are times of year at which the oviposition times of an insect and its offspring are separated by exactly one year, i.e. $t_o^n = G(t_o^n) - 365$. These fixed points dominate the dynamics of the circle map when it is iterated over multiple generations [35], since oviposition times rapidly converge to these points regardless of initial oviposition time (see Figure 2.2). Hence, univoltine fixed points can synchronize phenology within a population, and the timing of these fixed points relative to biotic and abiotic factors can have a profound effect on the average fitness of a population. The existence of fixed points is structurally stable; fixed points are maintained under small perturbations of development time curve parameters or the underlying temperature series [35]. This stability plays an important role in the dynamics of our evolution model, because individuals with slightly different phenotypes have slightly different G functions.

2.2.2 Development time as a quantitative trait

We model variation in development time by allowing a single developmental parameter, α , to vary continuously within a population. Let α scale some base development time curve $\tau_k(T)$ so that the development time in stage k for an individual with phenotype α is $\alpha\tau_k(T)$. Variance in α corresponds with realistic variance structure in development time; the same variation in α results in more variation at longer development times than at shorter development times as is often observed in development data. This means, for example, that an individual with phenotype $\alpha = 2$ takes twice as long to develop as an individual with phenotype $\alpha = 1$ at the same constant

temperature. Variation in α may be linked to variation in insect size at maturity. The extension of our phenology model to account for α is straightforward: the time that an insect with phenotype α completes stage k given that it began at time t , $g_{k,\alpha}(t)$, satisfies

$$1 = \int_t^{g_{k,\alpha}(t)} \frac{ds}{\alpha\tau_k(s)},$$

similar to (2.3). For illustration purposes, we let development time vary within a single life stage. In this case, the emergence time of an individual with phenotype α that was oviposited at time t (its G function (2.4)), is

$$G_\alpha(t) = (g_m \circ g_{m-1} \circ \dots \circ g_{k+1} \circ g_{k,\alpha} \circ g_{k-1} \circ \dots \circ g_2 \circ g_1)(t).$$

Figure 2.3 shows examples of $G_\alpha(t)$ for various values of α .

Under periodic temperatures, $G_\alpha(t)$ taken modulo 365 provides a circle map for each value of α , and this map may have univoltine fixed points. Conversely, given an oviposition time t there may be a phenotype, α_t , that results in a univoltine fixed point at time t , i.e. $t = G_{\alpha_t}(t) - 365$, (see Figure 2.3). If we differentiate the definition of α_t with respect to t , upon rearrangement,

$$\dot{\alpha}_t = \frac{1 - \frac{\partial}{\partial t} [G_\alpha(t)]|_{\alpha=\alpha_t}}{\frac{\partial}{\partial \alpha} [G_\alpha(t)]|_{\alpha=\alpha_t}},$$

where ‘ \cdot ’ indicates differentiation with respect to t . Increasing α increases development time, so the denominator is positive. If t is a stable fixed point of G_{α_t} , then $\frac{\partial}{\partial t} [G_\alpha(t)]|_{\alpha=\alpha_t} < 1$, so that the numerator is also positive, making $\dot{\alpha}_t > 0$. Similarly, $\dot{\alpha}_t < 0$ whenever t is a unstable fixed point of G_{α_t} . Stability of the univoltine fixed points in Figure 2.3 can therefore be determined by the slope of α_t . Univoltine fixed points play a crucial role in organizing the dynamics of development within a popu-

lation with developmental variability, since oviposition times are attracted to stable fixed points and repelled by unstable fixed points.

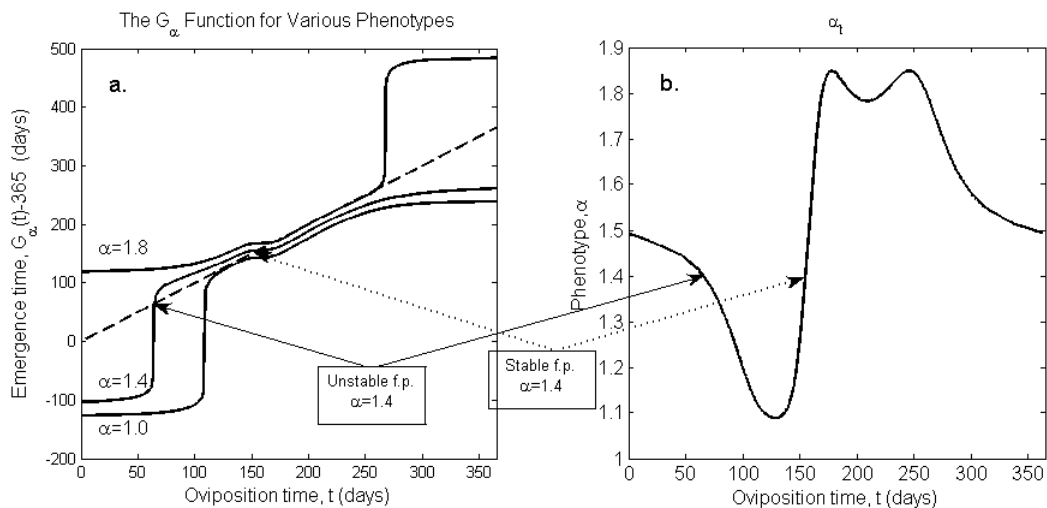


Fig. 2.3: **a.** The G_α function for various values of α . Given the oviposition time t of an individual with phenotype α , the individual's emergence time is $G_\alpha(t)$. Although α varies continuously within a population, this plot shows only a few representative curves. **b.** Given an oviposition time t , α_t is the unique phenotype that results in a univoltine fixed point for the G_α function at time t , i.e. $G_{\alpha_t}(t) = t + 365$. These fixed points are stable ($\frac{\partial}{\partial t}[G_{\alpha_t}(t)] < 1$) where α_t is increasing and unstable where α_t is decreasing (see text). The arrows point to the same unstable (solid) and stable (dotted) univoltine fixed points in both parts of the figure for individuals with phenotype $\alpha = 1.4$.

2.2.3 Evolution map

In this section we describe how the phenotype-dependent phenology model is incorporated into a model of the evolution of phenology within a population. Let $p_o^n(\alpha, t)$ be the density of insects in generation n with phenotype α and oviposition time t ; the evolution model maps $p_o^n(\alpha, t)$ to $p_o^{n+1}(\alpha, t)$. If selection acts only on emergence time and emergence density, then there are no selective pressures acting on the population during development, and the evolution map can be broken into two components: development and selection/reproduction (see Figure 2.4). Development

maps the oviposition distribution for generation n to the emergence distribution for generation n , i.e. $p_o^n(\alpha, t) \xrightarrow{D} p_e^n(\alpha, t)$. Selection and reproduction occur when the population emerges, mapping the emergence density for generation n to the oviposition distribution for generation $n + 1$, i.e. $p_e^n(\alpha, t) \xrightarrow{S,R} p_o^{n+1}(\alpha, t)$.

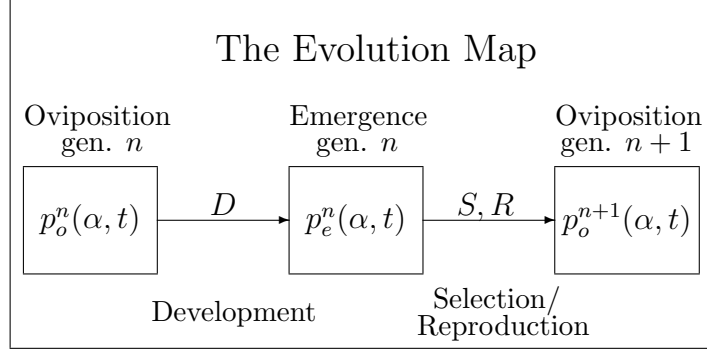


Fig. 2.4: A diagram of the evolution map. Development (D) maps the oviposition distribution to the emergence distribution for generation n . Selection/reproduction (S,R) maps the emergence distribution for generation n to the oviposition distribution for generation $n + 1$.

Now we derive an explicit representation for the development map in terms of the phenology model, leaving discussion of the selection and reproduction maps for §§2.2.4-2.2.5. If the number of insects is conserved during development (no mortality or immigration), then insects emerging between times t_1 and t_2 were oviposited between times $G_\alpha^{-1}(t_1)$ and $G_\alpha^{-1}(t_2)$;

$$\int_{t_1}^{t_2} p_e^n(\alpha, t) dt = \int_{G_\alpha^{-1}(t_2)}^{G_\alpha^{-1}(t_1)} p_o^n(\alpha, t) dt. \quad (2.5)$$

Changing variables results in

$$\int_{t_1}^{t_2} p_e^n(\alpha, t) dt = \int_{t_1}^{t_2} p_o^n(\alpha, G_\alpha^{-1}(t)) \frac{\partial}{\partial t} [G_\alpha^{-1}(t)] dt.$$

Since this equation must hold for all choices of t_1 and t_2 , it follows that

$$p_e^n(\alpha, t) = p_o^n(\alpha, G_\alpha^{-1}(\alpha, t)) \frac{\partial}{\partial t} [G_\alpha^{-1}(\alpha, t)]. \quad (2.6)$$

Both forms of the conservation law (2.5 and 2.6) explicitly define the development map.

2.2.4 Natural selection

We discuss natural selection on emergence time and emergence density. In both cases, selection affects phenotypic variation indirectly, because insects with the same emergence time have the same fitness regardless of phenotype. In the first selection model, truncation selection acts on emergence time. If $S_1(t)$ is the fitness of individuals emerging at time t (the number of female eggs per female adult), then

$$S_1(t) = \begin{cases} \gamma_1, & t \in [t_{early}, t_{late}), \\ 0, & \text{otherwise.} \end{cases} \quad (2.7)$$

This selection function models the need for some insect species to emerge within a certain time interval to coincide with resource availability or to avoid lethal temperatures. We require that $365 \leq t_{early} < t_{late} \leq 730$, which confines cohorts to emerging within a single calendar year (univoltinism). Univoltinism is often necessary for a population to maintain adaptive seasonality [27].

In the second selection model the fitness of an emerging individual depends on its emergence time and the density of simultaneous emergers. The emergence density at time t in generation n is

$$N_e^n(t) = \int p_e^n(\alpha, t) d\alpha. \quad (2.8)$$

The fitness of individuals emerging at time t , $S_2(t)$, has the following form:

$$S_2(t) = \begin{cases} F(N_e^n(t)), & t \in [t_{early}, t_{late}), \\ 0, & \text{otherwise,} \end{cases} \quad (2.9)$$

where F describes how fitness depends on emergence density. Here,

$$F(N) = \frac{\gamma_2 N}{N^2 + b^2}, \quad (2.10)$$

where γ_2 and b are positive parameters. $F(N)$ increases for $N < b$ and decreases for $N > b$, giving an Allee effect, since fitness increases with emergence density at low densities. F also accounts for saturation at high densities ($F(N) \rightarrow 0$ as $N \rightarrow \infty$).

2.2.5 Sexual reproduction

Whereas the selection model determines the number of offspring produced per emerging female, the reproduction model determines their phenotypes. For simplicity, we assume that mating occurs immediately following emergence and results in the immediate production of $S(t)$ female eggs per female emerging at time t . Hence mating only occurs between insects that emerge simultaneously, and the densities of parents and their offspring are related by

$$N_o^{n+1}(t) = S(t)N_e^n(t), \quad (2.11)$$

where $N_o^{n+1}(t)$ is the density of eggs oviposited at time t . We assume that the phenotypes of eggs laid at time t are normally distributed, so that the oviposition

distribution in generation n is given by

$$p_o^n(\alpha, t) = \frac{N_o^n(t)}{\sqrt{2\pi\nu_o^n(t)}} \exp\left[-\frac{(\alpha - \mu_o^n(t))^2}{2\nu_o^n(t)}\right], \quad (2.12)$$

where $\mu_o^n(t)$ and $\nu_o^n(t)$ are the mean phenotype and phenotypic variance for the eggs laid at time t . The assumption of phenotypic normality is common in the quantitative genetic literature (e.g. [21, 23, 43]). By using a normal distribution of phenotypes, we introduce negative and unbounded phenotypes into the population, but this effect is negligible if the mean phenotype is sufficiently large relative to the phenotypic variance.

We assume that progeny inherit their mean parent phenotype plus some error with zero mean and fixed variance σ_ε^2 . This is similar to the approach introduced by Slatkin [42]. The reproductive variance is assumed to be small ($\sigma_\varepsilon^2 \ll 1$) and accounts for the combined effects of different sources of variation including heterozygosity [42], maternal effects, environmental variability, and mutation. The phenotypes of females and males emerging simultaneously can be thought of as random variables F and M . Then, the phenotype of their eggs is also a random variable, O , and

$$O = \frac{F}{2} + \frac{M}{2} + \varepsilon,$$

where ε is the reproductive error. If F and M are identically and independently distributed, with mean μ_e and variance ν_e , then O has mean $\mu_o = \mu_e$, due to linearity of the mean, and variance $\nu_o = \nu_e/2 + \sigma_\varepsilon^2$, due to bilinearity of the covariance. Since most phenotypic variance can be attributed to reproductive variance [42], we rescale the phenotypic variance to obtain the order 1 quantity $v_e = \lambda\nu_e$, where $\lambda = 1/\sigma_\varepsilon^2$. Hence, if the mean phenotype and rescaled phenotypic variance of parents emerging at time t in generation n are $\mu_e^n(t)$ and $v_e^n(t)$, then the mean phenotype and rescaled

phenotypic variance of their offspring are

$$\mu_o^{n+1}(t) = \mu_e^n(t), \quad (2.13)$$

$$v_o^{n+1}(t) = v_e^n(t)/2 + 1. \quad (2.14)$$

2.2.6 Characterization of the evolution map

The normality assumption (2.12) and the relationships between the densities (2.11), mean phenotypes (2.13), and rescaled phenotypic variances (2.14) of parents and offspring define the selection/reproduction component of the evolution model, mapping the emergence distribution for generation n to the oviposition distribution for generation $n + 1$. Hence, the evolution map (e.g. Figure 2.4) is characterized by these relationships and how development maps the density, mean phenotype, and rescaled phenotypic variance from oviposition to emergence:

$$\{N_o^n(t), \mu_o^n(t), \nu_o^n(t)\} \xrightarrow{D} \{N_e^n(t), \mu_e^n(t), \nu_e^n(t)\} \xrightarrow{S,R} \{N_o^{n+1}(t), \mu_o^{n+1}(t), \nu_o^{n+1}(t)\}.$$

In the remainder of this section we provide the details of this characterization. The oviposition distribution for generation n (2.12) is

$$p_o^n(\alpha, t) = \sqrt{\frac{\lambda}{2\pi}} \left(\frac{N_o^n(t)}{\sqrt{v_o^n(t)}} \right) \exp \left[-\lambda \frac{(\alpha - \mu_o^n(t))^2}{2v_o^n(t)} \right], \quad (2.15)$$

Following development (2.6), the emergence distribution for generation n is

$$p_e^n(\alpha, t) = \sqrt{\frac{\lambda}{2\pi}} \left(\frac{N_o^n(G_\alpha^{-1}(t)) \frac{\partial}{\partial t} [G_\alpha^{-1}(t)]}{\sqrt{v_o^n(G_\alpha^{-1}(t))}} \right) \exp \left[-\lambda \frac{(\alpha - \mu_o^n(G_\alpha^{-1}(t)))^2}{2v_o^n(G_\alpha^{-1}(t))} \right]. \quad (2.16)$$

For notational simplicity we define the following functions of α :

$$f_t(\alpha) = \frac{N_o^n(G_\alpha^{-1}(t)) \frac{\partial}{\partial t}[G_\alpha^{-1}(t)]}{\sqrt{v_o^n(G_\alpha^{-1}(t))}}, \quad (2.17)$$

and

$$h_t(\alpha) = \frac{(\alpha - \mu_o^n(G_\alpha^{-1}(t)))^2}{2v_o^n(G_\alpha^{-1}(t))}. \quad (2.18)$$

Then, the emergence distribution (2.16) is given by

$$p_e^n(\alpha, t) = \sqrt{\frac{\lambda}{2\pi}} f_t(\alpha) \exp[-\lambda h_t(\alpha)].$$

The development map is characterized by the following integrals that give the density of individuals in generation n emerging at time t , their mean phenotype, and their rescaled phenotypic variance:

$$N_e^n(t) = \sqrt{\frac{\lambda}{2\pi}} \int_{-\infty}^{\infty} f_t(\alpha) \exp[-\lambda h_t(\alpha)] d\alpha, \quad (2.19)$$

$$\mu_e^n(t) = \frac{\sqrt{\lambda}}{N_e^n(t) \sqrt{2\pi}} \int_{-\infty}^{\infty} \alpha f_t(\alpha) \exp[-\lambda h_t(\alpha)] d\alpha, \quad (2.20)$$

$$v_e^n(t) = \frac{1}{N_e^n(t) \sqrt{2\pi\lambda}} \int_{-\infty}^{\infty} (\alpha - \mu_e^n(t))^2 f_t(\alpha) \exp[-\lambda h_t(\alpha)] d\alpha. \quad (2.21)$$

Following development, the selection/reproduction map is applied giving,

$$N_o^{n+1}(t) = S(t) N_e^n(t),$$

$$\mu_o^{n+1}(t) = \mu_e^n(t),$$

$$v_o^{n+1}(t) = v_e^n(t)/2 + 1.$$

The preceding six equations completely characterize the evolution map.

2.3 Analytical results

We use Laplace's method (a special case of the method of steepest descent) to approximate each of the integrals defining the development map (2.19-2.21) by the leading order term of its asymptotic expansion as $\lambda \rightarrow \infty$ (see [8, 14] for a discussion of the method). The results are used in §2.3.2 to approximate steady distributions in which the temporal structure of the mean phenotype and phenotypic variance are invariant under the evolution map with periodic temperatures. These steady distributions represent populations that are well adapted to stable climate conditions and are important in understanding the dynamics of the evolution model in general.

2.3.1 Approximation of the development map

Asymptotic expansions of development integrals

Applying Laplace's method to (2.19) results in the asymptotic expansion

$$N_e^n(t) = \frac{f_t(\alpha_t^*) \exp[-\lambda h_t(\alpha_t^*)]}{\sqrt{h_t''(\alpha_t^*)}} + O\left(\frac{\exp[-\lambda h_t(\alpha_t^*)]}{\lambda}\right),$$

as $\lambda \rightarrow \infty$, where α_t^* is the value at which $h_t(\alpha)$ achieves a (in this case unique) minimum. Using an asymptotic expansion as $\lambda \rightarrow \infty$ is reasonable if the reproductive variance is small (i.e. $\sigma_\varepsilon^2 \ll 1$), since $\lambda = 1/\sigma_\varepsilon^2$. Truncating after the first term results in an approximation for the emergence density,

$$N_e^n(t) \approx \frac{f_t(\alpha_t^*) \exp[-\lambda h_t(\alpha_t^*)]}{\sqrt{h_t''(\alpha_t^*)}}. \quad (2.22)$$

A similar approach gives the asymptotic expansion for the mean phenotype (2.20)

$$\mu_e^n(t) = \alpha_t^* + O\left(\frac{1}{\lambda}\right),$$

as $\lambda \rightarrow \infty$, provided that $f_t(\alpha_t^*) \neq 0$. The leading order term gives an approximation for the mean phenotype at emergence,

$$\mu_e^n(t) \approx \alpha_t^* \quad (2.23)$$

For the rescaled phenotypic variance we must use a higher order expansion (see [14]), since the first two terms in the asymptotic expansion for (2.21) are zero. Consequently,

$$v_e^n(t) = \frac{1}{h_t''(\alpha_t^*)} + O\left(\frac{1}{\lambda}\right).$$

Truncating after the first term gives

$$v_e^n(t) \approx \frac{1}{h_t''(\alpha_t^*)}. \quad (2.24)$$

Critical points of $h_t(\alpha)$

To find α_t^* that minimizes $h_t(\alpha)$, we seek α_t^* such that $h_t'(\alpha_t^*) = 0$ and $h_t''(\alpha_t^*) > 0$, where primes denote derivatives with respect to α . First, note that

$$\begin{aligned} h_t'(\alpha) = & \frac{\alpha - \mu_o^n(G_\alpha^{-1}(t))}{2[v^n(G_\alpha^{-1}(t))]^2} \left(2v^n(G_\alpha^{-1}(t)) \left(1 - \dot{\mu}_o^n(G_\alpha^{-1}(t)) \frac{\partial}{\partial \alpha} [G_\alpha^{-1}(t)] \right) \right. \\ & \left. - (\alpha - \mu_o^n(G_\alpha^{-1}(t))) \dot{v}^n(G_\alpha^{-1}(t)) \frac{\partial}{\partial \alpha} [G_\alpha^{-1}(t)] \right) \end{aligned} \quad (2.25)$$

where ‘ $\dot{\cdot}$ ’ denotes a derivative in time. In order for α_t^* to be a critical point of $h_t(\alpha)$, either factor in (2.25) must be zero when $\alpha = \alpha_t^*$. Setting the first factor in (2.25)

equal to zero gives

$$\alpha_t^* - \mu_o^n(G_{\alpha_t^*}^{-1}(t)) = 0. \quad (2.26)$$

Setting the second factor in (2.25) equal to zero gives

$$0 = 2v^n(G_{\alpha_t^*}^{-1}(t)) \left(1 - \dot{\mu}_o^n(G_{\alpha_t^*}^{-1}(t)) \frac{\partial}{\partial \alpha} [G_{\alpha}^{-1}(t)] \Big|_{\alpha=\alpha_t^*} \right) - \left(\alpha_t^* - \mu_o^n(G_{\alpha_t^*}^{-1}(t)) \right) \dot{v}^n(G_{\alpha_t^*}^{-1}(t)) \frac{\partial}{\partial \alpha} [G_{\alpha}^{-1}(t)] \Big|_{\alpha=\alpha_t^*}.$$

Here we focus on the first case, in which $\alpha_t^* = \mu_o^n(G_{\alpha_t^*}^{-1}(t))$, since it is consistent with numerical steady distribution results and leads to the simplest analysis. In this case, we know that $h_t(\alpha)$ achieves a minimum at α_t^* , since

$$h_t''(\alpha_t^*) = \frac{\left(1 - \dot{\mu}_o^n(G_{\alpha_t^*}^{-1}(t)) \frac{\partial}{\partial \alpha} [G_{\alpha}^{-1}(t)] \Big|_{\alpha=\alpha_t^*} \right)^2}{v(G_{\alpha_t^*}^{-1}(t))} > 0. \quad (2.27)$$

2.3.2 Steady distributions of the evolution map

Under stable conditions we expect that a well-adapted population will achieve some level of equilibrium with the local climate. To find equilibrium states we seek oviposition distributions with structure that is invariant under the evolution map with periodic yearly temperatures. Non-trivial steady states of the evolution map under periodic yearly temperatures may not exist if selection acts directly on emergence time and not on emergence density. Instead, steady distributions are sought in which the phenotypes of eggs oviposited at a particular time of year are invariant under the evolution map. These distributions are characterized by invariance of the mean

phenotype and rescaled phenotypic variance, i.e.

$$\mu_o^{n+1}(t + 365) = \mu_o^n(t), \quad (2.28)$$

$$v_o^{n+1}(t + 365) = v_o^n(t). \quad (2.29)$$

These conditions can be rewritten exclusively in terms of the development map, since $\mu_o^{n+1}(t + 365)$ and $v_o^{n+1}(t + 365)$ are given in terms of $\mu_e^n(t + 365)$ and $v_e^n(t + 365)$ by the reproductive map (2.13-2.14). The results are the following conditions for a steady distribution:

$$\mu_e^n(t + 365) = \mu_o^n(t), \quad (2.30)$$

$$v_e^n(t + 365) = 2v_o^n(t) - 2. \quad (2.31)$$

Approximate steady distributions

We use the approximations generated using Laplace's method to characterize steady distributions at leading order. In particular, we replace $\mu_e^n(t + 365)$ and $v_e^n(t + 365)$ in the steady distribution conditions (2.30-2.31) by their approximations (2.23-2.24), giving

$$\mu_o^n(t) = \alpha_{t+365}^*, \quad (2.32)$$

$$2v_o^n(t) - 2 = \frac{1}{h_t''(\alpha_{t+365}^*)}. \quad (2.33)$$

Recall that α_{t+365}^* minimizes $h_t(\alpha)$ if (2.26) is satisfied, i.e. if

$$\alpha_{t+365}^* = \mu_o^n \left(G_{\alpha_{t+365}^*}^{-1}(t + 365) \right).$$

Substituting into (2.32) yields

$$\mu_o^n(t) = \mu_o^n \left(G_{\mu_o^n(t)}^{-1}(t + 365) \right), \quad (2.34)$$

a sufficiency condition for the mean phenotype at a steady distribution.

Note that (2.34) is satisfied if $G_{\mu_o^n(t)}^{-1}(t + 365) = t$, which occurs, by definition, if

$$\mu_o^n(t) = \alpha_t. \quad (2.35)$$

In this case the mean phenotype at time t results in a univoltine fixed point of G_α . We expect such a steady distribution to be stable when t is a stable fixed point of G_α , because emergence times are attracted to these points.

A condition for $v_o^n(t)$ when $\mu_o^n(t) = \alpha_t$ can be derived by working directly with (2.33). However, it is more informative to assume that the mean has reached its steady state $\mu_o^n(t) = \alpha_t$, and consider the evolution of $v_o^n(t)$. Given the periodicity of α_t and (2.27), the Laplace approximation for the rescaled variance (2.24) becomes

$$v_e^n(t) \approx \frac{v_o^n(t)}{\left(1 - \dot{\alpha}_t \frac{\partial}{\partial \alpha} [G_\alpha^{-1}(t)] \Big|_{\alpha=\alpha_t} \right)^2}. \quad (2.36)$$

Taken together, these give an approximation for the rescaled phenotypic variance when $\mu_o^n(t) = \alpha_t$. The squared quantity in the denominator has a particularly simple representation. Differentiating $t = G_{\alpha_t}^{-1}(t)$ with respect to t gives

$$1 = \dot{\alpha}_t \frac{\partial}{\partial \alpha} [G_\alpha^{-1}(t)] \Big|_{\alpha=\alpha_t} + \frac{\partial}{\partial t} [G_\alpha^{-1}(t)] \Big|_{\alpha=\alpha_t}.$$

This implies that the denominator in (2.36) is $\left(\frac{\partial}{\partial t}[G_\alpha^{-1}(t)]\Big|_{\alpha=\alpha_t}\right)^2$, so that

$$v_e^n(t) \approx v_o^n(t) \left(\frac{\partial}{\partial t}[G_\alpha(t)]\Big|_{\alpha=\alpha_t}\right)^2, \quad (2.37)$$

using the fact that

$$\frac{\partial}{\partial t}[G_\alpha^{-1}(t)]\Big|_{\alpha=\alpha_t} = \left(\frac{\partial}{\partial t}[G_\alpha(t)]\Big|_{\alpha=\alpha_t}\right)^{-1}.$$

The effect of the reproduction map on the rescaled phenotypic variance is given by

$$v_o^{n+1}(t) = \frac{v_e^n(t)}{2} + 1.$$

Substituting the Laplace approximation (2.37) for $v_e^n(t)$ gives

$$v_o^{n+1}(t) \approx \frac{v_o^n(t)}{2} \left(\frac{\partial}{\partial t}[G_\alpha(t)]\Big|_{\alpha=\alpha_t}\right)^2 + 1.$$

Repeated application of the evolution map under periodic temperature conditions results in the following:

$$v_o^{n+m}(t) \approx v_o^n(t)[x(t)]^m + [x(t)]^{m-1} + [x(t)]^{m-2} + \dots + x(t) + 1,$$

where

$$x(t) = \frac{1}{2} \left(\frac{\partial}{\partial t}[G_\alpha(t)]\Big|_{\alpha=\alpha_t}\right)^2.$$

Assuming that $x(t) < 1$, the first term on the right hand side vanishes as $m \rightarrow \infty$.

Hence,

$$\lim_{m \rightarrow \infty} v_o^{n+m}(t) \approx \sum_{m=0}^{\infty} [x(t)]^m.$$

This geometric series converges to the limit $\frac{1}{1-x(t)}$ for values of t where $x(t) < 1$. This gives us the following result:

$$\lim_{n \rightarrow \infty} v_o^n(t) = \frac{1}{1 - \frac{1}{2} \left(\left. \frac{\partial}{\partial t} [G_\alpha(t)] \right|_{\alpha=\alpha_t} \right)^2},$$

for values of t where

$$\left. \frac{\partial}{\partial t} [G_\alpha(t)] \right|_{\alpha=\alpha_t} < \sqrt{2}. \quad (2.38)$$

A quick check shows that

$$v_o^n(t) = \frac{1}{1 - \frac{1}{2} \left(\left. \frac{\partial}{\partial t} [G_\alpha(t)] \right|_{\alpha=\alpha_t} \right)^2}, \quad (2.39)$$

satisfies the steady state condition (2.33).

Oviposition density dynamics at a steady distribution

We investigate the dynamics of the oviposition density, $N_o^n(t)$, at a steady distribution where $\mu_o^n(t) = \alpha_t$. The Laplace approximation (2.22) for the oviposition density at this steady distribution becomes

$$N_e^n(t) \approx \frac{f_t(\alpha_t)}{\sqrt{h_t''(\alpha_t)}}, \quad (2.40)$$

where (2.17) gives

$$f_t(\alpha_t) = \frac{N_o^n(t)}{\sqrt{v_o^n(t) \left. \frac{\partial}{\partial t} [G_\alpha(t)] \right|_{\alpha=\alpha_t}}}.$$

Substituting the expression for $h_t''(\alpha_t)$ from (2.37) into equation (2.40) results in

$$N_e^n(t + 365) \approx N_o^n(t).$$

This gives us the relationship between the oviposition densities for generations n and $n + 1$,

$$N_o^{n+1}(t + 365) = S(t + 365)N_o^n(t). \quad (2.41)$$

The resulting dynamics are remarkably simple, since development and reproduction can be ignored at a steady distribution where $\mu_o^n(t) = \alpha_t$. The oviposition density is determined by the time of year and the density at the same time of year in the preceding generation. In the case of density dependent selection (2.9), $N_o^{n+1}(t) = H(N_o^n(t))$, where $H(N) = NF(N)$. The result is a discrete dynamical system, with dynamics characterized by properties of the function $H(N)$. In particular, oviposition density dynamics are determined by fixed points of $H(N)$ and their stability.

Summary and implications of steady distribution results

The analytical results suggest that populations experiencing periodic temperatures may evolve to steady distributions at times that are stable fixed points of the G_α function. We expect the temporal structure of the mean phenotype to evolve toward stable univoltine fixed points G_α as these points attract nearby emergence times. Our results also predict the phenotypic variance at steady distributions. The oviposition densities at stable fixed points of G_α are described by a simple dynamical map, H , from the oviposition density in one generation to the oviposition density in the next that is determined only by the selection function. We are careful here to distinguish between the three different types of steady state behavior that are important in the dynamics of the evolution model: steady distributions of the evolution map where the mean phenotype and phenotypic variance at oviposition is maintained from one generation to the next, fixed points of G_α where oviposition times are the same

for parents with phenotype α and their offspring, and fixed points of H where the oviposition density of progeny is the same as the emergence density of their parents.

Although the structure of a steady distribution at unstable fixed points of G_α is not examined analytically, we expect it will be largely determined by the phenotypes of individuals leaked from nearby stable fixed points. For example, individuals with large phenotypes (large α s) will leak from late stable fixed points to unstable fixed points that are later in the year. Hence, large phenotypes will probably dominate at these unstable fixed points. Due to the repulsive effect of unstable fixed points of G_α on emergence times, we expect emergence densities to be lower than at stable fixed points.

2.4 Numerical simulations

We numerically simulated the evolution of phenology for a model insect with two life stages. The purpose of these simulations was twofold: to verify our analytical results and to provide examples of dynamics of the evolution model. However, we do not intend to present a comprehensive analysis here of all possible dynamics. Instead we restrict our attention to two long-term periodic temperature experiments with different selection functions and one short-term warming experiment with shifting resource phenology. A detailed description of the numerical implementation of the evolution map is given in the appendix.

2.4.1 Two-stage model insect

The two-stage (egg and adult) model insect used here was constructed to have qualitatively similar phenology to most insects with temperature-dependent development. Since a two-stage life cycle has similar developmental dynamics to life cycles with more than 2 stages [34], our results generalize to more complicated systems.

Table 2.1: Development time curve parameters for 2-stage model insect used in numerical simulations.

Stage	a	b	c	d	θ
Egg	81.000	6.899	0.156	0.101	25
Adult	28.036	8.658	0.351	1.022	25

The model insect has piecewise exponential development time curves (2.1) shown in Figure 2.5 with parameters in Table 2.1. Realistic parameters were obtained by fitting development time data for two mountain pine beetle life stages [4], then scaling the curves to allow the model insect to be univoltine. Genetic variation in development time occurs in the adult stage. The development time of an adult is obtained by scaling the base adult development time curve by its phenotype, α . The reproductive variance for the model insects is set at $\sigma_\varepsilon^2 = 0.001$, which is consistent with developmental variation observed in mountain pine beetle populations.

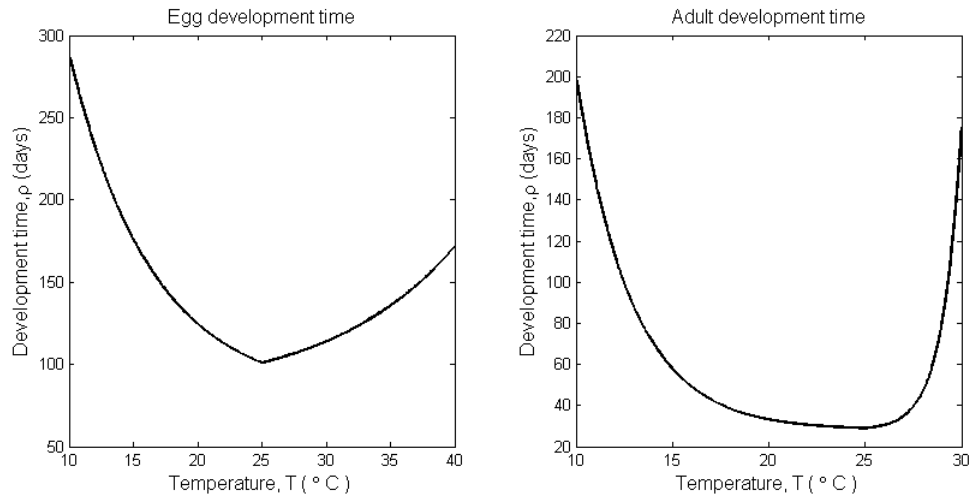


Fig. 2.5: Development time curves for the two-stage model insect. These curves are scaled mountain pine beetle development time curves.

2.4.2 Simulations: periodic temperature

To numerically investigate the structure of a population that is well-adapted to stable climate conditions and to test our analytical steady distribution approximations, we performed two periodic temperature simulations with different selection functions. The periodic temperature series is a cosine curve such that the mean annual temperature is $8^\circ C$, the seasonal variation is $18^\circ C$, and the minimum temperature occurs on January 1, i.e. $T(t) = 8 - 18 \cos(2\pi t/365)$. In both simulations, only insects emerging within a 100 day time window produce offspring (emergence time dependent truncation selection). In the first simulation this is the only selection that occurs, so that selection is modeled by (2.7). In the second simulation selection also depends on emergence density with an Allee effect according to (2.9-2.10). Selection parameters for both periodic temperature experiments are listed in Table 2.2. In the first simulation, we normalize the oviposition distribution at the beginning of each generation, because there is no density dependence to restrict population growth or decline. Given the parameter choices used in the second simulation (see Table 2.2), the emergence densities $N = 0$ and $N = 40,000$ are stable fixed points of $H(N)$, and $N = 10,000$ is an unstable fixed point of $H(N) = NF(N)$. Hence, when emergence density drops below 10,000 the next generation's oviposition density declines, and when emergence density is above 10,000 the next generation's oviposition density is attracted to 40,000. The initial oviposition distributions are uniform over the phenotype-time rectangle $R = [0.8, 2.0] \times [0, 365]$, with $p_o^0(\alpha, t) = 10^5$ if $(\alpha, t) \in R$, and $p_o^0(\alpha, t) = 0$ otherwise. Simulations are run for 1000 generations, after which $N_o^{1000}(t)$, $\mu_o^{1000}(t)$, and $v_o^{1000}(t)$ are computed for each time t and compared to the approximate steady distribution obtained by the Laplace method.

Table 2.2: Parameters for the selection functions in the periodic temperature simulations. In simulation 1 there is emergence time dependent truncation selection. In simulation 2 there is emergence time dependent truncation selection and density dependent selection with an Allee effect. The values listed for t_{early} and t_{late} are for generation n .

Simulation	Parameter	Value
1 & 2	t_{early}	$365n + 100$
1 & 2	t_{late}	$365n + 200$
1	γ_1	1
2	γ_2	50,000
2	b	20,000

The results of the first periodic temperature simulation with no density dependent selection are shown in Figure 2.6. After 1000 generations there is negligible change in the shape of the oviposition distribution in successive generations suggesting that a steady distribution is achieved. Most insects are oviposited at stable univoltine fixed points of G_α (see Figure 2.6a). At these points, the mean phenotype closely follows the phenotype that allows a univoltine fixed point of the G_α function (see Figure 2.6b). Hence, near stable fixed points the mean agrees with the steady distribution prediction that $\mu_o^n(t) \approx \alpha_t$. Furthermore, except near marginal (semistable) fixed points the rescaled variance closely matches the corresponding steady distribution prediction (2.39) at stable fixed points of G_α (see Figure 2.6c). At unstable fixed points, the numerical results do not match the steady distribution predictions. However, the oviposition density at these points is very low-the number of misbehaving insects is small relative to the total population.

The results of the second periodic temperature simulation with density-dependent selection are shown in Figure 2.7. Similar to the first simulation, a steady distribution is reached within 1000 generations and the validity of the steady distribution predictions depend on the stability of fixed points of G_α . At stable fixed points, the mean phenotype and rescaled phenotypic variance agree well with the phenotype that

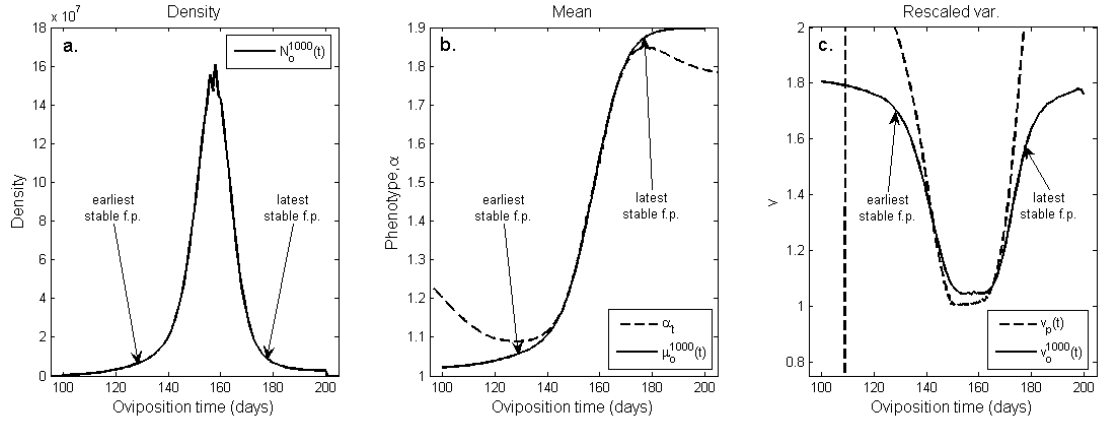


Fig. 2.6: Results after 1000 generations of the first periodic temperature simulation with truncation selection on emergence time. The time of year of oviposition is shown on the horizontal axes. **a.** Oviposition density. Most mass occurs at stable fixed points (between arrows). **b.** Mean phenotype (solid) and α_t (dashed), the phenotype that makes t a univoltine fixed point of G_α . Consistent with analytical results, $\mu_o^n(t) \approx \alpha_t$ at stable fixed points. The prediction fails at unstable fixed points, where there is little mass and the population structure is mainly determined by the phenotypes of individuals leaked from nearby stable fixed points. **c.** Rescaled phenotypic variance (solid) and $v_p(t)$ (dashed), the predicted rescaled variance at a steady distribution where $\mu_o^n(t) = \alpha_t$. Numerical rescaled variance results also agree with analytical predictions at all but the earliest and latest stable fixed points. The prediction does not hold at unstable fixed points where there is little mass.

results in a univoltine fixed point and the corresponding prediction for the rescaled variance (see Figure 2.7b-c). Near stable fixed points of G_α , the emergence density is reasonably close to the expected emergence density of 40,000 (see Figure 2.7a). The emergence density declines at unstable fixed points but much less rapidly than in the first simulation, due to density dependent selection pushing it upward.

It is not surprising that the approximation $\mu_o^n(t) \approx \alpha_t$ fails near unstable fixed points at a steady distribution; the emergence times of individuals with phenotypes close to α_t are actually repelled by these points, so it is unlikely that the population could evolve toward them. The steady state approximations do allow us to understand the structure of steady distributions at unstable fixed points. Near marginal

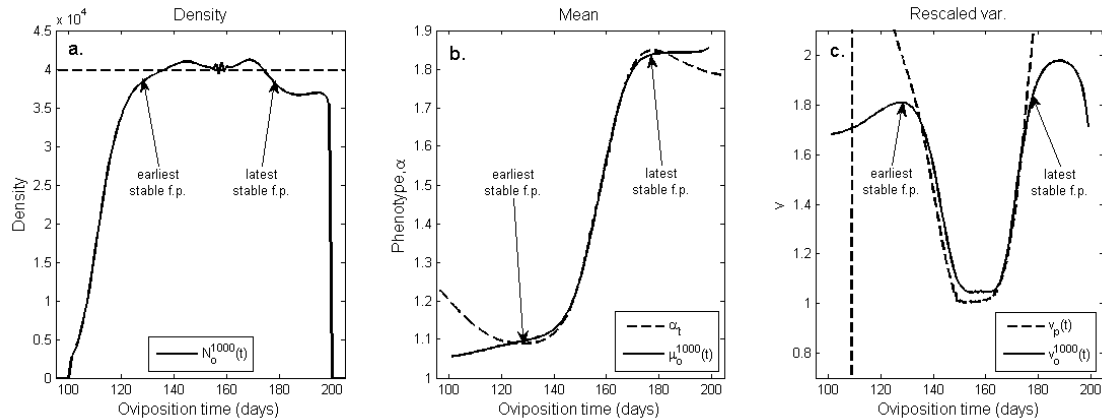


Fig. 2.7: Results after 1000 generations of the second periodic temperature simulation with selection on emergence time and emergence density. The time of year of oviposition is shown on the horizontal axes. **a.** Oviposition density (solid) and the predicted density (dash-dot) at a steady state where $\mu_o^n(t) = \alpha_t$ (40,000 is the non-trivial fixed point of $H(N)$). Most mass occurs at stable fixed points (between arrows). More mass is leaked to the unstable fixed points in this experiment than in the first periodic temperature experiment. This mass persists due to positive pressure from density dependent selection. **b.** Mean phenotype (solid) and α_t (dashed), the phenotype that makes t a univoltine fixed point of G_α . Consistent with analytical results, $\mu_o^n(t) \approx \alpha_t$ at stable fixed points. The prediction fails at unstable fixed points, where the population structure is mainly determined by the phenotypes of individuals leaked from nearby stable fixed points. **c.** Rescaled phenotypic variance (solid) and $v_p(t)$ (dashed), the predicted rescaled variance at a steady distribution where $\mu_o^n(t) = \alpha_t$. Numerical rescaled variance results also agree with analytical predictions at stable fixed points, but not at unstable fixed points.

(semistable) fixed points individuals with certain phenotypes are leaked from stable to unstable fixed points. For example, individuals with large phenotypes (large α s) oviposited at late stable fixed points will emerge later the next year on unstable fixed points. Hence, the phenotypes at unstable fixed points in a steady distribution are largely determined by the phenotypes of individuals leaking from nearby stable fixed points. This is apparent in Figures 2.6b and 2.7b, where the phenotypes of individuals oviposited at times to the right (left) of the region of stable fixed points have larger (smaller) phenotypes than individuals oviposited at nearby marginal points. These

results hold for a wide range of temperatures and parameters, except in the case where there are two or more disjoint regions of stable fixed points within the emergence time window. In this case, other numerical simulations show that the steady distribution approximation holds for the earliest region, but later regions tend to also be impacted by individuals leaked from the earlier stable fixed points. We expect that this discrepancy is due to the asymptotic nature of approximation, since as λ gets large reproductive variance gets small and there is less mixing between neighboring oviposition times. Hence the approximation becomes worse as there is more mixing between regions of stable fixed points due to higher reproductive variance.

Our periodic temperature results suggest that variation in development time and phenology persist in a well-adapted population under stable climate conditions, both of these are observed in natural populations and in laboratory reared insects. Our analytical prediction that the mean phenotype at a steady distribution results in a univoltine fixed point of G_α agrees with numerical results at stable fixed points and is useful in understanding the population structure at nearby unstable fixed points. An interesting consequence of the structure of steady distributions is reproductive isolation of individuals with substantially different phenotypes. For example, individuals with large phenotypes emerge later than individuals with small phenotypes at a steady distribution causing their reproductive periods to be disjoint. This creates the potential for rapid local evolution if a disturbance during the emergence period removes early or late phenotypes.

2.4.3 Simulation: increasing temperature and advancing resource phenology

As an example of the dynamics of the evolution model under global warming, we simulated the evolution of a population of two-stage model insects with increasing

Table 2.3: Parameters for the selection functions in the warming temperature simulations. There is truncation selection on emergence time with a shifting emergence window. There is also density dependent selection with an Allee effect. The values listed for t_{early} and t_{late} are for generation n .

Parameter	Value
t_{early}	$515 + (365 - 24/100)n$
t_{late}	$535 + (365 - 24/100)n$
γ_2	50,000
b	20,000

mean annual temperature and advancing resource phenology (emergence window). The mean annual temperature is increased 6°C over 100 years by adding $6/100^\circ\text{C}$ per year to the temperature series used in the preceding simulations: $T(t) = 8 - 18 \cos(2\pi t/365) + (6/100)n$, where n is the number of calendar years that have passed at time t since the beginning of the simulation. This amount of warming is at the high end of current projections for some regions [11], but the results generalize to less drastic scenarios. Selection depends on emergence time and density according to (2.9-2.10) with parameters in Table 2.3. The density dependence is the same as in the second periodic temperature experiment. In this simulation, individuals must emerge within a 20 day time window that advances 24 days over 100 years at a constant rate in order to reproduce, modeling changing resource phenology. This rate of phenology advance is similar to that observed in [29]. The simulation begins with a population that is well-adapted to temperatures at the beginning of the experiment; the initial oviposition distribution is the from 1,000th generation in the second periodic temperature simulation. The increasing temperature simulation was run for 100 generations (100 years), and the number of insects oviposited in each generation, $\int_{365n}^{365(n+1)} N_o^n(t) dt$, was tracked.

The results of this simulation are shown in Figure 2.8. The population declined slowly at first, but remained fairly large. After about 60 generations, the popu-

lution dropped dramatically with zero insects remaining after 83 generations. The steep population decline coincides with a loss of stable fixed points within the shifting emergence time window (see Figure 2.9). As temperatures increase, the time intervals over which G_α has stable fixed points change. The population evolves toward phenotypes that allow it to track changing stable fixed points as temperature increases, but when these fixed points do not overlap with the emergence time window the population rapidly declines. Outside of the region of stable fixed points individuals are pushed out of the emergence time window. The Allee effect keeps the population from rebounding if the system later evolves so the emergence time window overlaps with stable fixed points.

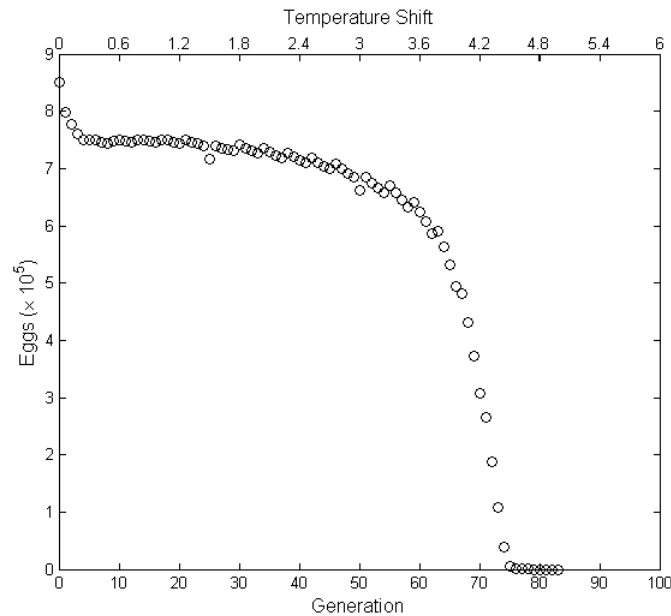


Fig. 2.8: Number of eggs laid per generation in the increasing temperature simulation. The generation number appears along the bottom horizontal axis, and the corresponding temperature shift appears along the top horizontal axis. In this simulation, mean annual temperature increases by 6°C over 100 years, and a 20 day long emergence window advances 24 days over 100 years. Density dependent selection is also imposed. The steep population decline between generations 60 and 73 corresponds to a loss of stable fixed points inside of the emergence time window.

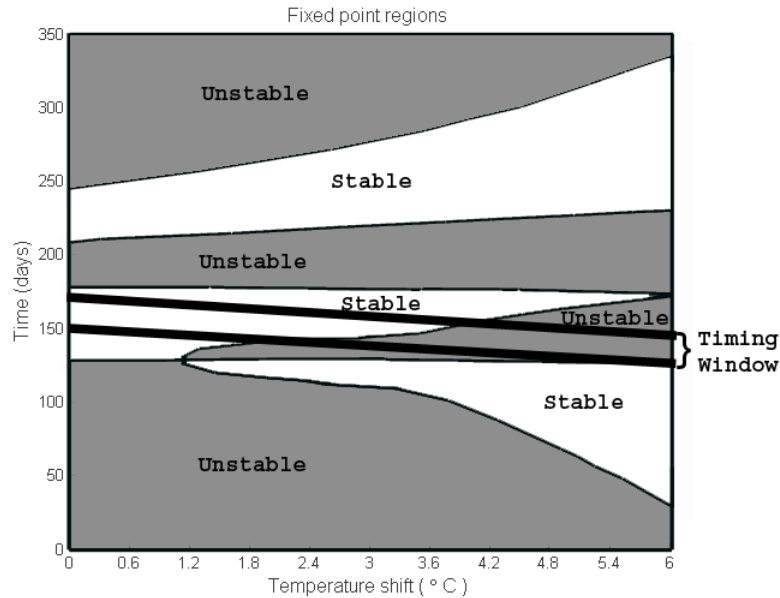


Fig. 2.9: A diagram of the stability of univoltine fixed points of the G_α function under different shifts of the temperature series $T(t) = 8 - 18 \cos(2\pi t/365)$ and the emergence time window for the increasing temperature simulation (between thick black lines). For the two-stage model insect there is a phenotype α that makes each emergence time a univoltine fixed point of the G_α map. The stability of these fixed points is indicated in the diagram, with stable fixed points occurring in white regions and unstable fixed points occurring in gray regions. Note that after the temperature shift reaches 4.1°C there are no stable fixed points within the emergence time window. The loss of stable fixed points coincides with population collapse in the increasing temperature simulation.

Our results show that genetic evolution may allow populations to persist for much longer than populations without evolution under global warming. To see this, we compare our results to the dynamics of a population with no developmental variation and no evolution of development time that experiences the same warming temperatures and shifting emergence window. Without evolution or variation of the plastic response of development time to temperature, populations can only remain viable if a stable fixed point of the G function is contained in the emergence time window. For example, if the entire population has phenotype $\alpha = 1.4$ and does not evolve, then

the population will persist for approximately 20 generations under the temperature conditions in this simulation, since beyond this $G_{1.4}$ does not have a univoltine stable fixed point within the emergence window. This is much shorter than the evolving population persists (approximately 80 generations). Hence, our results show that evolution may allow a population to persist, but there is a limit; populations can only persist as long as the emergence time window overlaps with stable fixed points. Although we focus on a single scenario here, Figure 2.9 can be used to predict population viability for the two-stage model insect under multiple scenarios of climate warming and resource phenology shifts. Plotting the corresponding emergence window, the population is expected to decline rapidly as the window leaves regions of stable fixed points.

2.5 Summary and future directions

The evolution model presented here extends previous temperature-dependent phenology models by introducing heritable variation in their parameters. The model is presented in a general manner that is applicable to many insect species. Variation in development time is allowed to evolve in response to indirect selection acting on phenology instead of the development parameters themselves. The evolution map is characterized by its effects on the temporal variation of density, mean phenotype, and phenotypic variance at oviposition. We used this characterization and the Laplace method to approximate the evolution map and to identify important steady distributions where the mean phenotype allows for a univoltine fixed point of G_α .

Our analytical results suggest (and our numerical results verify) that populations that are well-adapted to stable climate conditions are organized by stable univoltine fixed points of G_α . Populations rapidly adapt to track these points through evolution of the temporal structure of mean phenotype and phenotypic variance. The result is

a population in which heritable variation in development time is maintained across successive generations. The stationary temporal structure of phenotypic variance at stable fixed points of G_α is determined by the slope of G_α . Steady distribution dynamics at unstable fixed points are largely determined by the population at neighboring stable fixed points, as individuals are leaked from stable to unstable fixed points depending on their phenotypes.

The numerical results also predict that populations may evolve to remain synchronized with resources as temperatures increase. However, this ability to adapt may disappear as overlap between stable univoltine fixed points of G_α and the timing of resource availability is lost. Unfortunately, this may cause sudden and otherwise unexpected local extinctions as observed in our numerical simulations.

The evolution dynamics presented here will provide a basis of comparison for future work in which more complex systems are analyzed. Our model is easily generalized by using different selection functions, phenology models, mating assumptions, or allowing different or multiple developmental parameters to vary. Variation in a scaling parameter results in variance in development time that is proportional to the square of mean development time. For simplicity, we ignored the effects of other types of developmental variance in this work. In the future we will incorporate additional variance structures into a phenology model for mountain pine beetle using a Fokker-Planck equation (the phenology model without variation in development time presented here can be formulated as an advection equation). We will compare the evolution of phenology with additional random environmental noise to the analytical predictions presented here.

CHAPTER 3

DEVELOPMENTAL VARIATION AND INSECT PHENOLOGY¹

3.1 Introduction

Describing variation in the link between temperature and insect phenology (the timing of developmental events such as oviposition, or adult emergence) is a crucial step toward predicting how insect populations will respond to climate change. The time required for an insect to complete a life stage (development time) depends on its thermal environment [47]; this response varies within and between populations [5]. Variation in development time within a population can be divided into persistent and random variation. We define persistent variation to be developmental variation that persists throughout a life-stage, including genetic variation in traits that affect development time (e.g. size at maturity), maternal effects (e.g. egg size), and persistent environmental variation (e.g. variation in resource quality across oviposition sites). Random variation in development time is due to random environmental fluctuations (e.g. due to variation in micro-habitat). Random variation may also arise in laboratory development experiments due to fluctuations in experimental conditions (e.g. small temperature oscillations in the thermal cabinet). Predicting how climate change will affect insect phenology must take both of these factors into account. In this paper we present three phenology models incorporating increasing amounts of developmental variation, while explicitly separating persistent and random variation. The models are fit to data from constant temperature laboratory experiments for mountain pine beetle (MPB), *Dendroctonus ponderosae* Hopkins [Coleoptera: Scolytidae], an eco-

¹Coauthored by Brian Yurk and James A. Powell.

nomically important pest insect. The parameterized models are used to simulate MPB phenology using temperatures measured in the field, and phenology predictions are compared to field observations.

The response of insect populations to global warming has been the focus of many recent studies, e.g. [10, 27, 29, 31, 46]. Temperature change has been linked to shifting phenology [31] and range expansion (e.g. [10]) in several natural populations. Insect fitness is highly dependent on phenology; development must be timed to coincide with favorable weather conditions and resource availability. In some populations development must also be synchronized; Synchronous emergence improves mating chances in small populations and, in the case of MPB, is necessary to overwhelm defended host trees (see Chapter 2). Since temperature change shifts phenology, global warming will result in strong selection on development time. Predicting how populations might evolve to cope with global warming requires a mechanistic understanding of how phenology depends on temperature before the evolution of that dependence can be modeled.

The work presented here is largely motivated by the need to understand how MPB phenology depends on temperature, how that dependence varies within a population, and how it might adapt to climate change. MPB is an eruptive bark beetle found in western North America that spends most of its life cycle beneath the bark of host pine trees. Development from egg to adult occurs within host trees, after which the beetles emerge to mate and attack new hosts where they lay the next generation of eggs (see [39] for a review of MPB biology). These attacks have resulted in massive timber loss (see, for example, www.for.gov.bc.ca), making MPB an important insect from both an ecological and economic perspective. MPB fitness is highly dependent on phenology [26]; they are found in areas where temperatures are lethal to certain life stages, so developmental timing is an important factor in population viability [6, 27].

In fact, exposure to cold temperatures is likely the most important mortality factor for MPB [12]. Furthermore, recruitment depends on the beetles' ability to overwhelm tree defenses and kill at least a portion of the host tree, necessitating a sufficient density of simultaneously emerging attackers [7]. At low population densities this can only occur if emergence is highly synchronized within the population.

Many insects possess physiological mechanisms that use environmental cues to control phenology, such as diapause or photoperiod sensitivity [47]. However, some insects, such as MPB, lack direct physiological mechanisms for determining phenology; instead they rely on temperature control of development time to achieve appropriate seasonality and developmental synchrony [4, 13]. Since the body temperature of poikilotherms is not internally regulated, their metabolic rates depend on ambient temperature [15, 41]. At low to moderate temperatures warming speeds development, while at high temperatures warming can be counterproductive and slows development [4]. Low temperatures can have a strong synchronizing effect on a population of insects, as development effectively stops for a large proportion of individuals in a certain life stage, possibly allowing individuals in earlier stages to catch up.

We develop a phenology modeling framework that describes temperature-dependent development and explicitly accounts for persistent and random variation in development time. Various models have been developed to describe temperature-dependent development. Some of these have focused on tracking development of the median individual (e.g. [34]), while others have accounted for variation in phenology using distributional models [17, 25, 40, 44]. These models either ignore developmental variation or do not separate the effects of persistent variation from random variation. It is important to model both sources of variation in order to accurately predict phenology in laboratory experiments and under field conditions. Genetic variation in traits that affect development time is present in both laboratory and field populations,

contributing directly to persistent variation. In the laboratory, efforts are made to control random environmental fluctuations in temperature and other environmental factors. However, these controls are not perfect (e.g. temperature controllers still allow small but significant fluctuations in ambient temperature), so a phenology model that quantifies random variation may better describe laboratory development data. Uncontrolled variation in temperature and other environmental factors abounds in the field. Since sources of random variation will differ from case to case, whereas persistent variation will not, parsing these sources of variance is essential to making accurate predictions.

Previous phenology models rely on temperature-dependent developmental rates to predict development time (developmental rate is the reciprocal of development time) [4, 17, 27, 34, 41]. Temperature-dependent phenology models are typically fit to data from laboratory experiments in which development time is measured at multiple constant temperatures. Bentz et al. [4] showed that fitting developmental rate curves to the reciprocal of laboratory development time data results in large errors when the curves are used to predict development time, especially at low temperatures. This error is due to transformation of the error variance that results from using the reciprocal of the laboratory data and does not occur when curves are fit directly to development time data. Within populations of insects whose phenology is under direct temperature control, developmental synchronization is attributed to long development times at cold temperatures [19]. Since developmental synchrony can be an important determinant of fitness, it is very important to accurately predict development time at low temperatures in these populations. Phenology models fit to laboratory development times rather than rates offer a clear advantage in this case due to greater accuracy at low temperatures.

In addition to fitting development time curves to laboratory development time data, our approach to modeling phenology is unique in that it is directly based on development time curves rather than developmental rate curves. Although curves were fit to development time data in [4] and subsequent studies (e.g. [27]), the phenology models developed in those papers were still based on the reciprocal curves (developmental rate curves), largely because rates fit more naturally into previous phenology modeling frameworks. In addition to necessitating transformation of laboratory data to parameterize the model, these rate-oriented phenology models require transformation of field data to obtain boundary conditions for simulations (e.g. [17]). In contrast, our parameters and initial conditions are directly related to laboratory and field measurements.

We take a maximum likelihood approach to determine parameters using constant temperature laboratory development time data for MPB. This is different than previous developmental parameterizations for MPB, in which a curve was fit directly to the median development rates or times at each constant temperature (e.g. [4, 27]). Using a maximum likelihood approach has two major advantages when fitting phenology models to laboratory development time data. First, temperatures at which fewer observations were made have less weight in fitting development time curve parameters. This is especially important if few observations are made at some temperatures, since fitting a development time curve directly to the median development times would give equal weight to these temperatures. Second, the maximum likelihood approach allows us to explicitly incorporate variation in development time and to simultaneously fit development time curve and variance parameters.

The MPB development time data that we use for model parameterization incorporate previously published data [4, 25, 27] as well as previously unpublished data that include development times at temperatures not observed in previous experiments.

We expect that inclusion of these new data will result in more accurate phenology predictions at these temperatures, especially in the teneral adult stage. Previous phenology models for MPB have assumed that development halts in this stage at temperatures below 17°C [27, 35]. New data show that development occurs at temperatures as low as 8°C in the teneral adult stage. This has important implications for MPB phenology. In particular, the warm developmental threshold in the teneral adult stage that was imposed in previous models may result in predictions of later emergence and more developmental synchrony than a model without this threshold.

In this paper we discuss how insect phenology depends on temperature and develop a model for tracking the development of an individual through a life stage. Next population phenology is modeled ignoring variation in development time using an advection equation. The model is extended to incorporate persistent variation by introducing a developmental phenotype that varies within a population; this phenotype is a parameter that scales the transient speed coefficient of the advection equation. Finally, random variation is incorporated into the model by adding a diffusion term, resulting in a Fokker-Planck development equation. The Fokker-Planck development equation is solved under constant temperatures and fit to development time data. The models are then used to simulate MPB phenology using phloem temperatures measured in the field and field counts of beetle attacks on successfully colonized lodgepole pine trees; the emergence distributions predicted by the phenology models are compared to emergence measured in the field.

3.2 Model development

3.2.1 Temperature-dependent individual phenology

We begin by developing a simple mathematical description of the temperature-dependent development of an individual insect through a single life stage. Let $\tau_i(T)$ be the time required for an individual to complete development through its i th life stage at constant temperature T . Development time is often U-shaped with a minimum at some developmentally optimal temperature (often $20 - 25^\circ\text{C}$) and increases at cooler and warmer temperatures [41, 45]. In practice, $\tau_i(T)$ is approximated by measuring development time at constant temperatures in a laboratory, then fitting an appropriate curve to the data [4, 24, 28]. Development time curves are used to predict phenology for insects under variable temperatures. Let $T(t)$ be the temperature at time t and $a(t)$ be the proportion of a life stage that an insect has completed at time t . Then a is between 0 and 1 and can be thought of as the insect's physiological age [24]. Since an insect takes $\tau_i(T)$ days to develop through the entire life stage at constant temperature T , the simplest developmental model predicts it will take $\Delta t = \tau_i(T)\Delta a$ days to develop through a fraction Δa of the life stage at that temperature. If the relationship $\Delta a/\Delta t = 1/\tau_i(T)$ holds for arbitrarily small values of Δt , i.e. $da/dt = 1/\tau_i(T(t))$, then development through stage i for an insect that began at time t_0 is described by the initial value problem

$$\frac{da}{dt} = \frac{1}{\tau_i(t)}, \quad a(t_0) = 0, \quad (3.1)$$

where $\tau_i(t) = \tau_i(T(t))$. The differential equation (3.1) is integrated to determine the insect's age at time t ,

$$a(t) = \int_{t_0}^t \frac{ds}{\tau_i(s)}.$$

Let $\Gamma_i(\Delta a, t)$ be the time that an insect completes Δa units of age given that it began at time t , defined by

$$\Delta a = \int_t^{\Gamma_i(\Delta a, t)} \frac{ds}{\tau_i(s)}. \quad (3.2)$$

Note that the time an insect will complete stage i if it began at time t is $\Gamma_i(1, t)$, and $\Gamma_i(0, t) = t$ for all times t . If the function Γ_i is known for each life stage for an individual, the timing of any developmental event (phenology) is completely determined for that insect.

3.2.2 Population phenology (no variation in development time)

The individual phenology model is extended to track phenology within a population of identical individuals. Let $p(a, t)$ be the density of individuals achieving age a at time t , so $\int_{t_1}^{t_2} p(a, t) dt$ is the number of individuals achieving age a between times t_1 and t_2 . We will show that development of a population with no developmental variation satisfies the advection equation

$$\frac{\partial}{\partial a} p(a, t) + \frac{\partial}{\partial t} [\tau_i(t) p(a, t)] = 0. \quad (3.3)$$

Since an individual develops from age a at time t to age $a + \Delta a$ at time $\Gamma_i(\Delta a, t)$, we expect the same number of individuals to achieve age $a + \Delta a$ between times $\Gamma_i(\Delta a, t_1)$ and $\Gamma_i(\Delta a, t_2)$ as achieved age a between time t_1 and t_2 if there is no mortality during development. This results in the conservation law

$$\int_{t_1}^{t_2} p(a, s) ds = \int_{\Gamma_i(\Delta a, t_1)}^{\Gamma_i(\Delta a, t_2)} p(a + \Delta a, s) ds, \quad (3.4)$$

which holds for all choices of Δa such that $0 \leq a + \Delta a \leq 1$. Changing variables gives

$$\int_{t_1}^{t_2} p(a, s) ds = \int_{t_1}^{t_2} p(a + \Delta a, \Gamma_i(\Delta a, s)) \frac{\partial}{\partial t} [\Gamma_i(\Delta a, s)] ds.$$

Since this holds for all choices of t_1 and t_2 , it follows that

$$p(a, t) = p(a + \Delta a, \Gamma_i(\Delta a, t)) \frac{\partial}{\partial t} [\Gamma_i(\Delta a, t)]. \quad (3.5)$$

Note that differentiating (3.2) with respect to t and solving for the time derivative yields

$$\frac{\partial}{\partial t} [\Gamma_i(\Delta a, t)] = \frac{\tau_i(\Gamma_i(\Delta a, t))}{\tau_i(t)}.$$

Consequently, the conservation law (3.5) can be rewritten as

$$\tau_i(t)p(a, t) = \tau_i(\Gamma_i(\Delta a, t))p(a + \Delta a, \Gamma_i(\Delta a, t)). \quad (3.6)$$

This implies that the product of development time and population density is constant along the characteristic curves $t(a) = \Gamma_i(a, t_0)$, where t_0 is any stage initiation time.

To derive the developmental advection equation (3.3), we differentiate (3.6) with respect to Δa giving

$$\begin{aligned} 0 &= \tau_i(\Gamma_i(\Delta a, t)) \frac{\partial}{\partial a} [p(a, \Gamma_i(\Delta a, t))] \Big|_{a=a+\Delta a} \\ &\quad + \frac{\partial}{\partial t} [\tau_i(t)p(a + \Delta a, t)] \Big|_{t=\Gamma_i(\Delta a, t)} \frac{\partial}{\partial \Delta a} [\Gamma_i(\Delta a, t)]. \end{aligned} \quad (3.7)$$

Differentiating (3.2) with respect to Δa and solving for the derivative yields

$$\frac{\partial}{\partial \Delta a} [\Gamma_i(\Delta a, t)] = \tau_i(\Gamma_i(\Delta a, t)).$$

Hence, (3.7) can be rewritten as

$$\frac{\partial}{\partial a} [p(a, \Gamma_i(\Delta a, t))] \Big|_{a=a+\Delta a} + \frac{\partial}{\partial t} [\tau_i(t)p(a + \Delta a, t)] \Big|_{t=\Gamma_i(\Delta a, t)} = 0.$$

Setting $\Delta a = 0$ (recall $\Gamma_i(0, t) = t$) gives the developmental advection equation (3.3),

$$\frac{\partial}{\partial a} p(a, t) + \frac{\partial}{\partial t} [\tau_i(t)p(a, t)] = 0.$$

3.2.3 Persistent variation

We model persistent variation in development time by scaling a base temperature-dependent development time curve by a parameter α that varies within a population. If $\tau_i(T)$ is the base development time curve for stage i , then an individual with phenotype α has development time $\alpha\tau_i(T)$. This is consistent with the model of developmental variation presented in Chapter 2. We assume each individual maintains its phenotype throughout the life stage, which is consistent with our definition of persistent variation. Consequently, an advection equation similar to (3.3) describes the development of individuals with phenotype α ,

$$\frac{\partial}{\partial a} p(a, t; \alpha) + \frac{\partial}{\partial t} [\alpha\tau_i(t)p(a, t; \alpha)] = 0. \quad (3.8)$$

In this case, $p(a, t; \alpha)$ is the density of individuals with phenotype α achieving age a at time t .

In practice we assume some distribution of phenotypes in the population $f(\alpha)$, which is either fit to laboratory data or allowed to evolve. Tracking α explicitly allows us to monitor the temporal distribution of phenotypes in a population, an important feature for studying the evolution of phenology.

3.2.4 Random variation

We model the effect of random environmental variation on population phenology by adding a diffusion term to the advection equation (3.8). The result is a Fokker-Planck equation [16, 32], which we derive from first principles,

$$\frac{\partial}{\partial a}p(a, t; \alpha) + \frac{\partial}{\partial t}[\alpha\tau_i(t)p(a, t; \alpha)] = \frac{\nu}{2} \frac{\partial^2}{\partial t^2}p(a, t; \alpha). \quad (3.9)$$

This model arises because individuals with the same phenotype may develop at different rates due to random differences in environmental conditions. Equation (3.9) along with knowledge of how α is distributed within a population allows us to predict phenology in the presence of persistent and random developmental variation.

Derivation of the age-oriented Fokker-Planck development equation

We consider individuals with a single phenotype α and attempt to describe developmental variation among individuals with that phenotype. Dependence of p on α is suppressed to simplify notation in this and the following section. Hence, $p(a, t)$ is a probability density function giving the probability that an individual insect (with phenotype α) achieves age a at time t .

We derive the Fokker-Planck equation following Risken [37]. Define $K(a_1, t_1|a_0, t_0)$ to be the transition probability density function describing the probability that an individual will be age a_1 at time t_1 given that it was age a_0 at time t_0 . If development is a Markov process, i.e. the distribution of times that any age is achieved is completely determined by the distribution times that any previous age is achieved (no memory effects), then the distribution of times for age a determines the distribution

of times at some later age $a + \Delta a$,

$$p(a + \Delta a, t) = \int_{-\infty}^{+\infty} K(a + \Delta a, t|a, t')p(a, t')dt'. \quad (3.10)$$

Define the n th moment of K at age a and time t' to be

$$M_n(a, \Delta a, t') = \int_{-\infty}^{+\infty} (t - t')^n K(a + \Delta a, t|a, t')dt.$$

For example, $M_1(a, \Delta a, t')$ is the mean time required to age from a to $a + \Delta a$ for an individual that is age a at time t' . We change variables in (3.10), letting $\tau = t - t'$, and expand the integrand in a Taylor series,

$$p(a + \Delta a, t) = \sum_{n=0}^{\infty} \frac{1}{n!} \left(-\frac{\partial}{\partial t} \right)^n p(a, t) \int_{-\infty}^{+\infty} \tau^n K(a + \Delta a, t + \tau|a, t)d\tau \quad (3.11)$$

Reversing the change of variables reveals that the integrals on the right hand side are moments of K . Noting that the 0th moment is unity, (3.11) becomes

$$p(a + \Delta a, t) - p(a, t) = \sum_{n=1}^{\infty} \frac{1}{n!} \left(-\frac{\partial}{\partial t} \right)^n p(a, t) M_n(a, \Delta a, t). \quad (3.12)$$

Applying Taylor's theorem again,

$$p(a + \Delta a, t) - p(a, t) = \Delta a \frac{\partial}{\partial a} p(a, t) + O(\Delta a^2),$$

and substituting into (3.12) yields,

$$\Delta a \frac{\partial}{\partial a} p(a, t) + O(\Delta a^2) = \sum_{n=1}^{\infty} \frac{1}{n!} \left(-\frac{\partial}{\partial t} \right)^n p(a, t) M_n(a, \Delta a, t). \quad (3.13)$$

Each moment is also expanded in a Taylor series,

$$M_n(a, \Delta a, t) = \Delta a \left. \frac{\partial}{\partial \Delta a} [M_n(a, \Delta a, t)] \right|_{\Delta a=0} + O(\Delta a^2). \quad (3.14)$$

Here we used the fact that $M_n(a, 0, t) = 0$. Define

$$D^{(n)}(a, t) = \left. \frac{\partial}{\partial \Delta a} [M_n(a, \Delta a, t)] \right|_{\Delta a=0}.$$

Then, from (3.14),

$$M_n(a, \Delta a, t) = \Delta a D^{(n)}(a, t) + O(\Delta a^2). \quad (3.15)$$

Substituting this into (3.13), dividing by Δa , then taking the limit as Δa approaches 0, gives the Kramers-Moyal expansion [22, 30],

$$\frac{\partial}{\partial a} p(a, t) = \sum_{n=1}^{\infty} \frac{1}{n!} \left(-\frac{\partial}{\partial t} \right)^n [D^{(n)}(a, t) p(a, t)]. \quad (3.16)$$

The series is truncated after two terms to obtain the one-dimensional Fokker-Planck equation,

$$\frac{\partial}{\partial a} p(a, t) = -\frac{\partial}{\partial t} [D^{(1)}(a, t) p(a, t)] + \frac{1}{2} \frac{\partial^2}{\partial t^2} [D^{(2)}(a, t) p(a, t)]. \quad (3.17)$$

Note that if we set $D^{(2)}(a, t) = 0$, then (3.17) becomes an advection equation. Hence, the Fokker-Planck equation (3.17) with $D^{(2)}(a, t) = 0$ should be identical to the advection phenology model (3.3) if development progresses at a rate that depends on temperature alone (the same assumption that was made in the deriving the advection model (3.3)). So, by extension, we set $D^{(1)}(a, t) = \tau_i(t)$. For simplicity, we assume that $D^{(2)}(a, t)$ is constant, and set $D^{(2)}(a, t) = \nu$. We show in §3.3 that ν is the

variance in development time at constant temperature. Substituting $\tau_i(t)$ and ν for the coefficients in (3.17) and reinstating dependence of p on α gives the Fokker-Planck development equation (FPDE),

$$\frac{\partial}{\partial a}p(a, t; \alpha) + \frac{\partial}{\partial t}[\alpha\tau_i(t)p(a, t; \alpha)] = \frac{\nu}{2}\frac{\partial^2}{\partial t^2}p(a, t; \alpha).$$

3.2.5 Summary of phenology models

We have derived three population phenology models, each incorporating different levels of developmental variation. The simplest model does not account for variation in development time. In this case, development is described by an advection equation,

$$\frac{\partial}{\partial a}p(a, t) + \frac{\partial}{\partial t}[\tau_i(t)p(a, t)] = 0.$$

This model is easily extended to account for persistent variation in development time by introducing the phenotype α that scales the base development time curve. This phenotype has some distribution within the population. In this case, development is described by an α -dependent advection equation,

$$\frac{\partial}{\partial a}p(a, t; \alpha) + \frac{\partial}{\partial t}[\alpha\tau_i(t)p(a, t; \alpha)] = 0.$$

Note that if every individual in the population has phenotype $\alpha = 1$, then this model reduces to the simpler advection model. Finally, additional developmental variation due to random effects is incorporated into a phenology model by adding diffusion term to the previous model. The result is the most complex of the three population phenology models, the Fokker-Planck development equation,

$$\frac{\partial}{\partial a}p(a, t; \alpha) + \frac{\partial}{\partial t}[\alpha\tau_i(t)p(a, t; \alpha)] = \frac{\nu}{2}\frac{\partial^2}{\partial t^2}p(a, t; \alpha).$$

In the case that every individual with phenotype α has the same development time (i.e. $\nu = 0$), then the Fokker-Planck development equation becomes the α -dependent advection equation. Hence, the three models are nested.

For both the advection and the phenotype-dependent advection models, the distribution of times that insects will complete a stage can be determined analytically if the distribution of times that begin the stage is known. Unfortunately, a similar solution has not been found for the Fokker-Planck development equation under varying temperature conditions.

3.3 Constant temperature solution

Laboratory development experiments are often carried out at constant temperatures [15, 28, 45]. A cohort of insects is held at a constant temperature, and the length of time required for each individual to complete the life stage is recorded. The experiment is repeated for other cohorts at multiple constant temperatures resulting in data that show how development time depends on temperature and how that response varies within the sample group of insects. Solving the FPDE at constant temperatures (constant coefficients) and assuming normality of the distribution of phenotypes within a cohort allows us to fit the nested phenology models to experimental data. Since each individual in a cohort begins the stage at the same time ($t = 0$) the FPDE is solved with the initial condition $p(0, t; \alpha) = f(\alpha)\delta(t)$, where $f(\alpha)$ is the distribution of phenotypes in the cohort, given by

$$f(\alpha) = \frac{N}{\sqrt{2\pi\sigma^2}} \exp\left[-\frac{(\alpha - \mu)^2}{2\sigma^2}\right], \quad (3.18)$$

and $\delta(t)$ is the delta distribution.

To solve the FPDE (3.9) at constant temperature T , we make the variable changes $z = t - \alpha\tau_i(T)a$ and $q(a, z; \alpha) = p(a, z + \alpha\tau_i(T)a; \alpha)$. Then (3.9) becomes a diffusion equation, and the initial condition is unchanged,

$$\frac{\partial}{\partial a}q(a, z; \alpha) = \frac{\nu}{2} \frac{\partial^2}{\partial z^2}[q(a, z; \alpha)], \quad (3.19)$$

$$q(0, z; \alpha) = f(\alpha)\delta(z). \quad (3.20)$$

The solution of this equation is

$$q(a, z; \alpha) = \frac{f(\alpha)}{\sqrt{2\pi\nu a}} \exp\left[-\frac{z^2}{2\nu a}\right].$$

Reversing the change of variables,

$$p(a, t; \alpha) = \frac{f(\alpha)}{\sqrt{2\pi\nu a}} \exp\left[-\frac{(t - \alpha\tau_i(T)a)^2}{2\nu a}\right].$$

Consequently, the distribution of stage completion times ($a = 1$) for individuals with phenotype α , given an initial pulse of $f(\alpha)$ insects entering the at $t = 0$, is normally distributed with mean τ_i and variance ν ,

$$p(1, t; \alpha) = \frac{f(\alpha)}{\sqrt{2\pi\nu}} \exp\left[-\frac{(t - \alpha\tau_i(T))^2}{2\nu}\right]. \quad (3.21)$$

Stage completion times are measured in the laboratory, but phenotypes cannot typically be measured directly. The distribution of completion times is

$$E(t) = \int_{-\infty}^{\infty} p(1, t; \alpha) d\alpha.$$

From (3.21) and (3.18), it follows that the distribution of stage completion times is

$$E(t) = \frac{N}{\sqrt{4\pi^2\nu\sigma^2}} \int_{-\infty}^{\infty} \exp \left[-\frac{(\alpha - \mu)^2}{2\sigma^2} - \frac{(t - \alpha\tau_i(T))^2}{2\nu} \right] d\alpha.$$

Upon integration, we obtain

$$E(t) = \frac{N}{\sqrt{2\pi(\nu + \sigma^2\tau_i(T)^2)}} \exp \left[-\frac{(t - \mu\tau_i(T))^2}{2(\nu + \sigma^2\tau_i(T)^2)} \right]. \quad (3.22)$$

Hence, the model predicts development time at constant temperature T to be normally distributed with mean $\mu\tau_i(T)$ and variance $\nu + \sigma^2\tau_i(T)^2$. The fact that the mean development time is the product of the mean phenotype and the base development time is no surprise. It is more interesting that the variance in development time is the sum of the variance contributed by random variation in development time and the product of the square of the base development time and the persistent variance. This means that as development time increases so does its variance, a pattern that is observed in experimental data (see Figure 3.1).

3.4 Mountain pine beetle parameter estimation

We fit development time curves $\tau_i(T)$ and variance parameters ν and σ^2 to development time data for each stage of the MPB life cycle. The MPB life cycle consists of seven developmental stages and an ovipositional stage. MPB eggs are oviposited in vertical galleries beneath the bark of host trees. Ovipositional females construct egg galleries at a rate that depends on temperature [2], so that the oviposition times of a single female's eggs are distributed in time and temperature-dependent. The next seven developmental stages, including egg, four larval instars, pupa, and teneral adult, also occur beneath the bark of host trees. At the completion of the teneral

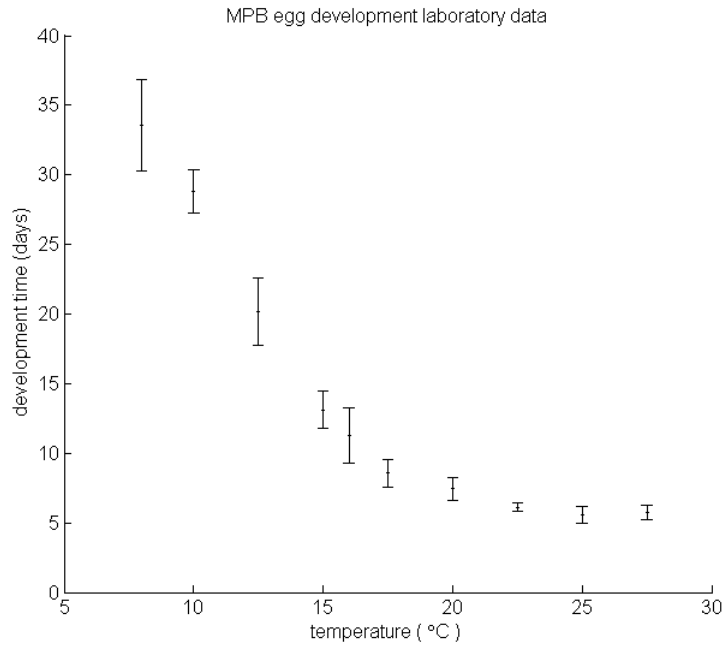


Fig. 3.1: Mean MPB egg development times measured at various constant temperatures. Error bars indicate \pm one standard deviation. Notice that the standard deviation of development time generally increases with development time.

adult stage, beetles emerge to attack new hosts, mate, and begin ovipositing the next generation.

The dependence of development time on temperature is well-studied for MPB. Development time has been measured in constant temperature laboratory experiments for each of the seven MPB developmental stages [4, 25]. Individuals from populations in central Idaho and northern Utah were collected from multiple trees in the field and reared at various constant temperatures. The time necessary for each individual to complete each developmental stage (development time) was recorded. Details of the experimental methods are given in [4]. These experiments were carried out between 1982 and 2005. Roughly 75% of the developmental data that we used to parameterize the phenology models presented in this paper were previously published by Logan and Amman [25], Bentz et al. [4], and in subsequent studies (e.g. [27]).

The remaining 25% of the data (collected in 2005) were not previously published. Most notably, these new data include development times for MPB teneral adults at 8, 12, and 15°C; previous phenology models for MPB have assumed that teneral adults cannot develop at these temperatures [27, 35]. Laboratory populations were usually observed daily during development experiments, so the number of insects that completed development through a stage between observation times are known. Since these experiments measured the development time of multiple individuals at constant temperature in each stage, the data are useful in estimating the variance structure of development time. The rate of egg gallery construction (cm/day) at different constant temperatures has also been measured in the laboratory [2].

For each developmental stage we simultaneously fit a development time curve and variance parameters to development time data from constant temperature laboratory experiments. The development time curve was either the sum of decreasing and increasing exponentials,

$$\tau_i(T) = c_1 + \exp[c_2 - c_3T] + \exp[c_4 + c_5T], \quad (3.23)$$

where c_3 and c_5 are positive, or a decreasing exponential,

$$\tau_i(T) = c_1 + \exp[c_2 - c_3T], \quad (3.24)$$

where c_1 and c_3 are positive. The first curve (3.23) captures the U-shaped dependence of development time on temperature that is often observed in insects [41, 45], while the second (3.24) is useful when the data do not support an increase in development time at high temperatures.

We take a maximum likelihood approach to fitting developmental parameters to laboratory data. To derive the likelihood function, a normal distribution of pheno-

types is assumed with mean $\mu = 1$ and variance σ^2 , so stage completion times are modeled by (3.22). In this case, $q_{i,j}$, the probability of a beetle completing a particular stage at the j th constant temperature T_j between observation times $t_{i,j}$ and $t_{i-1,j}$, is given by

$$q_{i,j} = \int_{t_{i-1,j}}^{t_{i,j}} \frac{1}{\sqrt{2\pi(\nu + \sigma^2\tau(T_j)^2)}} \exp\left[-\frac{(t - \mu\tau(T_j))^2}{2(\nu + \sigma^2\tau(T_j)^2)}\right] dt, \quad (3.25)$$

if the base development time curve $\tau(T)$ and the variance parameters σ^2 and ν are known. In practice these are unknown, so $q_{i,j}$ depends on the five development time curve parameters, c_1 through c_5 , and the variance parameters, i.e. $q_{i,j} = q_{i,j}(\theta)$, where

$$\theta = [c_1, c_2, c_3, c_4, c_5, \sigma^2, \nu].$$

If $n_{i,j}$ is the number of beetles completing a stage between observation times $t_{i,j}$ and $t_{i-1,j}$ at constant temperature T_j , then the probability of observing a particular completion time distribution in the laboratory, $\{n_{1,j}, n_{2,j}, \dots, n_{N_j,j}\}$, where N_j is the number of times that observations were made at constant temperature T_j , is given by the multinomial distribution

$$Q_j(n_{1,j}, n_{2,j}, \dots, n_{N_j,j}; \theta) = \frac{m_j!}{\prod_{i=1}^{N_j} n_{i,j}!} \prod_{i=1}^{N_j} (q_{i,j}(\theta))^{n_{i,j}},$$

where m_j is the total number of observations at temperature T_j . Since development times of the different groups exposed to different constant temperatures in the laboratory are independent of each other, the probability of observing a particular complete set of emergence times (i.e. at all temperatures) is given by the product of the Q_j 's taken over all of the temperatures at which observations were made. Hence, the negative log-likelihood of the parameter vector θ , given the array of observed completion

counts $\{n_{1,j}, n_{2,j}, \dots, n_{N_j,j}\}$, for $j = 1 \dots J$ (J is the number of temperatures), is

$$LL(\theta) = - \sum_{j=1}^J \left[\log(m_j!) + \sum_{i=1}^{N_j} (n_{i,j} \log(q_{i,j}(\theta)) - \log(n_{i,j}!)) \right]. \quad (3.26)$$

The development time curve parameters and variance parameters were fit for each stage by minimizing the negative log-likelihood function with respect to θ using standard optimization tools in MATLAB. For some life stages we failed to reject simpler developmental models in favor of models with additional parameters using the likelihood ratio test with 5% significance level. If the more complicated U-shaped development time curve (3.23) did not result in a better fit than the less complicated decreasing development time curve (3.24), the simpler curve was chosen. In some stages $c_1 \neq 0$ did not provide a better fit, so we set $c_1 = 0$. Most importantly, $\nu > 0$ did not improve the fit in most stages; in these we set $\nu = 0$. The parameters that minimized the negative log-likelihood function are shown in table 3.1 for all of the MPB developmental stages. The corresponding development time curves are shown in Figure 3.3 along with the mean development times measured in the laboratory experiments. Figure 3.2 also shows the observed standard deviation in development time and the predicted standard deviation in development time for MPB eggs. These development time curve parameterizations can be applied to all three of the population phenology models, since in the two simplest models, the extraneous variance parameters can be treated as nuisance parameters.

It is important to note that in all but the fourth larval instar, incorporating random variance ($\nu > 0$) did not improve the fit of the model, and in that stage ν was extremely small. This suggests that random variation in temperature and other environmental factors that affect development time in the laboratory (e.g. variation in phloem thickness) were well controlled in the developmental experiments for MPB and

Table 3.1: Parameterization for MPB development time curves and variance parameters for each life stage (egg-teneral adult(TA)). $L1 - L4$ indicate larval instars 1-4. These parameters were fit to data from constant-temperature laboratory experiments. The parameterization for MPB burrowing time curve is also shown (OA). These parameters were also fit to data from constant-temperature laboratory experiments. The negative log-likelihood (LL) is shown for the best fit parameters. In the cases that 5 development time parameters (c_i) are listed, the development time curve was the sum of decreasing and increasing exponential functions. In the cases that 3 development time parameters are listed, the development time curve was a decreasing exponential function. Note that in all developmental stages but the fourth larval instar, incorporating a diffusion term (random variation) did not improve the fit.

stage	c_1	c_2	c_3	c_4	c_5	σ^2	ν	LL
egg	0	4.802	0.154	-2.573	0.139	0.017	0	188
L1	-18.01	4.961	0.133	0.850	0.074	0.232	0	248
L2	4.744	9.196	0.499	-	-	0.324	0	185
L3	0.016	6.670	0.244	-12.334	0.553	0.237	0	145
L4	0	5.332	0.149	-18.386	0.799	0.129	0.006	108
pupa	4.240	10.577	0.509	-	-	0.030	0	92.7
TA	0	5.260	0.113	-	-	0.343	0	258
OA	0	1.003	0.085	-	-	-	0.057	-0.475

that most of the variance observed in laboratory development time can be attributed to persistent sources (e.g. genetic variation).

We used a similar method to fit a negative exponential model (3.24) to the time required for an ovipositional adult to construct 1 cm of gallery at different constant temperatures. However, in this case variance in burrowing time was not strongly related to the magnitude of burrowing time (Figure 3.4), so a normal distribution with mean $\tau_i(T)$ and variance ν was used to model the probability of observing a particular burrowing time. The resulting parameterization is shown in table 3.1, and the burrowing time curve is shown in Figure 3.4.

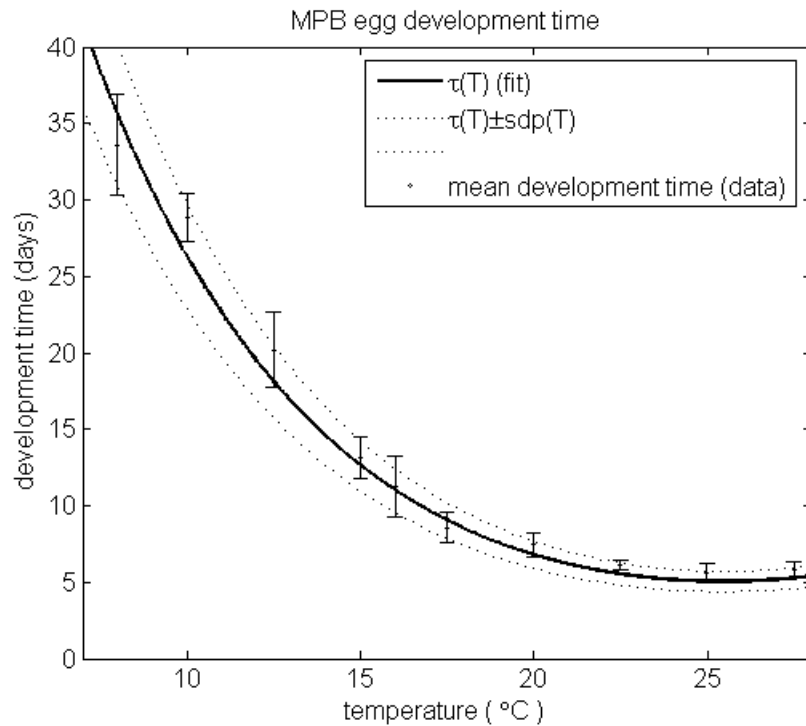


Fig. 3.2: Base development time curve fit to MPB egg development times measured at various constant temperatures (solid curve). Base development time \pm the predicted standard deviation of development time (sdp) is also plotted (dotted curves). Observed mean development times are plotted (dots), as well as error bars indicating \pm one standard deviation about the sample mean. Note that the likelihood fitting procedure employed here does not fit curves directly to mean development times (see text).

3.5 Simulation of MPB phenology and comparison to field data

3.5.1 Field data

In early June of both 2001 and 2002 seven approximately 30cm DBH trees were selected at two sites in the Sawtooth National Recreation Area of central Idaho, at the headwaters of the Salmon River. This region had recently experienced an outbreak of MPB population (see [35]). Selected trees were in apparent good health, with no broken limbs, significant damage to the bole, or obvious symptoms of disease. Trees

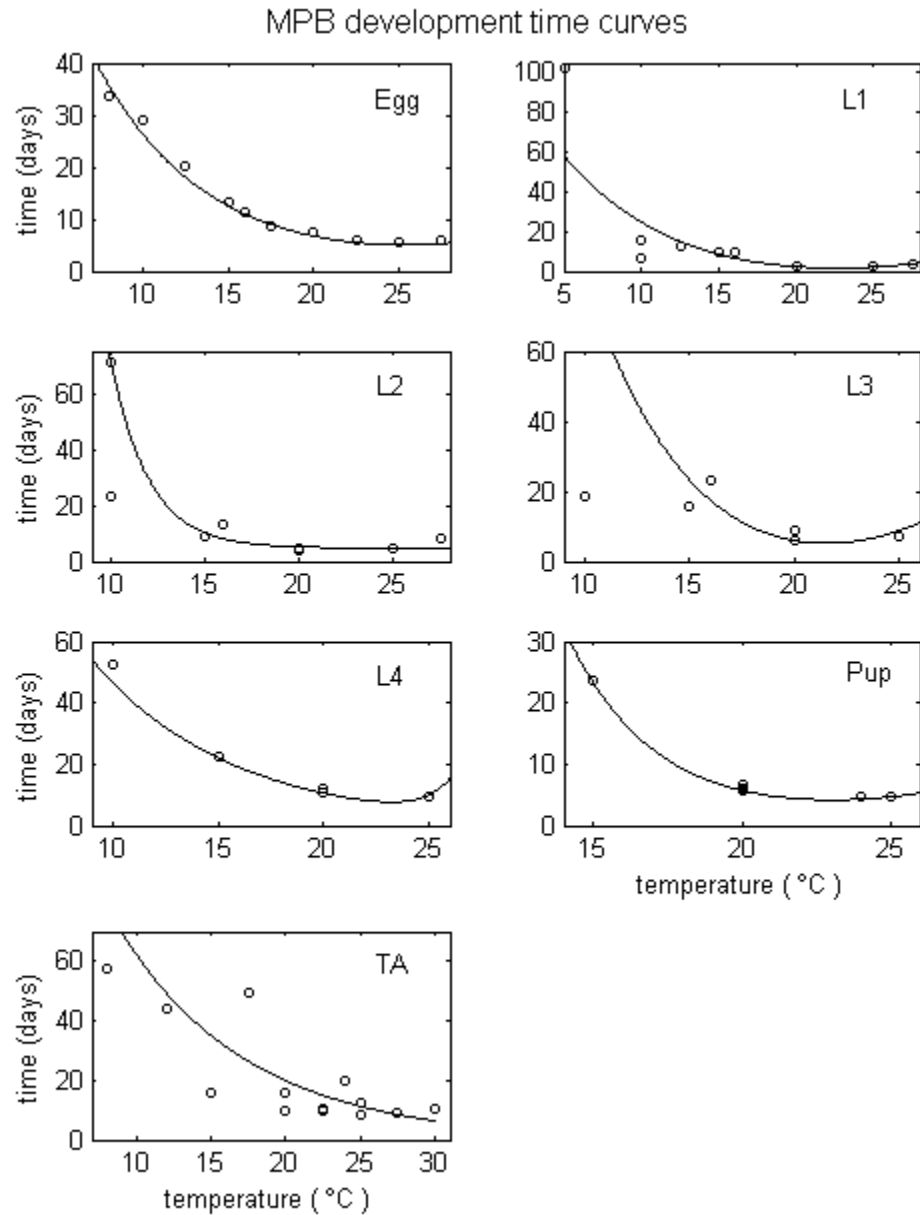


Fig. 3.3: Base development time curves fit to MPB development times for each developmental stage. Two means were plotted when there were two separate development experiments performed at the same temperature. Note that the likelihood fitting procedure employed here does not fit curves directly to mean development times (see text). The means are not equally weighted by the fitting algorithm. For example, the mean development time for the third larval instar at 10°C has relatively little weight in the fit, because four beetles were observed at that temperature, whereas 29 and 42 beetles were observed at 16°C and 20°C .

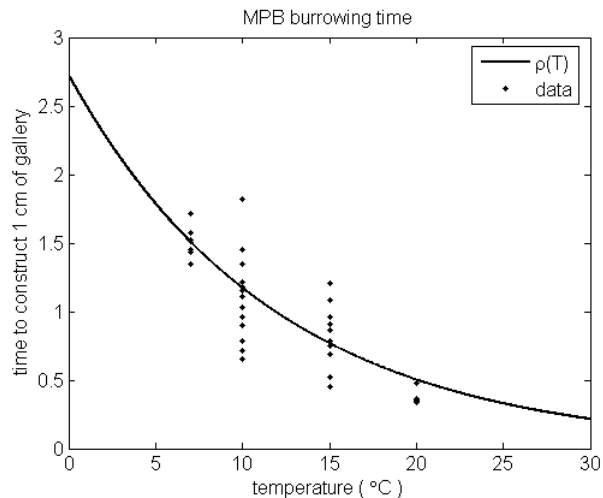


Fig. 3.4: Burrowing time curve $\rho(T)$ for MPB ovipositional adult (solid curve) fit to burrowing times measured in constant-temperature laboratory experiments (dots). Burrowing time is the time necessary for a MPB female to construct one centimeter of gallery at a given temperature.

were all partially shaded, sheltered by nearby trees but near the edge of stands for ease of access. Study locations were at approximately 2100 meters in elevation.

Thermocouples were inserted into the phloem at 4 feet above ground level on both northern and southern aspects of each tree. Temperature data from the phloem were recorded hourly (see [3] for details of phloem temperature monitoring techniques). Fourteen months later the data was downloaded, giving a complete picture of temperatures in the developmental environment under the bark (e.g. Figure 3.5).

On each tree a counting area was taped off between two feet and six feet above ground level, after which each tree was baited with a pheromone lure (Pherotech, Inc.). The pheromone lure remained on the tree until four successful attacks were recorded in the counting area, at which point the lure was removed. Each day thereafter the census area was inspected for new attacks; stick pins of differing colors were inserted next to each burrow during each count to avoid repeat counting. Daily

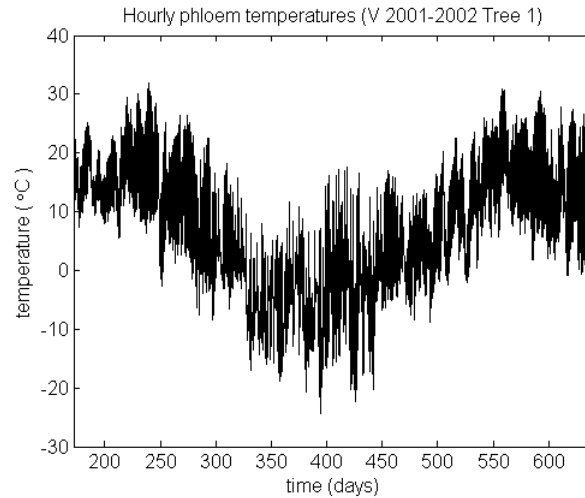


Fig. 3.5: Average of north and south side temperatures measured hourly in the phloem of tree 1 at site V from 2001 until 2002.

counts were continued until no new attacks appeared for three days, after which trees were inspected on a weekly basis.

In fall the entire census area was enclosed in rectangular nylon mesh emergence cages (see [3] for details). Bark at cage edges was shaved to even the surface and the cages continuously stapled to the bark around their perimeter to keep beetles from escaping. Each cage had a funnel base leading to a collection bottle. In the subsequent year emerging MPB were collected in the catch tubes and counted every two days. Thus, for several trees over two years we collected input and output distributions and temperatures controlling development times underneath the bark – all the data necessary for validation of the distributional models above.

3.5.2 Simulations

We used the phenotype-dependent advection model parameterized with data from constant-temperature laboratory experiments (table 3.1) to simulate MPB phenology under the temperature conditions measured in each of the seven trees ob-

served in the field. The simpler phenotype-dependent advection model was chosen over the FPDE for two reasons. First, incorporating random variance in the FPDE did not improve fits to laboratory data. Second, even without the diffusion term, the phenotype-dependent advection model tended to over-predict variance in a single tree under field conditions. Simulations were performed with the average of north and south side phloem temperatures measured at each of the seven trees. Initial conditions for the simulations were the attack time distributions counted at the same trees. The phenology model was used to predict emergence time distributions for each tree, and the results were compared to the observed emergence time distributions.

Successful attack of a host tree is followed by initiation of egg gallery construction. We assume that 20 female eggs are laid in each gallery, a number that is consistent with MPB field demographic data [36]. Eggs were laid at a rate of 1 female egg per centimeter within the gallery [36]. The position of the median egg was chosen to fit the mean predicted oviposition times to the observed means for the 7 trees at which data were collected, giving 70cm as the position of the median egg, although the median egg in the field is likely laid significantly earlier. Temperature-dependent burrowing was simulated one centimeter at a time using the advection model with no variance (3.3) with the burrowing time curve shown in Figure 3.4 and initial condition given by the measured attack time distribution. This resulted in a distribution of completion times for each of the 20 centimeters of gallery in which a female egg was laid after an observed attack on a tree. These distributions were summed to obtain an oviposition time distribution for the entire tree.

Following oviposition, development was simulated consecutively through each developmental stage (egg through teneral adult) using the phenotype-dependent population phenology model. The initial condition for each stage was the completion time distribution from the previous stage. The initial distribution of phenotypes (α 's) was

assumed to be normal with mean 1 and variance σ^2 , parameterized using data from constant-temperature laboratory experiments (see table 3.1). There was no temporal structure in phenotypes at the beginning of each stage and the distributions of phenotypes in different stages were assumed to be independent. Temperatures used in the simulation models were the average of north and south side temperatures measured hourly at each tree. We used a finite volume characteristic method (described in the appendix) with 1 age step per stage to solve the phenotype-dependent advection equation (3.8). Solving the partial differential equations, the population distributions were tracked using a daily temporal discretization, although characteristics were computed using hourly temperatures. The equations were solved at each of 50 equally spaced α -nodes ranging from 0.04 to 2.0. The resulting stage completion time distributions at each phenotype node were summed with weights according to the initial phenotype distribution to obtain a phenotype-independent completion time distribution. This distribution became the initial condition for the next developmental stage.

The predicted emergence distributions and the observed emergence distributions are plotted in Figure 3.6 for all seven trees. The models generally over-predicted the emergence time variance. Although the position of the median egg within the egg galleries was chosen to fit the predicted mean emergence time to the observed mean emergence time, the agreement between the predicted and observed means is still notable. Since the value of this parameter was chosen to fit the means to the data for all seven tree simultaneously, it is significant that the predicted mean emergence times fit the mean observed emergence times at each tree fairly well (see Figure 3.6).

3.6 Discussion and conclusion

Our results suggest that the phenotype-dependent advection model (3.8) provides the best description of MPB phenology in the laboratory and in single trees

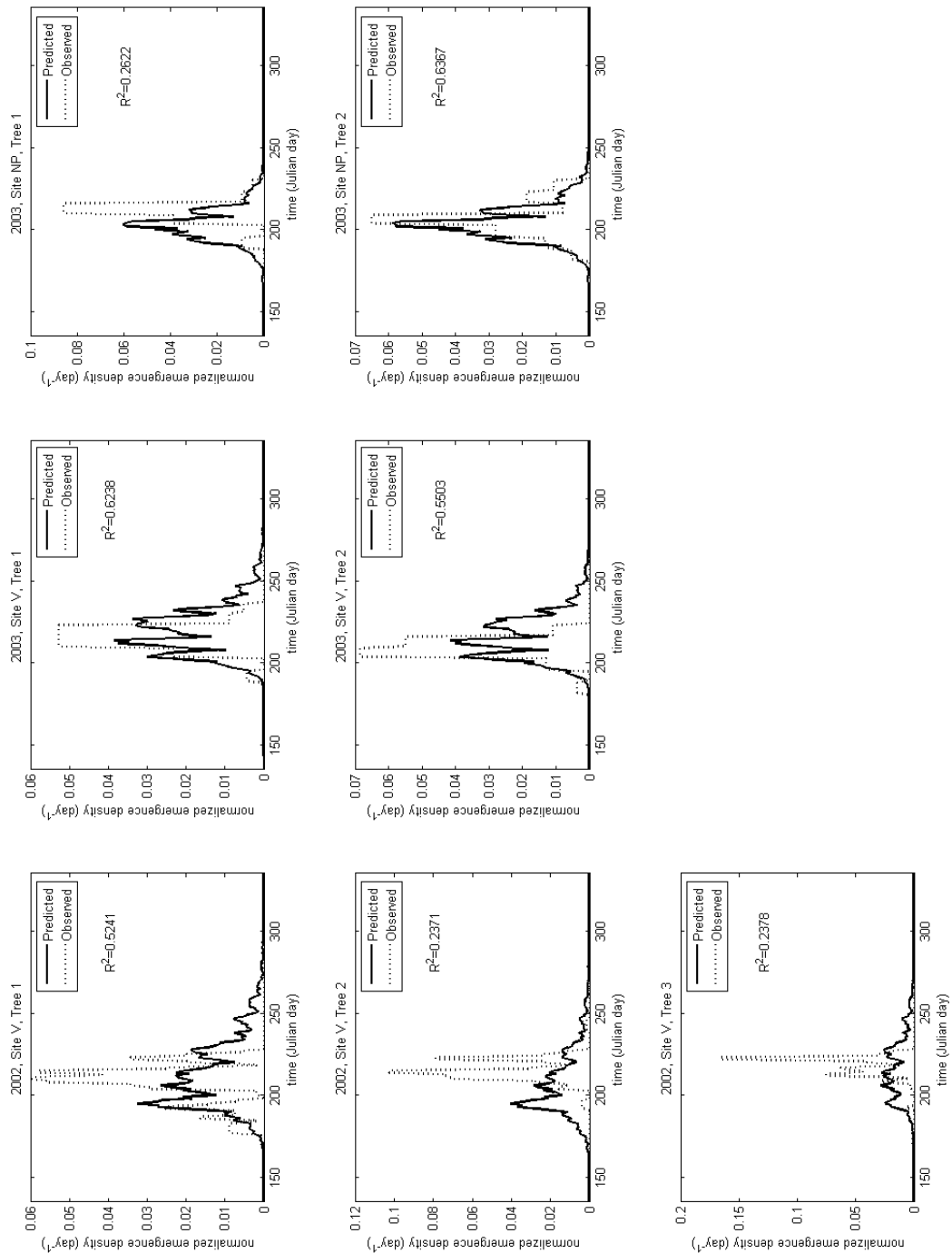


Fig. 3.6: Plots of predicted (solid) and observed (dotted) emergence distributions for seven trees from central Idaho in 2002 and 2003, along with R^2 values. Data was collected at 2 sites, V and NP, where hourly phloem temperatures, attack time distributions and emergence time distributions were measured. Predicted emergence time distributions were obtained using the phenotype-dependent advection model. Note that the position of the median egg in the egg gallery was chosen to fit the mean emergence time predictions to the observed means.

in the field. This model accurately represents the variance structure of development times from constant temperature laboratory experiments, and the incorporation of a diffusion term (resulting in the FPDE model (3.9)) does not significantly improve the fit. It is also clear from the simulation results that incorporating additional (random) variation would worsen agreement between emergence time predictions and observations at single trees in the field, because the phenotype-dependent advection model generally over-predicts variance in the field.

There are several reasons that the phenotype-dependent advection model, parameterized using laboratory development time data, might over-predict variation in the field for MPB. The model does not allow for interactions between individuals beneath the bark of the host that may act to synchronize emergence. Also, it is likely that mountain pine beetles do not enter the pupal stage until phloem temperatures exceed a specific temperature threshold (Barbara Bentz, personal communication April 21, 2009); this threshold is not incorporated into the phenology model but could act to synchronize emergence. Finally, the phenology model does not account for mortality beneath the bark of the tree, which may reduce field emergence densities, especially in the tails of the emergence distribution due to sampling effects.

Incorporating new development time data for MPB teneral adults in parameterizing the phenology models caused the time required to develop through that stage to be significantly shorter than in previous MPB phenology simulations using field temperatures. As a consequence, it was necessary to let oviposition occur farther down the egg gallery than in previous simulations. It may not be realistic for MPB to lay their median egg in the 70th centimeter of the gallery. This suggests that further investigation of temperature dependent development of MPB may be required, particularly in the teneral adult stage.

Solving the phenotype-dependent advection equation is much simpler than solving the more complicated FPDE or phenology models that rely on a diffusion term alone to capture developmental variation, such as the extended von Foerster equation presented in [17]. Although the phenotype-dependent advection equation, the FPDE, and other diffusion models can be solved analytically at constant temperatures, only the phenotype-dependent advection equation has been solved analytically at varying temperatures. Furthermore, the phenotype-dependent advection equation is much simpler to solve numerically under varying temperatures than diffusion-based phenology models. The phenotype-dependent advection model is the differential form of a conservation law; the integral form of this law (7.4) can be used directly for numerical solution of the model (see Appendix). Diffusion-based phenology models must be solved using more complicated numerical schemes, typically requiring much more computation time.

The phenotype-dependent advection model also offers flexibility in describing the shape of the distribution of development times. Throughout this paper we have assumed that phenotypes are normally distributed within a population at the beginning of a life-stage. This assumption can be easily modified without affecting the analytical or numerical solvability of the equation. For example, it may be desirable to use a phenotype distribution with positive support, such as a log-normal or truncated normal distribution. It is difficult, if not impossible, to achieve such a distribution using a phenology model that relies on a diffusion term alone to describe developmental variation.

Another advantage of the phenotype-dependent advection model is that it can be easily extended to study the evolution of phenology, since it explicitly incorporates persistent variation in development time. The evolution of phenology of a simple model insect was presented in Chapter 2; in that chapter the integral form of the

phenotype-dependent advection model was used to describe persistent variation in development time within a single life-stage.

The importance of the FPDE in modeling insect phenology should not be discounted. As a model that explicitly separates persistent and random variation, it may be useful in describing the development of laboratory populations of a wide range of insects. This is particularly true if random sources of developmental variance cannot be well controlled. The FPDE may also be a better model of insect phenology in the field if the population is observed over multiple trees in a stand, while ambient temperatures are only available from a single site. In these cases, the diffusion term may allow the model to capture developmental variance resulting from differences between trees or due to variation between ambient and phloem temperatures.

CHAPTER 4

EVOLUTION OF MOUNTAIN PINE BEETLE PHENOLOGY¹

4.1 Introduction

Understanding the evolution of insect phenology (the timing of developmental events, such as oviposition or adult emergence) is a crucial step toward predicting how insect populations will respond to climate change. It is particularly important to understand how climate change will affect outbreak insects due to their economic and ecological importance. There are strong selective pressures on insects to maintain appropriate phenology, including synchrony with resources and within populations. Insect phenology changes plastically (without underlying genetic evolution) as yearly temperature changes, because the time necessary for an insect to complete its life cycle is largely dependent on temperature [47]. This plastic response may be insufficient to maintain adaptive phenology within some populations given the degree of temperature change predicted to occur over the next 100 years. Instead, these populations must migrate, adapt through genetic evolution, or face extinction. In order for development time to evolve in response to selection on phenology, there must be heritable variation in that trait. Heritable variation in development time within and between populations has been shown experimentally by Bentz et al. [5]. In this article we extend and apply a model of phenology evolution (see Chapter 2) to investigate the evolution of mountain pine beetle (an important outbreak insect) development time in response to natural selection on emergence time, particularly how mountain pine beetles might evolve to cope with climate change.

¹Coauthored by Brian Yurk, James A. Powell, and Barbara J. Bentz.

The fitness of an individual insect depends on its phenology relative to the timing of biotic and abiotic factors as well as the phenology of other individuals in the population. It is essential that development is timed to take advantage of the phenology of biotic resources and to avoid the coincidence of sensitive life stages with extreme weather to lessen the risk of desiccation in the summer and cold-induced mortality in the winter [27]. Developmental synchrony within a population is another phenology-driven determinant of fitness. Finding mates at low densities may require a high degree of reproductive synchrony (i.e. a high proportion of the population with overlapping reproductive periods) [9]. The need for developmental synchrony in a population means that fitness increases with emergence density (at low population densities); this is known as an Allee effect [1].

Temperature plays a major role in determining the phenology of poikilothermic organisms, such as insects, whose body temperatures depend on ambient temperatures. Shifting phenology has been linked to temperature change in several natural populations [31]. Although some insects possess physiological mechanisms that use cues other than temperature to control phenology (e.g. diapause or photoperiod sensitivity) [47], for others, phenology is directly controlled by the dependence of development time on temperature [13]. Since their metabolic rates depend on ambient temperature, insects develop at different rates at different temperatures [15, 41, 45]. Increasing temperature speeds metabolism at low to moderate temperatures, resulting in a shorter time period required for development. However, increasing temperature can be counterproductive at high temperatures, resulting in longer development time [4]. Consequently, the response of phenology to temperature is a highly plastic trait (phenology can change in response to yearly temperature change with no underlying molecular evolution). The dependence of development time on temperature varies between developmental stages. This can have a strong synchronizing effect on a pop-

ulations; at low temperatures development can effectively halt for individuals in one stage allowing individuals in earlier stages to catch up [19]. Since changing temperature shifts phenology, and insect fitness is highly dependent on phenology, it follows that global warming will result in strong selection on development time.

Predicting how populations might evolve to cope with global warming requires a mechanistic understanding of how phenology depends on temperature before the evolution of that dependence can be modeled. Laboratory experiments have measured development time at various constant temperatures for many insect species (e.g. [4, 15, 17, 28, 41]). We are careful to make the distinction between development time, the time it takes for an insect to develop through a life stage or life cycle, and phenology, the timing (i.e. time of year) of developmental milestones. In these experiments, insects are held at constant temperatures and allowed to develop through a life stage. The time it takes to complete the stage (development time) is recorded. These experiments are carried out at many different temperatures for each life stage. Empirical models (discussed in detail later) are then developed to describe the dependence of development time on temperature in each stage. These models are used to predict development time under both constant temperatures and varying temperatures in the laboratory and in the field.

In order for a trait like development time to evolve it must vary within a population, and some portion of that variation must be heritable [18]. Development time can be considered to be a continuous trait (also known as a quantitative or multifactorial trait) as opposed to a discrete trait (see [21, 23]). This is justified because development time is affected by enzyme kinetics and environmental variation and therefore likely influenced by many genes, whereas a discrete trait is controlled by only a few genes. Consequently, we assume development time varies continuously within a population.

Quantitative genetic models describe how selection affects variation in quantitative traits and how that variation is inherited by successive generations [20, 42, 43]. Selection acts on heritable traits through differential fitness, so that phenotypes associated with higher fitness are better represented in the next generation. The simplest quantitative genetic model is the breeder's equation (see e.g. [18]). This model relates the change in the mean phenotype in the next generation (the response to selection) to the difference between the mean phenotype of individuals that reproduce and the mean phenotype of all individuals in this generation (the selection differential). The breeder's equation does not allow for phenotypic mating structure (e.g. temporal structure in the case of development time), as there is the inherent assumption that every individual in the population is capable of breeding with every other individual. This assumption is violated for development time, since individuals with similar phenotypes are more likely to mate than individuals with dissimilar phenotypes. For example, slow developers are more likely to mate with other slow developers, because they are more likely to be in their reproductive phases at the same time (late in the reproductive season). In other quantitative genetic models assumptions are typically made about the shape of the phenotype distribution within a population (e.g. normality [21]), and the models describe how selection and reproduction affects the mean and variance of the phenotype distribution for the next generation [42].

Yurk and Powell (see Chapter 2) took a more direct approach to modeling the evolution of insect development time in response to selection on emergence time. Development was tracked and emergence time distributions were predicted for each developmental phenotype, in this case the individual development time relative to a base development time. A selection function was then applied, assigning fitness based on emergence time and density (individuals emerging on the same day have the same fitness regardless of phenotype). The phenotypes of offspring laid as eggs

on a particular day were assumed to be normally distributed with the same mean as their parents and variance related to their parents' phenotypic variance, consistent with [42]. A clear benefit of this approach is that it allows a complex evolutionary scenario (indirect, density-dependent selection on a highly plastic, temporally structured quantitative trait) to be represented in a fairly simple way. Additionally, the simplicity of this approach admits analysis using classical tools of applied mathematics (see Chapter 2).

The Yurk and Powell evolution model was applied to study the evolution of a model two-stage insect (see Chapter 2). Asymptotic analysis of the model led to analytic approximations of evolutionary steady distributions under periodic temperature conditions (no change in the yearly temperature series from year to year). At these steady distributions, the temporal structures of population density, mean phenotype, and phenotypic variance of emergent adults are invariant across generations. It was demonstrated analytically and numerically that populations of model insects will evolve so that the mean phenotype at any emergence time is the one that allows completion of exactly one generation per year (strict univoltinism), with predictable temporal structure for emergence densities and phenotypic variances. In particular, the populations evolve so that emergence occurs at times of year that are stable fixed points of a developmental circle map (described in detail later). They also demonstrated the importance of these steady distributions under warming temperatures; if adaptation does not allow for stable fixed points, the population rapidly goes extinct.

In this article, we use these methods to study the evolution of mountain pine beetle phenology in response to selection on emergence time. The mountain pine beetle (*Dendroctonus ponderosae* Hopkins, MPB) is an eruptive bark beetle found in western North America that spends most of its life cycle beneath the bark of host pine trees. MPB outbreaks have resulted in massive timber loss (see, for example,

www.for.gov.bc.ca), making MPB an important insect from both an ecological and economic perspective. Recent MPB range expansion and increased outbreak frequency have been linked to climate change [10]. For MPB, development from egg to adult occurs within hosts, after which the beetles emerge to mate and attack new hosts where they lay the next generation of eggs. In order to reproduce successfully MPB must kill at least part of their host, which requires a high attack rate (a mass attack) to overwhelm the resin response mechanism of the tree [7]. Mounting mass attacks requires a sufficient density of beetles to simultaneously complete development and emerge from their hosts to find and attack new ones, resulting in an Allee effect [1] for MPB. On the other hand, intraspecific competition becomes the dominant effect at high emergence densities, and increasing attack density reduces fitness [7]. Additionally, it is important that MPB emergence is timed so that they are in the appropriate stage to survive cold fall and winter temperatures. In fact, the northern extent of the MPB range is thought to be largely determined by exposure to cold temperatures [6, 12]. A comprehensive review of MPB biology is presented in [39].

Previous models of MPB phenology that do not account for evolution of development time predict that developmental synchrony within a population can only be maintained within a narrow range of mean annual temperatures, spanning approximately 2.5°C [27]. An increase of 2°C (well within current projections in the MPB range [11]) would push temperatures outside of this range [27]. Without evolution, populations will lose developmental synchrony and be exposed to extreme weather conditions in sensitive life stages [27]. These predictions reinforce the idea that evolution of the temperature-dependence of development time will be necessary for local populations to successfully adapt to changing climate and indicate the need to understand how phenology might evolve.

Variation in development time within MPB populations has been observed in the laboratory (e.g. Chapter 3 and [17]) and in the field (see Chapter 3). Bentz et al. [5] showed that variation in development time exists between MPB populations and is heritable through breeding experiments involving individuals from populations in central Idaho and southern Utah.

We extend the Yurk and Powell model to study the evolution of MPB phenology. The current treatment is novel because the evolution map is founded on a phenology model that has been parameterized for MPB (see Chapter 3). We also use a more realistic selection function that is based on a fecundity model developed by Powell and Bentz [33] to study the relationship between MPB phenology and demography. Additionally, we implement an oviposition mechanism that incorporates distributed oviposition (female MPB lay one egg at a time within their egg galleries at a rate that depends on temperature), an important source of phenology variability (see Chapter 3).

We address the evolution of MPB phenology under both stable, periodic temperatures and warming temperatures. One goal of this work is to predict whether MPB populations will evolve to steady distributions under stable periodic temperatures. This is addressed by numerically simulating the evolution of phenology in response to many generations of natural selection on emergence time and density under stable phloem temperatures measured in the field at MPB infestation sites in central Idaho and southern Utah. Another goal is to determine if MPB can adapt to warming temperatures and to discover possible limitations to the rate of adaptation—an idea that was not addressed in Chapter 2. Warming is simulated by uniformly shifting from the central Idaho phloem temperatures to the southern Utah phloem temperatures. This shift is implemented over different numbers of generations to simulate different warming rates, and a population that is well adapted to central Idaho temperatures

is allowed to evolve under the different warming scenarios so that limits on the rate of adaptation can be determined.

4.2 Model development

4.2.1 Temperature-dependent development time curves

The phenology model that we develop is based on development time curves. These curves describe how long it takes an individual to complete a life stage at different constant temperatures. Typically, development time is U-shaped with a minimum at some developmentally optimal temperature (often 20 – 25°C); development time increases as temperatures become cooler or warmer than the optimum [41, 45]. In practice, the curves are constructed by measuring development time at various constant temperatures in the laboratory, then fitting an appropriate curve to the data [4, 24, 28].

Development time curves for each MPB life stage (Figure 4.1) have been fit to constant temperature development time data using a maximum likelihood approach (see Chapter 3). The individuals measured in the experiment were collected from multiple trees at MPB infestation sites in central Idaho and northern Utah . Details of the experimental methods are given in [4] and the data are described in Chapter 3 and [4, 25]. The rate at which female adult MPB construct their egg galleries (the number of centimeters constructed per day) also depends on temperature, and gallery construction can be treated as a life stage. The length of MPB gallery constructed per day at different temperatures has been measured in laboratory experiments [2]. This data was transformed to find the time required to complete one centimeter of gallery at each temperature (burrowing time), and a curve (Figure 4.2) was fit to the transformed data (see Chapter 3).

Table 4.1: Parameterization for MPB development time curves for each life stage (egg-general adult). The parameterization for MPB burrowing time curve is also shown (ovi. adult). $L1 - L4$ indicate larval instars 1-4. These parameters were fit to data from constant-temperature laboratory experiments. In cases that five parameters (c_i) are listed, the development time curve was the sum of decreasing and increasing exponential functions. In the cases that three parameters are listed, the development time curve was a decreasing exponential function.

stage	c_1	c_2	c_3	c_4	c_5
egg	0	4.802	0.154	-2.573	0.139
L1	-18.014	4.961	0.133	0.850	0.074
L2	4.744	9.196	0.499	-	-
L3	0.016	6.670	0.244	-12.334	0.553
L4	0	5.332	0.149	-18.386	0.799
pupa	4.240	10.577	0.509	-	-
ten. adult	0	5.260	0.113	-	-
ovi. adult	0	1.003	0.085	-	-

We define $\tau_i(T)$ to be the time required for an individual to complete development through its i th life stage at constant temperature T (its development time curve). The development time curve fit to each MPB life stage (including egg gallery construction) is either the sum of decreasing and increasing exponentials,

$$\tau_i(T) = c_1 + \exp[c_2 - c_3T] + \exp[c_4 + c_5T], \quad (4.1)$$

where c_3 and c_5 are positive, or a decreasing exponential if the data does not support an increase in development time at high temperatures (see table 4.1),

$$\tau_i(T) = c_1 + \exp[c_2 - c_3T], \quad (4.2)$$

where c_1 and c_3 are positive.

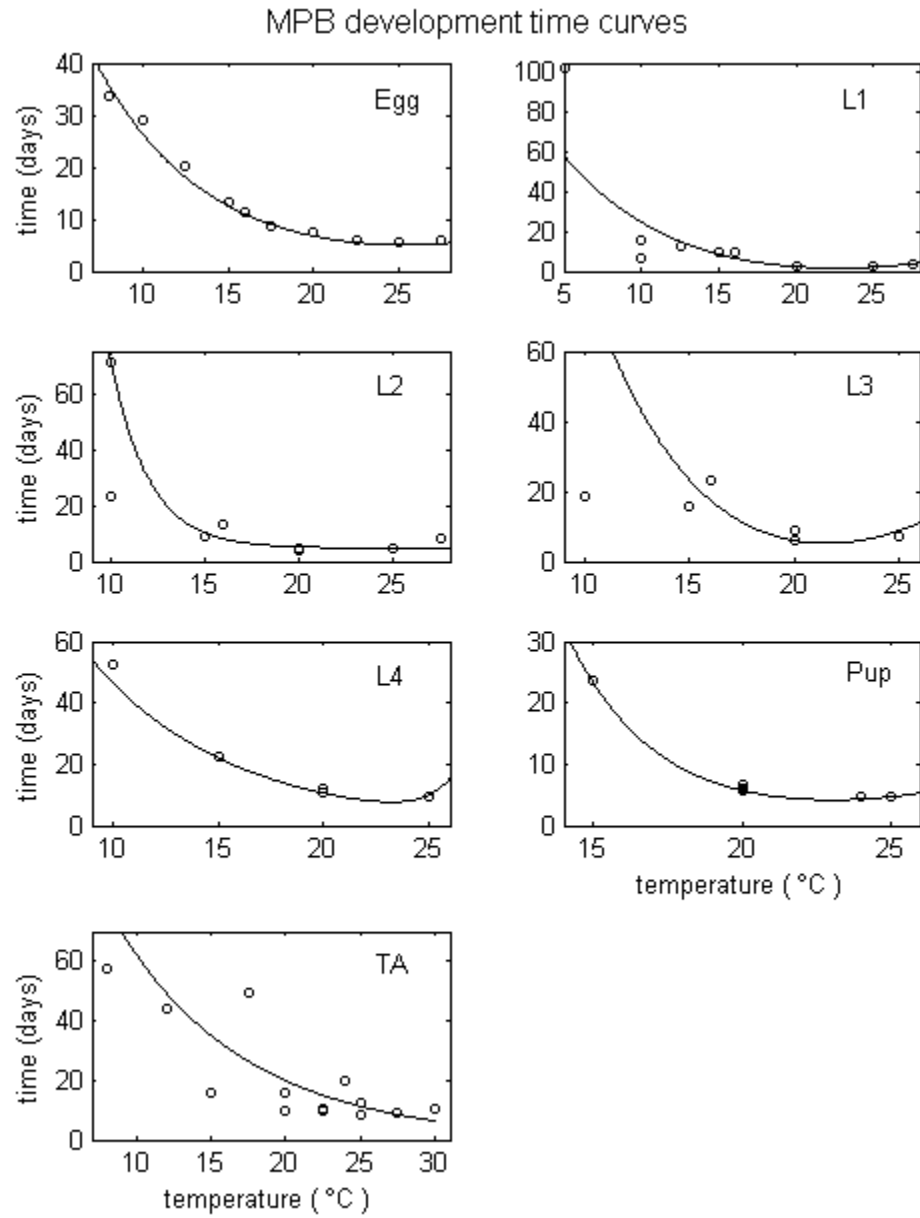


Fig. 4.1: Base development time curves fit to MPB development times for each developmental stage. Two means are plotted at the same temperature if there were two separate development experiments performed at that temperature.

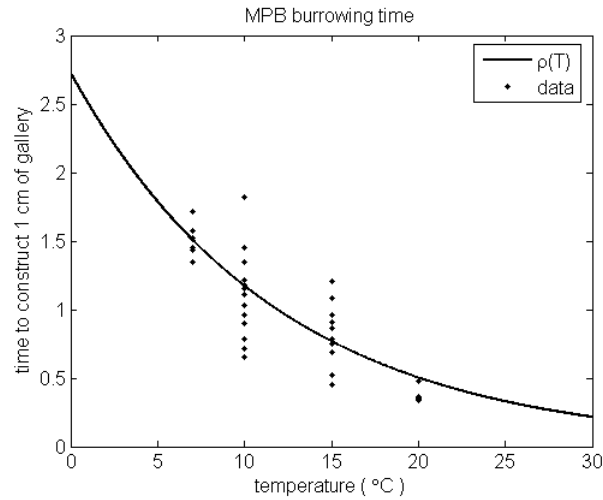


Fig. 4.2: Burrowing time curve $\rho(T)$ for MPB ovipositional adult (solid curve) fit to burrowing times measured in constant-temperature laboratory experiments (dots). Burrowing time is the time necessary for a MPB female to construct on centimeter of gallery at a given temperature.

4.2.2 Simple individual phenology model

Development time curves are used to predict development time under varying temperatures. We define $a(t)$ to be the proportion of a life stage that an insect has completed at time t ; a takes values between 0 and 1 and can be thought of as the insect's physiological age [24]. Since an insect takes $\tau_i(T)$ days to develop through the entire life stage at constant temperature T , the simplest developmental model predicts it will take $\Delta t = \tau_i(T)\Delta a$ days to develop through a fraction Δa of the life stage at that temperature.

Under varying temperatures, let $T(t)$ be the temperature at time t . If the relationship $\Delta a/\Delta t = 1/\tau_i(T)$ holds for arbitrarily small values of Δt , then development through stage i for an insect that began at time t_0 is described by the initial value problem

$$\frac{da}{dt} = \frac{1}{\tau_i(t)}, \quad a(t_0) = 0, \quad (4.3)$$

where $\tau_i(t) = \tau_i(T(t))$. We integrate the differential equation (4.3) to determine the insect's age at time t ,

$$a(t) = \int_{t_0}^t \frac{ds}{\tau_i(s)}.$$

In practice, it is useful to be able to predict the time that a developmental milestone occurs. To this end, define $\Gamma_i(\Delta a, t)$ to be the time that an insect completes Δa units of age given that it began at time t . Then $\Gamma_i(\Delta a, t)$ satisfies

$$\Delta a = \int_t^{\Gamma_i(\Delta a, t)} \frac{ds}{\tau_i(s)}. \quad (4.4)$$

If the function Γ_i is known for each life stage of an individual, the timing of any developmental event (phenology) is completely determined for that insect. An important special case is $\Gamma_i(1, t)$, the time an insect completes stage i if it began at time t ; we define $g_i(t) = \Gamma_i(1, t)$. Then $g_i(t)$ satisfies

$$1 = \int_t^{g_i(t)} \frac{ds}{\tau_i(s)}. \quad (4.5)$$

4.2.3 The G-function

The individual phenology model is easily extended to describe development through an entire life cycle. We define $G(t)$ to be the time that an insect lays the next generation of eggs if it was oviposited at time t . At present, we ignore the distributed nature of MPB oviposition (for the sake of clarity) and let $G(t)$ be the oviposition time of the median egg; this restriction will be relaxed later. For MPB, which has an 8-stage life cycle (counting oviposition as a life-stage),

$$G(t) = (g_8 \circ g_7 \circ \dots \circ g_2 \circ g_1)(t), \quad (4.6)$$

because upon completing a life stage the insect enters the next stage. A G -function for MPB is shown in Figure 4.3.

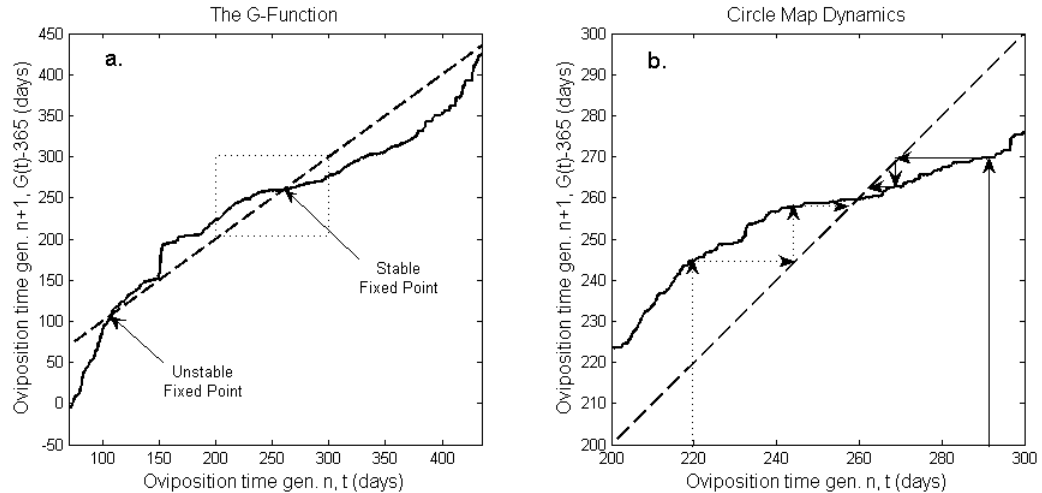


Fig. 4.3: **a.** An example of a G function (solid) for MPB. Given the oviposition time t of an insect in generation n , the oviposition time of its median egg in generation $n + 1$ is $G(t)$. $G(t) - 365$ is plotted to show the time of year of emergence relative to the time of year of oviposition. Also plotted is the fixed point line (dashed); times at which the G function intersects the fixed point line (fixed points) correspond to times of year where oviposition occurs at exactly the same time of year in successive generations. **b.** A developmental circle map for MPB and its fixed point dynamics. The circle map is the solid curve, and the fixed point line $G(t_o^n) = t_o^n$ is dashed. The circle map corresponds to the G function in the left panel. As the map is iterated, oviposition times converge (arrows) to stable fixed points (fixed points that occur where slope of the circle map curve is less than one).

In previous work the G function has been employed to understand how phenology depends on temperature [27, 35]. Under stable yearly temperatures, the G -function, taken modulo 365 days, is a periodic circle map between the time of year that an individual in generation n is oviposited and the time of year that its offspring are oviposited in generation $n + 1$. The dynamics of the circle map are dominated by univoltine (one generation per year) fixed points of the circle map, where the oviposition times of an insect and its offspring are exactly one year apart. Oviposition

times rapidly converge to stable fixed points as the circle map is iterated over multiple generations (see Figure 4.3). As a consequence, stable univoltine fixed points synchronize phenology within a population and play an important role in insect fitness (see Chapter 2). A fixed point of the G -function is stable if $\frac{dG}{dt} < 1$ there; this makes sense from a biological perspective, because individuals that are oviposited earlier than such a fixed point (but sufficiently close to it) will produce offspring that are oviposited later in the next generation. On the other hand, individuals that are oviposited later than the fixed point will produce offspring that are oviposited earlier in the next generation.

4.2.4 Population phenology model

We now extend the phenology model to track development time within a population of identical individuals (no variation in development time). Later, this will be extended to account for developmental variation. Let $p(a, t)$ be the density of individuals that achieve age a at time t ; then $\int_{t_1}^{t_2} p(a, t) dt$ is the number of individuals that achieve age a between times t_1 and t_2 . According to (4.4), an individual that was age a at time t will be age $a + \Delta a$ at time $\Gamma_i(\Delta a, t)$. Consequently, the same number of individuals will achieve age $a + \Delta a$ between times $\Gamma_i(\Delta a, t_1)$ and $\Gamma_i(\Delta a, t_2)$ as achieved age a between time t_1 and t_2 , assuming there is no mortality during development. This gives the conservation law

$$\int_{t_1}^{t_2} p(a, s) ds = \int_{\Gamma_i(\Delta a, t_1)}^{\Gamma_i(\Delta a, t_2)} p(a + \Delta a, s) ds, \quad (4.7)$$

which can also be written in differential form as an advection equation (see Chapter 3),

$$\frac{\partial}{\partial a} p(a, t) + \frac{\partial}{\partial t} [\tau_i(t) p(a, t)] = 0. \quad (4.8)$$

Solutions of the advection equation are of the form

$$\tau_i(t)p(a, t) = \tau_i(\Gamma_i(\Delta a, t))p(a + \Delta a, \Gamma_i(\Delta a, t)); \quad (4.9)$$

here, the product of development time and population density is constant along the characteristic curves $t(a) = \Gamma_i(a, t_0)$, where t_0 is any stage initiation time (see Chapter 3). In particular, the density of insects exiting a stage is related to the density of insects entering by the equation

$$\tau_i(t)p(0, t) = \tau_i(g_i(t))p(1, g_i(t)), \quad (4.10)$$

or equivalently by the conservation law

$$\int_{t_1}^{t_2} p(0, s)ds = \int_{g_i(t_1)}^{g_i(t_2)} p(1, s)ds. \quad (4.11)$$

4.2.5 Development time as a quantitative trait

We model variation in development time by allowing a single developmental parameter, α , to vary continuously within a population. This parameter relates individual development time to a standard development time for all temperatures. For simplicity, we allow variation within a single life stage (the teneral adult stage). Although developmental variation exists in all life stages, variation in earlier stages may be less important than in the teneral stage due to the synchronizing effects of low temperatures [34] decreasing phenology variation. Bentz et al. [5] showed that variation in MPB development time is heritable for MPB.

Let α scale a base development time curve $\tau_7(T)$ for the teneral stage (e.g. the mean development time curve) so that the development time for an individual in

the teneral stage with phenotype α is $\alpha\tau_7(T)$. Then an individual with phenotype $\alpha = 2$ takes twice as long to develop through the teneral stage as an individual with phenotype $\alpha = 1$ at the same constant temperature. The temperature-dependent phenology model is easily extended to account for the developmental phenotype α . Define $g_{7,\alpha}(t)$ to be the time that an insect with phenotype α will complete the teneral stage if it began at time t . Then,

$$1 = \int_t^{g_{7,\alpha}(t)} \frac{ds}{\alpha\tau_7(s)},$$

similar to (4.5). We also generalize the G -function (4.6) to incorporate α in the teneral stage; let $G_\alpha(t)$ be the time that an individual with phenotype α that was oviposited at time t in generation n oviposits its offspring in generation $n + 1$. Then,

$$G_\alpha(t) = (g_8 \circ g_{7,\alpha} \circ g_6 \circ \dots \circ g_2 \circ g_1)(t).$$

Figure 4.4 shows examples of $G_\alpha(t)$ for various values of α .

Similar to the G -function, $G_\alpha(t)$ taken modulo 365 provides a circle map under periodic temperatures for each phenotype, and each map may have univoltine fixed points. Conversely, given an oviposition time t there may be a phenotype, α_t , that results in a univoltine fixed point at time t (see Figure 4.4). This new function is defined by the relationship

$$t = G_{\alpha_t}(t) - 365. \tag{4.12}$$

The function α_t has an important effect on organizing the dynamics of the G_α map; as the map is iterated over multiple generations the individuals that are attracted to a particular oviposition time t will have phenotype α_t if t is a stable fixed point of G_{α_t} . Differentiating the definition (4.12) with respect to time and solving for the

derivative of α_t gives

$$\dot{\alpha}_t = \frac{1 - \frac{\partial}{\partial t} [G_\alpha(t)]|_{\alpha=\alpha_t}}{\frac{\partial}{\partial \alpha} [G_\alpha(t)]|_{\alpha=\alpha_t}},$$

where ‘ \cdot ’ indicates differentiation with respect to t . Since increasing α increases development time, the denominator is positive. If t is a stable fixed point of G_{α_t} , then $\frac{\partial}{\partial t} [G_\alpha(t)]|_{\alpha=\alpha_t} < 1$, so that the numerator is also positive, making $\dot{\alpha}_t > 0$. Similarly, $\dot{\alpha}_t < 0$ whenever t is an unstable fixed point of G_{α_t} . Therefore, stability of the univoltine fixed points in Figure 4.4 can be determined by the slope of α_t . This relationship makes sense from a biological perspective; since individuals oviposited at a time later than a stable fixed point take less than one year to develop, only an increase in development time can cause those individuals to complete development in exactly one year; this is achieved by increasing the phenotype (α). Hence, locally, phenotypes that result in later stable fixed points are larger than phenotypes that result in earlier stable fixed points.

An advection equation similar to (4.8) describes the development of individuals with phenotype α through the teneral stage,

$$\frac{\partial}{\partial a} p(a, t; \alpha) + \frac{\partial}{\partial t} [\alpha \tau_7(t) p(a, t; \alpha)] = 0. \quad (4.13)$$

In this case, $p(a, t; \alpha)$ is the density of individuals with phenotype α achieving age a at time t . In other stages, the development time of an insect with phenotype α does not depend on α . Consequently, development through stage i for an individual with phenotype α is described by the advection equation

$$\frac{\partial}{\partial a} p(a, t; \alpha) + \frac{\partial}{\partial t} [\tau_i(t) p(a, t; \alpha)] = 0. \quad (4.14)$$

for $i \neq 7$. In order to track development of the entire population through the complete

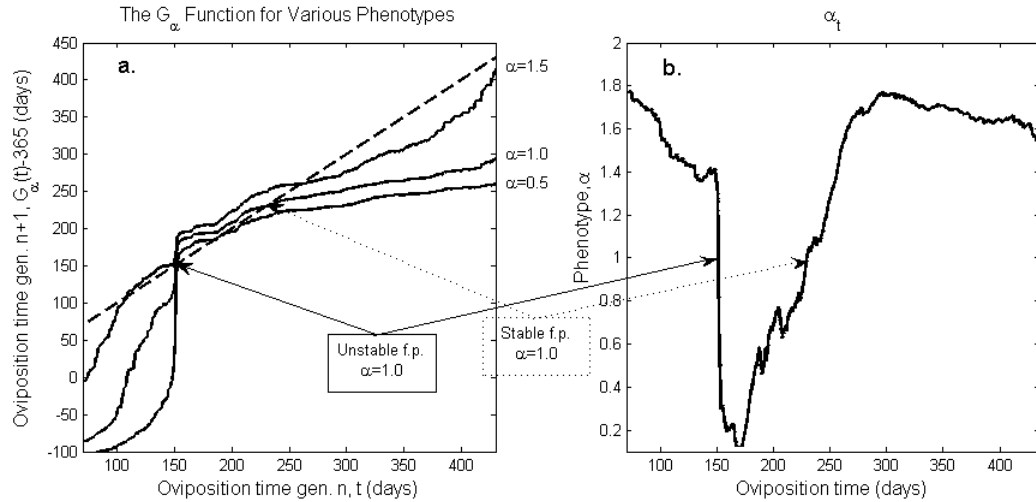


Fig. 4.4: **a.** The G_α function for MPB for various values of α . An individual with phenotype α that was oviposited at time t in generation n will lay its median egg at time $G_\alpha(t)$ in the next generation. Although α is assumed to vary continuously within a population, this plot shows only a few representative curves. Also plotted is the fixed point line. Note that individuals with different phenotypes have different fixed points. **b.** Given an oviposition time t , α_t is the unique phenotype that results in a fixed point for the G_α function at time t , i.e. $G_{\alpha_t}(t) = t + 365$. These fixed points are stable ($\frac{\partial}{\partial t}[G_{\alpha_t}(t)] < 1$) where α_t is increasing and unstable where α_t is decreasing (see text). The arrows point to the same unstable (solid) and stable (dotted) univoltine fixed points in both parts of the figure for individuals with phenotype $\alpha = 1.0$.

life-cycle, the distribution of phenotypes in the population must be known at oviposition. This can be estimated using development time data from constant temperature laboratory experiments, since development times are monitored for multiple individuals (see Chapter 3). Variation in development time in the teneral stage (and in the other MPB life stages) has been quantified in Chapter 3. Specifically, if a normal distribution of phenotypes (α 's) is assumed in the teneral stage, the phenotypic variance (fit to development time data from multiple constant temperature experiments) is 0.343 (see Chapter 3).

4.2.6 Evolution map

The phenotype-dependent phenology model is incorporated into a model of the evolution of phenology similar to the one introduced in Chapter 2. We define $p_o^n(\alpha, t)$ to be the density (with respect to time) of insects in generation n with phenotype α and oviposition time t , and $p_e^n(\alpha, t)$ to be the corresponding density at emergence. We also define $N_o^n(t)$ and $N_e^n(t)$ to be the (phenotype-independent) oviposition density and emergence density in generation n at time t , obtained by integrating $p_o^n(\alpha, t)$ and $p_e^n(\alpha, t)$ over all phenotypes, e.g.

$$N_o^n(t) = \int_0^\infty p_o^n(\alpha, t) d\alpha.$$

These quantities are important because selection acts on phenology and not directly on α and is defined in terms of these quantities. We assume that all selective forces acting on phenology can be described in terms of selection on emergence time and density (e.g. winter mortality of offspring can be attributed to emergence at the wrong time of year by their parents); this is consistent with the phenology-demography model proposed by Powell and Bentz [33]. Then the evolution model can be broken into 3 consecutive processes: development (from egg to emergent adult), selection (on emergence time and density), and reproduction. Development is described by the phenotype-dependent phenology model. Selection determines the net-fecundity of individuals that emerge at a particular time. The reproduction model determines the phenotypes and oviposition times of offspring. Since MPB net-fecundity is described in terms normalized emergence density and not the absolute number of emergers [33], we focus here on capturing the evolution of normalized oviposition and emergence distributions (e.g. $\iint p_e^n(\alpha, t) d\alpha dt = 1$).

Development through each life stage before the teneral stage is described by the advection equation (4.13), whereas development through the teneral stage is described by the phenotype-dependent advection equation (4.14). To track development through the entire life-cycle for each phenotype the advection equations are solved consecutively for each life stage. The initial condition for the first stage is taken to be the oviposition distribution $p_o^n(\alpha, t)$, and the initial condition for each later stage is taken to be the distribution of completion times (at $a = 1$) for the preceding stage. Figure 4.5 shows the effect of the development map on an oviposition distribution. For clarity, the figure shows only the phenotype-independent oviposition and emergence densities, although the oviposition and emergence densities do, in fact, depend on α .

4.2.7 Natural selection

In MPB populations natural selection acts on both emergence time and emergence density. We define $N_s^n(t)$ to be the density of females emerging in generation $n + 1$ that are produced by females emerging in generation n at time t , which we call the post-selection density. Then the effects of natural selection can be quantified in terms of the function $S(t)$, defined by

$$S(t) = \frac{N_s^n(t)}{N_e^n(t)}.$$

As such, $S(t)$ is proportional to the net fecundity of females emerging at time t . A reasonable selection function for the MPB is

$$S(t) = \begin{cases} \gamma \max(N_e^n(t) - A', 0), & t \in [152, 245], \\ 0, & \text{otherwise.} \end{cases} \quad (4.15)$$

Development

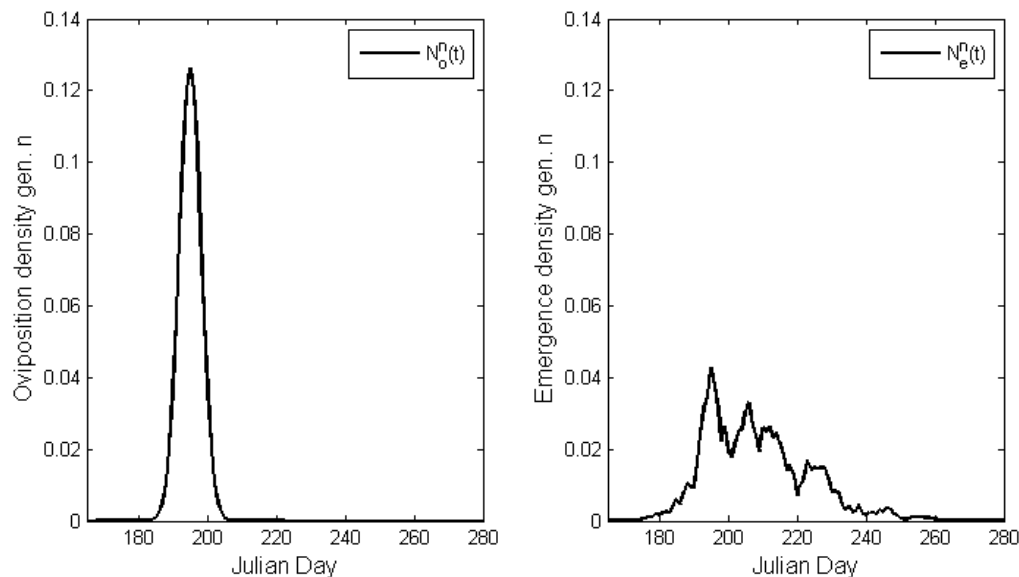


Fig. 4.5: An example of the effects of the development map on an oviposition distribution. Development maps an oviposition distribution to an emergence distribution for the same generation according to the phenotype-dependent phenology model. Note that although the oviposition and emergence distributions depend on phenotype, only the phenotype-independent distributions are shown for clarity.

This selection function is based on a model of phenology-dependent MPB effectiveness presented by Powell and Bentz [33]. It reflects the need for MPB to emerge within a reasonable time window between June 1 and August 30 (JD 152 and 245) in order to be in the appropriate life stage to survive cold fall and winter temperatures [6]. The model also simulates the need for MPB to emerge with sufficient density (above attack density threshold A') to overwhelm host tree defenses. The parameter γ gives the net fecundity of an “effective” beetle (an individual that survives a successful attack that has emerged within the emergence window) in terms of the number of emergers it will produce in the next generation. It is important to emphasize that this selection function affects phenotypic variation indirectly, because insects with the

same emergence time have the same fitness regardless of phenotype. An example of the effects of selection on an emergence distribution is shown in Figure 4.6.

Natural Selection

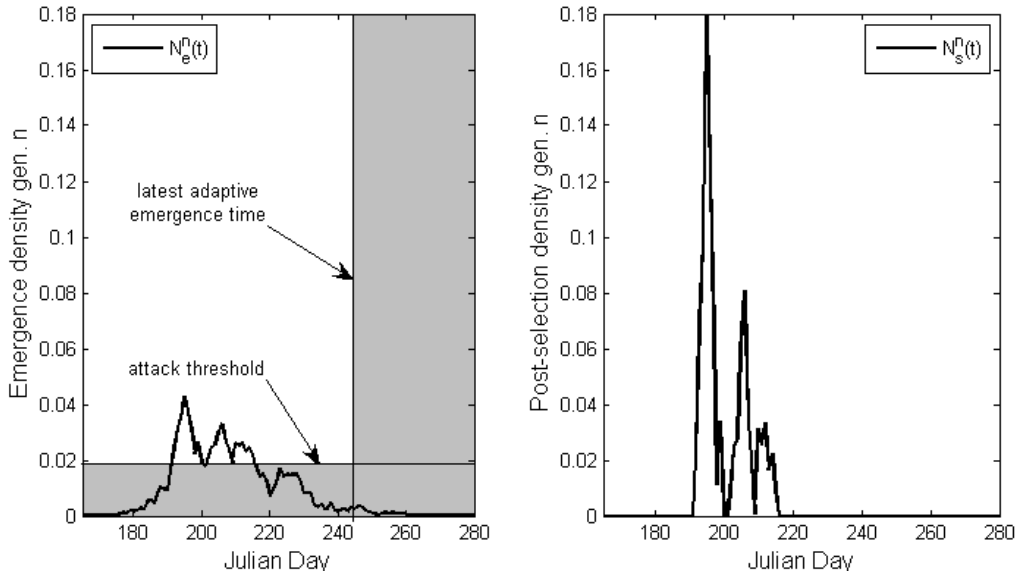


Fig. 4.6: An example of the effect of natural selection on emergence time and density ($N_e^n(t)$). Beetles that do not emerge at densities greater than the attack threshold (A') or within the emergence time window (i.e. beetles that emerge within the gray regions in the left panel) do not reproduce successfully. The post-selection density ($N_s^n(t)$) is shown in the right panel. The post-selection density is the density of females in generation $n + 1$ produced by females emerging in generation n at time t .

The attack density threshold parameter A' and the net fecundity parameter γ are combinations of different parameters in the Powell and Bentz phenology-demography model [33]. In terms of their parameters, A' is given by the ratio of the number of emerging MPB on a daily basis required to overwhelm host tree defenses to the number of adults that emerge from one successfully attacked tree (their A divided by their sf). The parameter γ is the same as their parameter α_1 . Powell and Bentz used eight years of MPB infestation data from an outbreak in central Idaho to estimate

sf and α_1 [33]; the best-fit parameter values that they obtained using the average of north and south side phloem temperatures were $sf = 13,000$ and $\alpha_1 = 6.45$. They chose $A = 250$ to correspond with the number of beetles necessary to achieve the threshold of 40 MPB/m² [36]. Based on these values, we set the attack density threshold at $A' = 250/13,000$, or $A' = 0.0192$.

One assumption of the Powell and Bentz model [33] is that each successfully attacked host tree produces a fixed number (sf) of emerging mountain pine beetles (regardless of the number of attackers in the previous generation); this allows the dependence of MPB success on phenology to be cast in terms of density of emergers instead of absolute numbers of emergers. In their article, Powell and Bentz incorporate the beetle effectiveness model into a demography model for MPB that also accounts for variation in host tree populations due to MPB infestation [33]. In the present treatment, we ignore host population effects; this is reasonable if we track probability density functions of emergence times instead of numbers of emergers and as long as there remains at least one host that is available for attack. Given that our model does not allow for host depletion and assumes that successfully attacked trees produce a fixed number of emerging MPB, extinction (zero emergence in the next generation) can only occur if the emergence density in this generation does not exceed the attack density threshold A' at any time within the emergence window. Consequently, this model inherently underestimates extinction risk in real MPB populations.

4.2.8 Sexual reproduction

Whereas the selection model determines the net fecundity of females emerging at a particular time, the reproduction model determines the phenotypes and oviposition times of their eggs. We assume that mating and egg gallery initiation occur immediately upon emergence so that mating only occurs between individuals that emerge

simultaneously. This is reasonable, because the flight period for an individual MPB is very short—less than two days for individuals that do not leave the stand [39]. Female MPB construct egg galleries, burrowing at a rate that depends on temperature and laying eggs at roughly two eggs per centimeter. The reproduction model developed here captures both the breeding structure due to the temporal isolation of emergers and the distributed nature and temperature dependence of MPB oviposition.

Phenotypes of offspring

The phenotypes of females and males emerging at a particular time can be thought of as random variables F and M . Then, the phenotypes of their eggs is also a random variable, S . If progeny inherit their mean parent phenotype plus some error with zero mean and constant variance σ_ε^2 , then

$$S = \frac{F}{2} + \frac{M}{2} + \varepsilon,$$

where ε is the reproductive error, which accounts for variation due to the combined effects of sources of variation including mutation, heterozygosity, and maternal effects. If F and M are identically and independently distributed (i.e. males and females in the population have the same phenotype distributions and mate independently of phenotypes at any particular emergence time), with mean μ_e and constant variance ν_e , then the offspring phenotype, S , has mean

$$\mu_s = \mu_e, \tag{4.16}$$

due to linearity of the mean, and variance

$$\nu_s = \nu_e/2 + \sigma_\varepsilon^2, \tag{4.17}$$

due to bilinearity of the covariance. This approach to describing offspring phenotype was used in Chapter 2 and is similar to the approach developed by Slatkin [42]. The assumption of identical and independent male and female phenotype distributions allows us to focus exclusively on the females in the population.

Since the mean phenotype and phenotypic variance may differ for each emergence time, we treat both as functions of time. Let $\mu_e^n(t)$ and $\nu_e^n(t)$ be the mean phenotype and phenotypic variance of adults emerging at time t in generation n . To compute the mean phenotype and phenotypic variance at a particular emergence time, evaluate the integrals

$$\mu_e^n(t) = \frac{1}{N_e^n(t)} \int_0^\infty \alpha p_e^n(\alpha, t) d\alpha, \quad (4.18)$$

and

$$\nu_e^n(t) = \frac{1}{N_e^n(t)} \int_0^\infty (\alpha - \mu_e^n(t))^2 p_e^n(\alpha, t) d\alpha. \quad (4.19)$$

Then the mean phenotype of offspring laid by females that emerge at time t in generation n is

$$\mu_s^n(t) = \mu_e^n(t),$$

and the phenotypic variance is

$$\nu_s^n(t) = \nu_e^n(t)/2 + \sigma_\varepsilon^2,$$

by (4.16) and (4.17). We assume that the phenotypes of eggs laid by females that emerge at time t in generation n are normally distributed, with mean $\mu_s^n(t)$ and variance $\nu_s^n(t)$. Assuming a normal distribution of phenotypes is common in the quantitative genetic literature (e.g. [21, 23, 43]) and reflects the fact that variation in quantitative traits is attributed to the combination of several additive effects, i.e.

the aggregation of the effects of genetic variation across multiple loci and multiple environmental effects.

Combining the assumption of phenotypic normality following reproduction with the selection model gives the (phenotype-dependent) post-selection distribution,

$$p_s^n(\alpha, t) = \frac{N_s^n(t)}{\sqrt{2\pi\nu_s^n(t)}} \exp\left[-\frac{(\alpha - \mu_s^n(t))^2}{2\nu_s^n(t)}\right], \quad (4.20)$$

which is the normalized phenotype-dependent density of females emerging in generation $n + 1$ that are produced by females emerging in generation n at time t . The post-selection distribution is analogous to the oviposition distribution in Chapter 2, because oviposition was assumed to occur immediately upon emergence (there was no oviposition stage) in that paper.

Here we set $\sigma_\varepsilon^2 = 0.1$ for MPB; although the true value of σ_ε^2 is unknown, this value is consistent with laboratory data for MPB, because the best-fit value for phenotypic variance in the teneral adult stage is 0.343 (see Chapter 3), and Yurk and Powell (Chapter 2) predicted that the phenotypic variance for well-adapted adults emerging on a single day should be 1-2 times σ_ε^2 . Since all of the individuals reared in the laboratory did not emerge simultaneously in the field, their phenotypic variance (0.343) should be greater than the predicted variance among simultaneous emergers (1-2 times σ_ε^2). Hence, $\sigma_\varepsilon^2 = 0.1$ is a reasonable estimate, and is probably within an order of magnitude of the true value.

Distributed oviposition

We let gallery construction and oviposition proceed according to the model developed and parameterized for MPB in Chapter 3. MPB egg galleries are constructed at a rate that depends on temperature [2]; this dependence is modeled by the bur-

rowing time curve shown in Figure 4.2. As the model galleries are constructed, 20 female eggs are laid per successful female adult at a rate of 1 egg/cm [36] starting in the 60th centimeter of the gallery. Yurk and Powell set the position of the median egg at 70 centimeters to fit mean emergence times predicted by the phenology model to mean emergence times observed at seven MPB infested trees in central Idaho (see Chapter 3), although the median egg in the field is likely laid significantly earlier.

In the evolution model, gallery construction is implemented in the same way as development through a life stage by treating oviposition of the j th egg in a gallery as a developmental milestone. Each of the 20 eggs has its own G_α -function; the G_α -function for the j th egg maps the oviposition time of a parent in generation n with phenotype α to the oviposition time of its j th egg in generation $n + 1$. Furthermore, different eggs have different fixed points and different α_t functions (recall that α_t is the phenotype that results in a fixed point at time t). The phenology model that describes development through a life stage (4.8) is also used to describe gallery construction and to predict the distribution of times that j th eggs are laid in a population. This maps the post-selection distribution, $p_s^n(\alpha, t)$, to an oviposition distribution for each of the 20 eggs (see Figure 4.7). The resulting oviposition distributions are summed and the resultant distribution is divided by 20 (normalizing the distribution) to determine the composite oviposition distribution, $p_o^{n+1}(\alpha, t)$, for generation $n + 1$ (see Figure 4.7).

4.2.9 Summary of the evolution map

In summary, implementation of the evolution map proceeds as follows:

1. The oviposition distribution for generation n , $p_o^n(\alpha, t)$, is mapped to the emergence distribution for generation n , $p_e^n(\alpha, t)$, using the phenotype-dependent phenology model (4.13-4.14). Details of the numerical implementation of the development map are given in the appendix.
2. The normalized net fecundity of emerging individuals (the post-selection density, $N_s^n(t)$) is determined based on emergence time and density (i.e. $N_e^n(t)$)

Distributed Oviposition

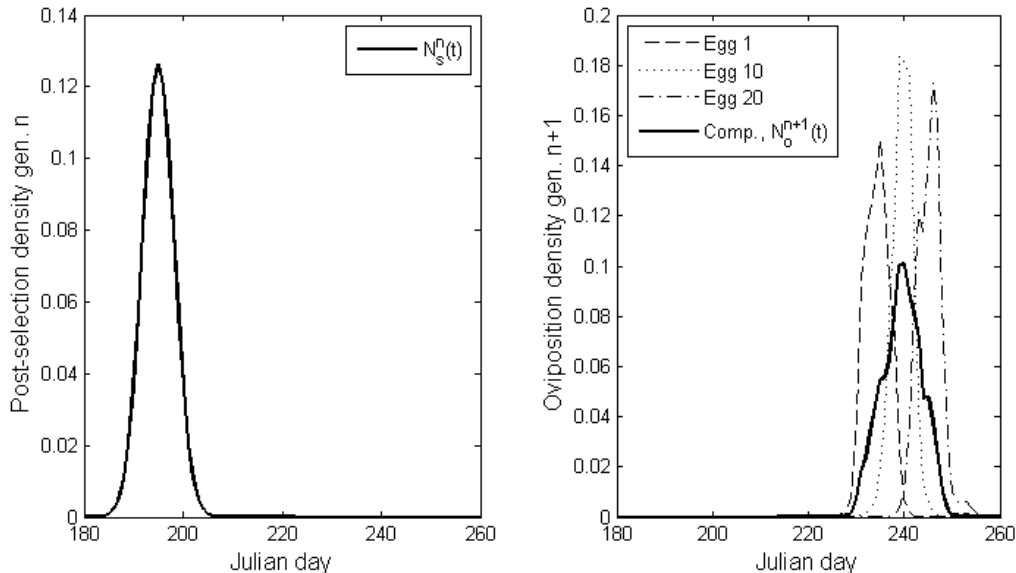


Fig. 4.7: An example of the effect of the distributed oviposition map on a post-selection distribution. The post-selection density $N_s^n(t)$ is shown in the left panel. Oviposition densities are shown for eggs 1 (dashed), 10 (dash-dotted), and 20 (dotted) in the left panel. The composite oviposition distribution (solid) is also shown (the entire oviposition distribution accounting for all 20 eggs, $N_o^{n+1}(t)$). Note that the dependence of post-selection and oviposition densities on phenotype is suppressed for clarity.

using the selection function, $S(t)$ (4.15).

3. The mean phenotype, $\mu_e^n(t)$, and phenotypic variance, $\nu_e^n(t)$, are computed for adults emerging at each time.
4. The phenotypes of offspring produced by individuals emerging at each time are taken to be normally distributed with mean $\mu_s^n(t)$ and variance $\nu_s^n(t)$ according (4.16) and (4.17). These and $N_s^n(t)$ determine the post-selection distribution (4.20).
5. Oviposition distributions are constructed for each of the twenty eggs by treating gallery construction as a developmental stage, and the overall oviposition distribution for generation $n + 1$, $p_o^{n+1}(\alpha, t)$, is determined by summing the oviposition distributions of the individual eggs and dividing by 20 to normalize.

4.3 Numerical results

4.3.1 Simulations: stable temperatures

We investigated the evolution of MPB phenology under two different stable temperature series. The first temperature series was obtained by measuring hourly phloem temperatures at a MPB infestation site in the Sawtooth National Recreation Area (SNRA) in central Idaho during 2001-2002. Methods for collecting phloem temperature data are described in detail in Chapter 3. A second hourly phloem temperature series was collected at an infestation site at Panguitch Lake, Utah (PAN) that was collected during 1996-1997. Both temperature series represent the average of north- and south-side phloem temperatures measured hourly at single trees. Minimum daily temperatures for both sites are shown in the left panel of Figure 4.8. On average, hourly temperatures were 2.56°C warmer at the Panguitch Lake site than at the central Idaho site.

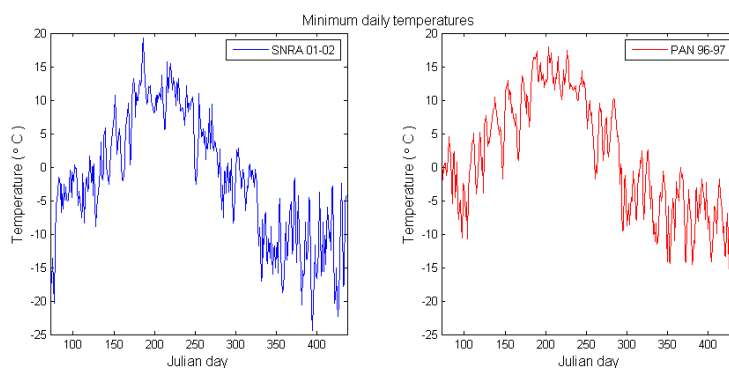


Fig. 4.8: Minimum daily phloem temperatures observed at two MPB infestation sites: the Sawtooth National Recreation Area (SNRA, left) in central Idaho and Panguitch Lake, Utah (PAN, right). The hourly temperature series from which these figures were generated is composed of the average of north- and south-side phloem temperature measurements made at a single tree at each site.

For each temperature series, the evolution map was implemented numerically for 1000 generations, so that a steady distribution was reached; this simulated evolutionary dynamics under stable climate conditions because the temperature series was not changed from year to year. The initial condition was a MPB attack time distribution measured in the field at the same tree that the SNRA temperature series was collected with phenotypes distributed uniformly between 0.06 and 3.0 at each time. The population was tracked at 49 evenly spaced phenotype values in this range on a daily time grid (although development was tracked hourly). At the end of each generation, the post-selection density was re-normalized, so the post-selection distributions predicted by the model can be thought of as probability density functions. This does not affect the dynamics of the evolution map due to the fact that the selection function (4.15) depends on the normalized emergence density rather than absolute numbers of emergers.

Under both temperature series, the population densities, mean phenotypes, and phenotypic variances at emergence converged to steady states. The steady post-selection densities and mean phenotypes are shown in Figure 4.9 for the SNRA temperature series and in Figure 4.10 for the warmer PAN temperature series. In both cases population density is concentrated at times that are stable fixed points of the G_α function for some value of α (see Figures 4.11 and 4.12).

It is interesting to note that at a steady state, the mean phenotype for the entire population was 0.5463 for the SNRA temperature series and 1.4309 for the PAN temperature series. This suggests that individuals that are well-adapted to Panguitch Lake temperatures should take substantially longer to complete development than individuals that are well-adapted to central Idaho temperatures under the same temperature conditions. This is consistent with experimental results obtained by Bentz et al. [5]; they reared individual MPB from both the Panguitch Lake population and

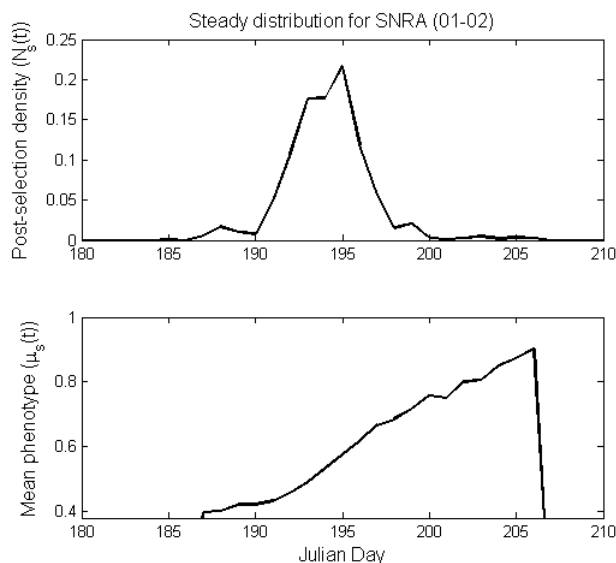


Fig. 4.9: Post-selection density (top) and mean phenotype (bottom) for the SNRA steady distribution. The evolution map was numerically implemented for 1000 generations with stable temperatures. The temperature series consisted of the average of north- and south-side hourly phloem temperatures measured at a tree in the Sawtooth National Recreation Area in central Idaho. The mean phenotype for the steady population is 0.5463.

the central Idaho population at the same constant temperatures and observed that individuals from the Panguitch Lake population emerged significantly later and were significantly larger than individuals from the central Idaho population.

Temporal variation in the mean phenotype at the steady distributions followed a pattern similar to that suggested in Chapter 2 (although that model did not incorporate distributed oviposition). For both temperature series, the mean phenotype at each emergence time took a value that was intermediate relative to the phenotypes that resulted in univoltine fixed points at that time (α_t) for each of the 20 eggs in the model egg gallery. In fact, the mean phenotype closely followed α_t for egg 10, in particular. Figure 4.11 shows the mean phenotypes at the steady distribution along with the phenotypes that result in univoltine fixed points (for eggs 1, 10, and 20)

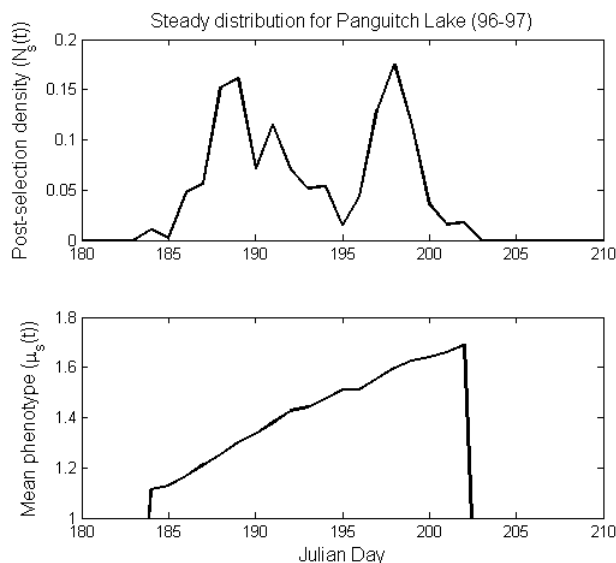


Fig. 4.10: Post-selection density (top) and mean phenotype (bottom) for the PAN steady distribution. The evolution map was numerically implemented for 1000 generations with stable temperatures. The temperature series consisted of the average of north- and south-side hourly phloem temperatures measured at a tree in Panguitch Lake, Utah. The mean phenotype for the steady population is 1.4309.

at each emergence time for the SNRA temperature series. Figure 4.12 shows similar plots for the PAN temperature series. Recall that regions where α_t is increasing correspond with stable fixed points of the G_α map, whereas regions where the function is decreasing correspond with unstable fixed points.

These results suggest that it is sufficient to focus on the median egg in order to understand the approximate behavior of the temporal variation of the mean phenotype with a full complement of eggs (at least at a steady distribution). Ignoring distributed oviposition in favor of only tracking median egg phenology greatly simplifies implementation of both the phenology and evolution models and allows for direct application of the analytical results obtained by Yurk and Powell (Chapter 2), since those results are based on a phenology model that does not incorporate distributed oviposition. That model predicts that the mean phenotype at oviposition

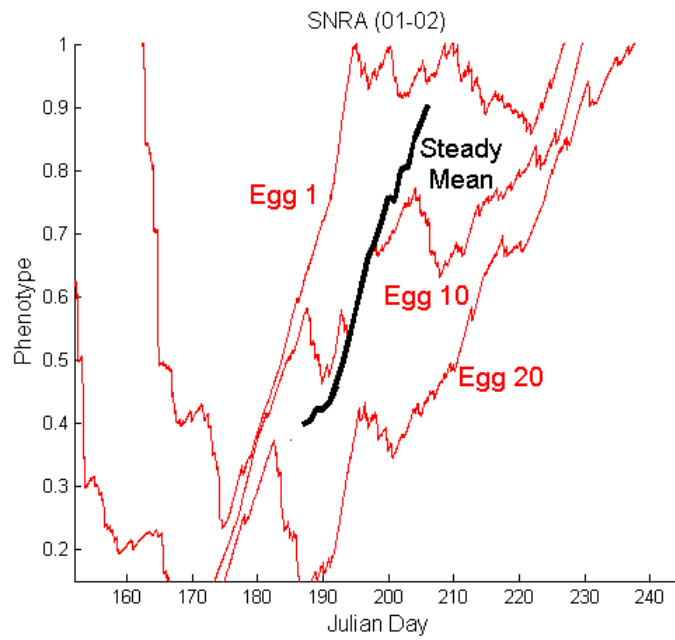


Fig. 4.11: Mean phenotype for the SNRA steady distribution (Steady Mean, black) and α_t for eggs 1, 10, and 20 (gray). α_t is the phenotype that results in a fixed point at time t . Fixed points are stable where α_t is increasing and unstable where α_t is decreasing.

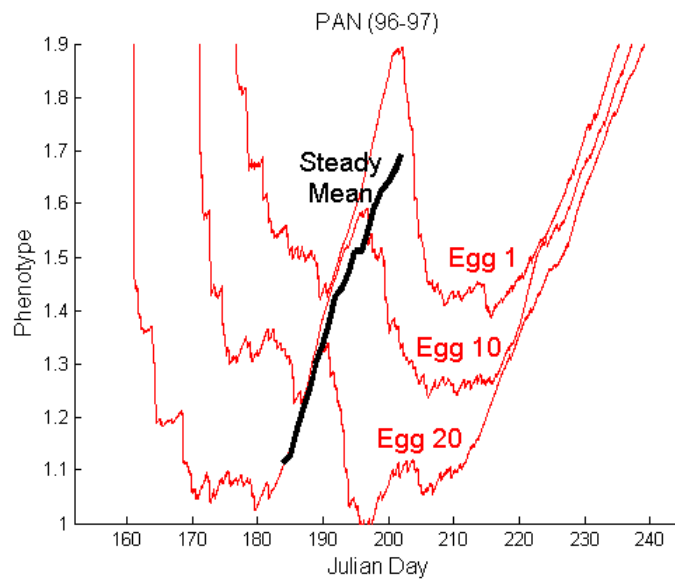


Fig. 4.12: Mean phenotype for the PAN steady distribution (Steady Mean, black) and α_t for eggs 1, 10, and 20 (gray).

time t should be α_t ; here we have demonstrated numerically that the mean phenotype in a population with distributed oviposition follows α_t for the median egg. On the other hand, ignoring distributed oviposition and focusing on the median egg ignores an important source of non-heritable variation in MPB phenology, which could affect model predictions regarding the rate of phenology evolution.

4.3.2 Simulations: increasing temperatures and rate of adaptation

Next, we simulated the evolution of phenology in response to warming by numerically implementing the evolution map with temperatures changing from central Idaho temperatures to Panguitch Lake, Utah temperatures (see Figure 4.8). The initial population was taken to be the steady population for the SNRA temperature series shown in Figure 4.9. Temperature change was implemented at different rates, so the rate of phenology adaptation could be studied. If \mathbf{T}_S and \mathbf{T}_P are the SNRA and PAN hourly temperature series, then the difference between them is $\mathbf{T}_{\text{diff}} = \mathbf{T}_P - \mathbf{T}_S$ (each element of this vector is the difference between corresponding hourly phloem temperatures at Panguitch Lake and the Sawtooth National Recreation Area). We used a linear ramp from SNRA to PAN temperatures; if the temperature change occurred over n generations, the temperature series in the m th generation (for $m \leq n$) was $\mathbf{T}_m = \mathbf{T}_S + (\frac{m}{n})\mathbf{T}_{\text{diff}}$. After the n th generation, temperatures were kept stable at the PAN temperature series.

We simulated warming over increasing numbers of generations, starting with a one-generation ramp and increasing the number of generations in the ramp until the population was able to persist for 1000 generations. For example, in the first simulation, the SNRA stable population was immediately exposed to PAN temperatures (a one-generation ramp) and went extinct after three generations. In the next simula-

tion, the SNRA stable population was ramped up to the PAN temperatures over two generations and went extinct after four generations. Here, extinction occurs when there are no successful offspring produced by a generation of emergers (i.e. when the emergence density does not exceed the attack threshold A' at any time within the MPB emergence window). The number of generations that the population persisted before going extinct under different temperature ramps is shown in Figure 4.13. For eight-generation ramps and greater, the population was able to adapt to the changing temperatures and survive for at least 1000 generations.

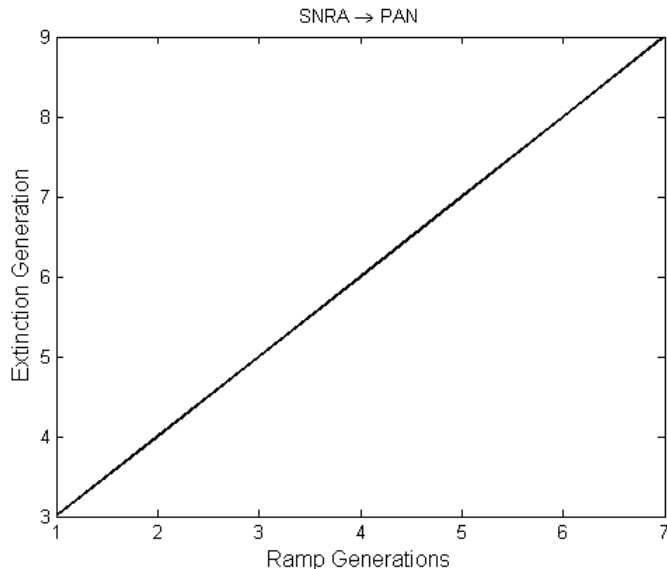


Fig. 4.13: Number of generations before extinction under different rates of temperature change. The initial population distribution for each simulation was well-adapted to SNRA 2001-2001 temperatures. Temperatures were ramped from hourly phloem temperatures measured during 2001-2002 in the Sawtooth National Recreation Area (SNRA) in central Idaho to hourly phloem temperatures measured during 1996-1997 at Panguitch Lake, Utah (PAN). Then temperatures were held at the Panguitch Lake values. Measured hourly phloem temperatures average 2.56°C warmer at the Panguitch Lake site than at the central Idaho site. In successive simulations, the temperature was ramped up over increasing numbers of generations (see text). The population was able to adapt to Panguitch Lake temperatures if the ramp occurred over eight or more generations.

These results suggest that the rate of temperature change is an important factor in determining the ability of a population to adapt. In this case, for MPB that are well-adapted to SNRA temperatures, adaptation to PAN temperatures requires little adaptation of development time in the teneral stage; the range of phenotypes that result in stable fixed points for at least one egg under SNRA temperatures is not significantly separated from the corresponding range of phenotypes under PAN temperatures (see Figures 4.11-4.12). In general, our results suggest that populations may be able to adapt to moderate rates of temperature increase, but the risk of extinction increases with the rate of temperature change. Furthermore, model populations were able to persist for short periods following drastic temperature change (the population survived for 2 generations after a 1-generation ramp from SNRA temperatures to PAN temperatures), suggesting that populations may remain viable despite short-term climate perturbations. Such perturbations are common in natural environments; for example, in the summer of 1993 summer temperatures in central Idaho were the coldest on record [35] following the Pinatubo eruption. During that summer, MPB populations were depressed in the Sawtooth Natural Recreation Area but recovered as temperatures warmed in following years [35].

4.3.3 Regions of stable fixed points and evolutionary consequences

Due to the importance of fixed points of the G_α -function and their stability in determining the evolutionary dynamics of phenology, it is useful to investigate patterns of fixed point existence and stability under different temperature regimes. To this end, we constructed G_α -functions on an hourly time-grid for egg 10 MPB with various values of α under different shifts of the SNRA temperature series. We focus on egg 10 because the stable temperature simulations suggest that the evolution of the popula-

tion closely tracks α_t for that egg. The shifted temperature series were obtained by adding constant temperatures (from $-6^\circ C$ to $6^\circ C$) to each hourly temperature in the SNRA series; in this manner 50 temperature series were generated with shifts evenly spaced between $-6^\circ C$ and $6^\circ C$. Although it is highly unlikely that climate change could proceed with such a uniform warming or cooling pattern, such an investigation reveals useful qualitative information about the potential impact of climate change on phenology. We restricted our attention to 49 values of α spaced evenly between 0.0612 and 3.0 (hence, the individual with the largest phenotype $\alpha = 3.0$ takes approximately 49 times as long to develop through the teneral stage as the individual with the smallest phenotype $\alpha = 0.06$ at the same constant temperature). The range of variation in α that exists or that is possible in natural populations is unknown, but it is certainly limited by physical and physiological constraints on development. Our lower-bound ($\alpha = 0.06$) is likely lower than the true lower bound for α , whereas the relationship of our upper-bound ($\alpha = 3.0$) to the true upper-bound is unknown.

Fixed points of each of the 2500 G_α -functions were identified by searching for sign changes in the quantity $G_\alpha(t) - t - 365$, which indicates their presence. The stability of each fixed point was evaluated by checking the derivative of the G_α -function; at a stable fixed point the slope of G_α is less than one, and at an unstable fixed point the slope of G_α is greater than one. The results are shown in Figure 4.14, where each circle indicates the presence of a stable fixed point at a particular time under a particular temperature shift. Fixed points are only shown within the MPB emergence time window (from JD 152 to JD 245), because individuals that emerge outside of this window do not yield emergent adults in the next generation.

An interesting results emerges from this exercise: Univoltine fixed points disappear at high and low temperatures. Specifically, there are no fixed points for any phenotype at temperature shifts less than approximately $-2.6^\circ C$ or greater than

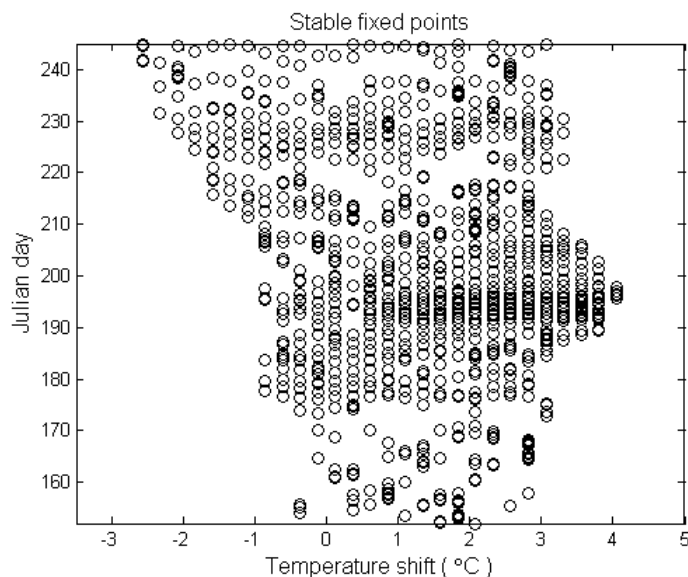


Fig. 4.14: Diagram of stable univoltine fixed points of the G_α function for egg 10 under different shifts of the SNRA 2001-2002 phloem temperature series. Only emergence time that are adaptive are shown (i.e. inside of the MPB emergence window). For each shifted temperature series, there may be a phenotype α that makes a particular emergence day a fixed point of the G_α map. If so, that fixed point is either stable or unstable. Note that at high and low temperatures there are no fixed points—at these temperatures reasonable adaptation in the teneral stage cannot result in strict univoltinism.

4.0°C. At temperature shifts less than -2.6°C , an individual that is oviposited at any time within the emergence window takes longer than 365 days to complete development through the pupal stage (the life stage before the teneral adult stage). Hence, at these temperatures, even an individual with no teneral stage ($\alpha = 0$) could not complete development in one year; this results in the complete absence of fixed points of the G_α functions at those temperatures. At temperatures warmer than 4.0°C development is rapid through the early stages, and there are no phenotypes less than $\alpha = 3$ that lengthen the teneral stage sufficiently for development to complete in a single year. Hence, the loss of fixed points at high temperatures is due to the upper-bound on the phenotype that we imposed. To illustrate this, Figure 4.15 shows the

G_3 -function (the G -function for egg 10 with phenotype $\alpha = 3.0$) for the temperature shifts $T_{shift} = 4.0^\circ C$ and $T_{shift} = 4.3^\circ C$. In the first case, the G_3 -function has fixed points; in the second case G_3 -function has no fixed points.

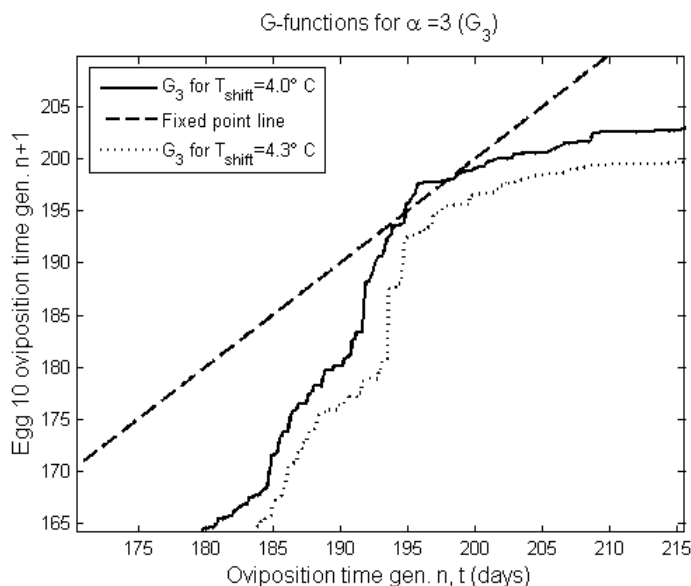


Fig. 4.15: The G_3 function for egg 10 under two different shifts of the SNRA temperature series ($T_{shift} = 4.0^\circ C$ and $T_{shift} = 4.3^\circ C$). Note that there are fixed points for $T_{shift} = 4.0^\circ C$, but there are no fixed points for $T_{shift} = 4.3^\circ C$.

Yurk and Powell demonstrated numerically that populations rapidly go extinct after stable fixed points are lost for a simple 2-stage model insect without distributed oviposition. To determine if MPB population success under warming conditions can be predicted based on the presence of stable fixed points of the G_α function for egg 10, we simulated the evolution of a population (with a full complement of eggs) as temperatures increased from the SNRA temperature series to the SNRA series under a $6.0^\circ C$ shift. The initial population was well-adapted to the SNRA temperature series (i.e. the stable distribution for the SNRA series). Temperatures were ramped up over 1000 generations to ensure that adaptation would not be limited by the warming rate. After 714 generations, the population went extinct, corresponding with a temperature

shift of 4.3°C , the same temperature at which fixed points are lost for egg 10 (see Figure 4.14). This result further suggests that the evolution of the population as a whole tracks the evolution of the median egg. It also supports the hypothesis that the presence of stable fixed points controls evolutionary dynamics, even under changing temperature conditions.

If fixed points are in fact necessary for population success, the results presented here suggest that evolution of phenology will allow populations to persist under a significantly broader range of temperature conditions than if populations are limited to responding plastically to climate change. The 6.8°C range of temperature shifts under which fixed points are present (assuming a maximum phenotype of $\alpha = 3.0$) is significantly broader than the 2.5°C range predicted by Logan and Powell [27] using a phenology model that did not account for variation in development time in the teneral stage. The broad range of adaptive temperatures at which fixed points occur is consistent with the fact that the MPB are successful in a broad range of temperature conditions in nature (their range extends from northern Mexico into Canada in western North America).

4.4 Summary and conclusion

In this paper we have developed a framework for modeling the evolution of MPB phenology in response to selection on emergence time and density. This model incorporates realistic aspects of MPB phenology, including development and burrowing time curves parameterized using data from constant temperature laboratory experiments as well as a distributed oviposition mechanism. The evolution model also reflects reasonable selection pressures on MPB phenology that are based on the results of a study that connected MPB phenology and demographics [33]. The model predicts several qualitative patterns observed in real MPB populations, including

longer time to complete the entire life cycle in southern populations than in northern populations, persistence of populations despite short-term perturbations to yearly temperatures, and a broad range of adaptive temperatures. The model also predicts that populations will evolve to steady states where the distribution of phenotypes and the timing of emergence do not vary across generations and that these steady states are determined by the presence and stability of univoltine fixed points. Furthermore, by studying the evolution of a population from SNRA temperatures to PAN temperatures, we were able to demonstrate that the rate of climate change is important in determining whether a population will be able to adapt to changing climate.

Perhaps the most important and consistent result of this work is that evolutionary dynamics are controlled largely by the existence and stability of univoltine fixed points of the G_α -function. A similar pattern was also suggested by Yurk and Powell in Chapter 2 based on a simpler phenology evolution model. We have also demonstrated that the evolutionary dynamics of mean development time in the teneral stage can be largely predicted using a simple median oviposition model rather than a distributed oviposition model. However, additional variation injected by distributed oviposition may affect the rate of adaptation.

The range of adaptive temperatures predicted by the evolution model depends on the range of phenotypes possible in a population. The extent of the possible phenotype range is unknown for MPB. Hence, further laboratory study is necessary to determine the degree of temperature change that will allow populations to adapt. A factor that may affect the ability of MPB to adapt to changing temperatures that is not considered here is the ability to complete two generations per year (bivoltinism) or one generation every two years (semivoltinism). At low temperatures, populations may be able to succeed by adopting semivoltine phenology, whereas at high temperatures they may succeed by adopting bivoltine phenology. Neither is possible in

the formulation of the evolution model presented here, but it could be extended in the future to incorporate either scenario. Furthermore, our results underestimate extinction risk for MPB populations under warming temperatures due to the fact that the model does not account for host population dynamics, which are coupled with mountain pine beetle population dynamics in real populations. Without incorporating forest dynamics, this model best describes populations that have unlimited access to host trees (e.g. populations expanding into new regions). Future work should incorporate host dynamics in order to better understand the evolution of phenology in localized MPB populations.

CHAPTER 5

SUMMARY AND CONCLUSION

In this dissertation we investigated the evolution of insect phenology in response to climate change with particular attention paid to MPB. This is a topic of great ecological and economic concern due to the importance of MPB as a forest outbreak insect. Phenology is a major determinant of fitness in insect populations; success depends on maintaining appropriate phenology relative to biotic and abiotic factors and developmental synchrony with other individuals in the population. Since insect phenology depends on temperature, populations will be forced to migrate, adapt, or go extinct to cope with climate change.

We developed a framework for modeling the evolution of insect phenology. The evolution model allows the distribution of a parameter that scales a base development time curve to evolve within a population in response to natural selection on emergence time and density. The evolution map was characterized by its effects on the temporal variation of the density, mean phenotype, and phenotypic variance of a population at oviposition. Using Laplace's method we found approximate steady states of the evolution map under stable (periodic) temperatures; at these steady states, the mean phenotype at any oviposition time is the one that results in a fixed point of the G_α circle map at that time. Biologically, this means that an individual oviposited at that time with that mean phenotype will take exactly one year to complete development. These results were verified numerically for a simple two-stage model insect. We also simulated evolution of the two-stage insect under warming temperatures and showed that evolution allowed the insect to adapt to climate change as long as stable fixed points of the G_α map existed within the window of adaptive emergence times.

Next, we developed a development time-oriented model of temperature-dependent phenology that accounts for both variation in development time that persists throughout a life stage and random variation. Persistent variation was modeled by incorporating a developmental phenotype that varies within a population, similar to the phenotype in the evolution model, and random variation was modeled using a diffusion term. The phenology model was fit to development time data for MPB collected in constant temperature laboratory experiments using a maximum likelihood approach. The incorporation of random variation did not improve fits to laboratory data. The phenology model also included a description of temperature-dependent distributed oviposition for MPB. We used the phenology model to predict emergence distributions given attack distributions for the previous generation and phloem temperatures measured in the field. The predicted mean emergence times agreed well with field observations, while the predicted variances were significantly greater than those observed in the field, further supporting the conclusion that random variation does not improve the MPB phenology model (although it may be an important factor in other insects).

Finally, we incorporated the temperature-dependent phenology model for MPB into the evolution model framework that we had developed. This evolution model also contained a realistic selection function based on a phenology-demography model for MPB developed by Powell and Bentz [33]. We simulated the evolution of MPB phenology under two stable phloem temperature series measured in central Idaho and southern Utah. In both cases populations evolved to steady distributions that were closely related to those predicted by the earlier analytical results; the mean phenotype at time t in a steady distribution closely followed the phenotype that resulted in a fixed point at time t (α_t) for the median egg. This suggests that the controlling effect of fixed points on evolutionary dynamics is a fairly robust phenomenon,

and that evolutionary dynamics can be approximated using a median oviposition model rather than a distributed oviposition mode. We also simulated the evolution of MPB phenology under warming temperatures by starting with a population that was well-adapted to central Idaho temperatures and shifting from the central Idaho temperature series to the southern Utah series at various rates. At rapid rates, the population went extinct, whereas at moderate and slow rates the population was able to persist. This suggests that the rate of climate change is an important factor, as well as the degree of climate change, in determining whether a population will be able to adapt.

Our approach to modeling the evolution of insect phenology can be adapted to study other insect species. The general approach presented in Chapter 2 can be extended to incorporate specific aspects of life-cycle and phenology for a particular species. For example, the evolution model presented in Chapter 4 extends the general approach to incorporate specific details about MPB (e.g. distributed oviposition, the necessity of mass-emergence within a specific time window, and a realistic phenology model). Although the general model is based on the assumption of direct temperature control of phenology, it can be extended to incorporate diapause or photoperiod sensitivity if either of these synchronizing mechanisms are apparent in a particular species. Under truncation selection on emergence time, the analytical steady distribution results in Chapter 2 hold under two conditions: First, phenology under a given temperature series is described in terms of a one parameter map (i.e. the G_α -function) that is differentiable with respect to the parameter. Second, selection acts directly on variation in phenology (i.e. the output of the map) rather than variation in the parameter. Consequently, the analytical steady distribution results are independent of our assumption that the phenotype α scales a base development time curve in a single life-stage. These results also hold if, for example, the single parameter α scales

development time across multiple life stages or represents a variable developmental threshold within a stage; offering a great deal of flexibility in describing variation in phenology.

In general, our results suggest that the ability of an insect population to adapt to climate change is largely dependent on its ability to maintain stable univoltine fixed points. This points to the need to develop phenology models that accurately describe temperature-dependent development and to understand the extent and heritability of variation in development time. Future modeling efforts should also focus on describing potential fitness trade-offs associated with the evolution of development time. For example, if development time is correlated with body size, it is likely that individuals that take longer to develop will also have higher fecundities because they are larger. Also, future models should allow for the possibility for adaptive semivoltine and bivoltine phenology.

REFERENCES

- [1] W.C. Allee, A.E. Emerson, O. Park, and K.P. Schmidt, *Principles of Animal Ecology*, Saunders, Philadelphia, 1949.
- [2] G.D. Amman, *Some factors affecting oviposition behavior of the mountain pine beetle*, Environ. Entomology, **1** (1972), no. 6, pp. 691–695.
- [3] B.J. Bentz, *Mountain pine beetle population sampling: inferences from Lindgren pheromone traps and tree emergence cages*, Canadian J. of Forest Res., **36** (2006), pp. 351–360.
- [4] B.J. Bentz, J.A. Logan, and G.D. Amman, *Temperature-dependent development of the mountain pine beetle (Coleoptera: Scolytidae) and simulation of its phenology*, The Canadian Entomologist, **123** (1991), pp. 1083–1094.
- [5] B.J. Bentz, J.A. Logan, and J.C. Vandygriff, *Latitudinal variation in Dendroctonus ponderosae (Coleoptera: Scolytidae) development time and adult size*, The Canadian Entomologist, **133** (2001), pp. 375–387.
- [6] B.J. Bentz and D.E. Mullins, *Ecology of mountain pine beetle (Coleoptera: Scolytidae) cold hardening in the intermountain west*, Environ. Entomology, **28** (1999), no. 4, pp. 577–587.
- [7] A.A. Berryman, B. Dennis, K.F. Raffa, and N.C. Stenseth, *Evolution of optimal group attack, with particular reference to bark beetles (Coleoptera: Scolytidae)*, Ecology, **66** (1985), no. 3, pp. 898–903.

- [8] N. Bleistein and R.A. Handelsman, *Asymptotic Expansion of Integrals*, Dover Publications, New York, 1986.
- [9] J.M. Calabrese and W.F. Fagan, *Lost in time, lonely, and single: reproductive asynchrony and the Allee effect*, *The American Naturalist*, **164** (2004), no. 1, pp. 25–37.
- [10] A. Carroll, S. Taylor, J. Régnière, and L. Safranyik, *Effects of climate change on range expansion by the mountain pine beetle in British Columbia*, Mountain Pine Beetle Symposium: Challenges and Solutions. Information report BC-X-399 (Klowna, British Columbia) (T.L. Shore, J.E. Brooks, and J.E. Stone, eds.), Natural Resources Canada, Canadian Forest Service, Pacific Forestry Centre, Victoria, B.C., October 2003, pp. 223–232.
- [11] J.H. Christensen et al., *Climate change 2007: The physical science basis. contribution from working group I to the fourth assessment report of the intergovernmental panel on climate change*, Cambridge University Press, Cambridge (United Kingdom) and New York (USA), 2007.
- [12] W.E. Cole, *Some risks and causes of mortality in mountain pine beetle populations: a long-term analysis*, *Researches on Population Ecology*, **23** (1981), no. 1, pp. 116–144.
- [13] H.V. Danks, *Insect Dormancy: An Ecological Prospective*, Monograph Series, vol. 1, Biological Survey of Canada (Terrestrial Arthropods), Ottawa, 1987.
- [14] N.G. de Bruijn, *Asymptotic Methods in Analysis*, Dover Publications, New York, 1981.

- [15] W.P. Eubank, J.W. Atmar, and J.J. Ellington, *The significance and thermodynamics of fluctuating versus static thermal environments on Helios zea egg development rates*, Environ. Entomology, **2** (1973), no. 4, pp. 491–496.
- [16] A.D. Fokker, *Die mittlere energie rotierender elektrischer dipole im strahlungsfeld*, Annalen der Physik, **43** (1914), pp. 810–820.
- [17] E. Gilbert, J.A. Powell, and J.A. Logan, *Comparison of three models predicting developmental milestones given environmental and individual variation*, Bull. Mathematical Biology, (2004), no. 66, pp. 1821–1850.
- [18] D.L. Hartl, *A Primer of Population Genetics*, 3rd ed., Sunderland, Massachusetts, 2000.
- [19] J.L. Jenkins, J.A. Powell, J.A. Logan, and B.J. Bentz, *Low seasonal temperatures promote life cycle synchronization*, Bull. Mathematical Biology, **63** (2001), no. 3, pp. 573–595.
- [20] T. Johnson and N. Barton, *Theoretical models of selection and mutation on quantitative traits*, Philosophical Trans. Royal Society B, **360** (2005), pp. 1411–1425.
- [21] M. Kimura, *A stochastic model concerning the maintenance of genetic variability in quantitative characters*, Proc. National Academy of Sciences of the United States of America, **54** (1965), pp. 731–736.
- [22] H.A. Kramers, *Brownian motion in a field of force and the diffusion model of chemical reactions*, Physica, **7** (1940), pp. 284–304.
- [23] R. Lande, *The maintenance of genetic variability by mutation in a polygenic character with linked loci*, Genetical Res., **26** (1975), pp. 221–235.

- [24] J.A. Logan, *Toward an expert system for development of pest simulation models*, Environ. Entomology, **17** (1988), no. 2, pp. 359–376.
- [25] J.A. Logan and G.D. Amman, *A distribution model for egg development in mountain pine beetle*, The Canadian Entomologist, **118** (1986), pp. 361–372.
- [26] J.A. Logan, P. Bolstad, B.J. Bentz, and D. Perkins, *Assessing the effects of changing climate on mountain pine beetle dynamics*, Interior West Global Change Workshop. General technical report RM-GTR-262 (Fort Collins, Colorado), USDA Forest Service, Rocky Mountain Forest and Range Experiment Station, April 1995, pp. 92–105.
- [27] J.A. Logan and J.A. Powell, *Ghost forests, global warming and the mountain pine beetle*, American Entomologist, **47** (2001), pp. 160–173.
- [28] J.A. Logan, D.J. Wollkind, S.C. Hoyt, and L.K. Tanigoshi, *An analytic model for description of temperature dependent rate phenomena in arthropods*, Environ. Entomology, **5** (1976), no. 6, pp. 1133–1140.
- [29] J. Memmott, P.G. Craze, N.M. Waser, and M.V. Price, *Global warming and the disruption of plant-pollinator interactions*, Ecology Letters, **10** (2007), pp. 710–717.
- [30] J.E. Moyal, *Stochastic processes and statistical physics*, J. Royal Statistical Society, Series B (Methodological), **11** (1949), no. 2, pp. 150–210.
- [31] C. Parmesan and G. Yohe, *A globally coherent fingerprint of climate change impacts across natural systems*, Nature, **421** (2003), pp. 37–42.

- [32] M. Planck, *Ueber einen satz der statistischen dynamik und eine erweiterung in der quantumtheorie*, Sitzungsberichte der Koniglich Preußischen Akademie der Wissenschaften, (1917), pp. 324–341.
- [33] J.A. Powell and B.J. Bentz, *Connecting phenological predictions with population growth rates for mountain pine beetle, an outbreak insect*, Landscape Ecology (submitted).
- [34] J.A. Powell, J.L. Jenkins, J.A. Logan, and B.J. Bentz, *Seasonal temperature alone can synchronize life cycles*, Bull. Mathematical Biology, **62** (2000), no. 5, pp. 977–998.
- [35] J.A. Powell and J.A. Logan, *Insect seasonality: circle map analysis of temperature-driven life cycles*, Theoretical Population Biology, **67** (2005), pp. 161–179.
- [36] K.F. Raffa and A.A. Berryman, *The role of host plant resistance in the colonization behavior and ecology of bark beetles (Coleoptera:Scolytidae)*, Ecological Monographs, **53** (1983), no. 1, pp. 27–49.
- [37] H. Risken, *The Fokker-Planck Equation: Methods of Solution and Applications*, 2nd ed., Springer, Berlin, 1996.
- [38] D. Roff, *Optimizing development time in a seasonal environment: the ‘ups and downs’ of clinal variation*, Oecologia, **45** (1980), pp. 202–208.
- [39] L. Safranyik and A.L. Carrol, *The mountain pine beetle: A synthesis of biology, management, and impacts on lodgepole pine*, pp. 3–66, Natural Resources Canada, Canadian Forest Service, Pacific Forestry Centre, Victoria, B.C., 2006.

- [40] P.J.H. Sharpe, G.L. Curry, D.W. DeMichele, and C.L. Cole, *Distribution model of organism development times*, J. Theoretical Biology, **66** (1977), pp. 21–38.
- [41] P.J.H. Sharpe and D.W. DeMichele, *Reaction kinetics of poikilotherm development*, J. Theoretical Biology, **64** (1977), pp. 649–670.
- [42] M. Slatkin, *Selection and polygenic characters*, Proc. National Academy of Sciences of the United States of America, **66** (1970), no. 1, pp. 87–93.
- [43] ———, *Frequency- and density-dependent selection on a quantitative character*, Genetics, **93** (1979), pp. 755–771.
- [44] R.E. Stinner, Jr. G.D. Butler, J.S. Bachelier, and C. Tuttle, *Simulation of temperature-dependent development in population dynamics models*, The Canadian Entomologist, **107** (1975), pp. 1167–1174.
- [45] F. Taylor, *Ecology and the evolution of physiological time in insects*, The American Naturalist, **117** (1981), no. 1, pp. 1–23.
- [46] M.E. Visser and L.J.M. Holleman, *Warmer springs disrupt the synchrony of oak and winter moth phenology*, Proc. Royal Society of London, **268** (2001), pp. 289–294.
- [47] V.A. Zaslavski, *Insect Development: Photoperiodic and Temperature Control*, Springer, Berlin, 1988.

APPENDIX

Numerical implementation of the phenology model

A typical goal of phenology modeling is to predict the distribution of times at which a population will complete a life stage given the distribution of times at which it began the life stage. If $p_b(t)$ is the distribution of times at which the population begins the life stage (at $a = 0$), and $p_c(t)$ is the distribution of times at which the population completes the life stage (at $a = 1$), then $p_b(t) = p(0, t)$ and $p_c(t) = p(1, t)$. We define $g_i(t)$ to be the time that an insect completes stage i given that it entered the stage at time t . Then, $g_i(t) = \Gamma_i(1, t)$. Setting $\Delta a = 1$ and $a = 0$ in (3.6) yields the following relationship between the distribution of stage completion times and initiation times:

$$\tau_i(t)p_b(t) = \tau_i(g_i(t))p_c(g_i(t)). \quad (7.1)$$

In practice the density of insects entering a stage at a particular time cannot be measured directly. Instead the number of insects entering the stage over a specified time interval (the integral of the density) is observed. Hence, the integral form of the conservation law (3.4) may be more useful than the differential form (the advection equation (3.3)). In this case, the number of insects entering the stage between times t_1 and t_2 is the same as the number of insects completing the stage between times $g_i(t_1)$ and $g_i(t_2)$; from (3.4),

$$\int_{t_1}^{t_2} p_b(s)ds = \int_{g_i(t_1)}^{g_i(t_2)} p_c(s)ds. \quad (7.2)$$

This equation is particularly useful for numerical solution of the advection phenology model and is the primary phenology relationship used in Chapter 2.

As in the advection model, the phenotype-dependent advection equation can be solved analytically if the distribution of times at which a population entered a stage

is known. If $p_b(t; \alpha)$ is the distribution of times at which the population begins the life stage (at $a = 0$), and $p_c(t; \alpha)$ is the distribution of times at which the population completes the life stage (at $a = 1$), then $p_b(t; \alpha) = p(0, t; \alpha)$ and $p_c(t; \alpha) = p(1, t; \alpha)$. Let $g_i(t; \alpha)$ be the time that an insect with phenotype α completes stage i given that it began at time t . Then, $g_i(t; \alpha)$ satisfies

$$\alpha = \int_t^{g_i(t; \alpha)} \frac{ds}{\tau_i(s)}.$$

By analogy to (7.1), the density of insects beginning the stage and the density of insects completing the stage are related by

$$\tau_i(t)p_b(t; \alpha) = \tau_i(g_i(t; \alpha))p_c(g_i(t; \alpha); \alpha). \quad (7.3)$$

Furthermore, the number of insects with phenotype α entering the stage between times t_1 and t_2 is the same as the number of insects with phenotype α completing the stage between times $g_i(t_1; \alpha)$ and $g_i(t_2; \alpha)$,

$$\int_{t_1}^{t_2} p_b(s; \alpha) ds = \int_{g_i(t_1; \alpha)}^{g_i(t_2; \alpha)} p_c(s; \alpha) ds. \quad (7.4)$$

We use (7.4) to develop a numerical scheme for implementing development of a population of insects using the phenotype-dependent advection equation (3.8). This scheme was used to simulate mountain pine beetle phenology. Development of a population through each life stage is treated separately and sequentially. Define $p_{b,i}(t; \alpha)$ to be the density of insects with phenotype α that begin stage i at time t and $p_{c,i}(t; \alpha)$ to be the density of insects with phenotype α that complete stage i at time t . We assume that phenotype is independent of time at the beginning of each stage. In particular, $p_{b,i}(t; \alpha)$ is gaussian in α with mean 1 and variance σ^2 at each

time t . We also impose the requirement that the same density (with respect to time) of insects begin stage i at time t as complete stage $i - 1$ at time t , i.e.

$$\int_{-\infty}^{\infty} p_{b,i}(t; \alpha) d\alpha = \int_{-\infty}^{\infty} p_{c,i-1}(t; \alpha) d\alpha.$$

Instead of tracking $p_i(t; \alpha)$ directly, we track integrals of $p_i(t; \alpha)$ over small time intervals (finite volumes) along characteristics, i.e. forward tracking from t to $g_i(t; \alpha)$ or backtracking from t to $g_i^{-1}(t; \alpha)$. With this in mind, we use slightly modified form of the conservation law (7.4),

$$\int_{t_1}^{t_2} p_{c,i}(t; \alpha) dt = \int_{g_i^{-1}(t_1; \alpha)}^{g_i^{-1}(t_2; \alpha)} p_{b,i}(t; \alpha) dt. \quad (7.5)$$

Recall that this conservation law follows from the assumption that insects with phenotype α that complete stage i between times t_1 and t_2 must have begun the stage between times $g_i^{-1}(t_1; \alpha)$ and $g_i^{-1}(t_2; \alpha)$. Finite volume methods are conservative, so there is no loss of population density due to truncation error. The benefit of using a characteristic method is that development is tracked from the beginning of a stage to the end of the stage in one step. We define an equally-spaced time grid spanning three years consisting of full-nodes, $\{1 = t_0, t_1, t_2, \dots, t_w = 1095\}$, and an equally-spaced time grid consisting of half-nodes, $\{t_{-1/2}, t_{1/2}, t_{3/2}, t_{5/2}, \dots, t_{w+1/2}\}$. In both cases $t_y = 1 + y\Delta t$, where $\Delta t = 1094/(w - 1)$. Let τ_j be the time interval $\tau_j = (t_{j-1/2}, t_{j+1/2}]$, noting that t_j is its midpoint. In the α direction, the population is represented at regularly spaced grid points on a finite phenotype domain, $\{\alpha_1, \alpha_2, \dots, \alpha_u\}$. Let $P_{j,k}^{b,i}$ be the number of insect with parameter α_k that begin stage i during the time interval τ_j :

$$P_{j,k}^{b,i} = \int_{t_{j-1/2}}^{t_{j+1/2}} p_i(t; \alpha_k) dt. \quad (7.6)$$

Similarly, we define $P_{j,k}^{c,i}$ be the number of insect with parameter α_k that complete stage i during the time interval τ_j .

The conservation law (7.5) provides a map between $P_{j,k}^{c,i}$ and $p_i(t; \alpha_k)$,

$$\begin{aligned}
P_{j,k}^{c,i} &= \int_{t_{j-1/2}}^{t_{j+1/2}} p_{i+1}(t; \alpha_k) dt, \\
&= \int_{g_i^{-1}(t_{j-1/2}; \alpha_k)}^{g_i^{-1}(t_{j+1/2}; \alpha_k)} p_i(t; \alpha_k) dt, \\
&= \int_{g_i^{-1}(t_{j-1/2}; \alpha_k)}^{t_{q-1/2}} p_i(t; \alpha_k) dt + \sum_{l=q+1}^{q+m-1} \left(\int_{t_{l-1/2}}^{t_{l+1/2}} p_i(t; \alpha_k) dt \right) \\
&\quad + \int_{t_{q+m-1/2}}^{g_i^{-1}(t_{j+1/2}; \alpha_k)} p_i(t; \alpha_k) dt, \tag{7.7}
\end{aligned}$$

where $t_{q-1/2}$ through $t_{q+m-1/2}$ make up all of the half-nodes strictly between $g_i^{-1}(t_{j-1/2}; \alpha_k)$ and $g_i^{-1}(t_{j+1/2}; \alpha_k)$. The first and last integrals on the right hand side of (7.7) are approximated, noting that $p_i(t; \alpha_k) \approx P_{j,k}^{b,i}/\Delta t$ for $t \in \tau_j$. The other integrals in (7.7) are of the form in (7.6) so that

$$\begin{aligned}
P_{j,k}^{c,i} &\approx \left(\frac{t_{q-1/2} - g_i^{-1}(t_{j-1/2}; \alpha_k)}{\Delta t} \right) P_{q-1,k}^{b,i} + \sum_{l=q+1}^{q+m-1} P_{l,k}^{b,i} \\
&\quad + \left(\frac{g_i^{-1}(t_{j+1/2}; \alpha_k) - t_{q+m-1/2}}{\Delta t} \right) P_{q+m,k}^{b,i}. \tag{7.8}
\end{aligned}$$

This equation is used to find the number of insects that complete a stage during the time interval τ_j given information about insects entering the stage. We use equation (7.8) as the basis for our numerical method.

We compute $g_i^{-1}(t_{j-1/2}; \alpha_k)$ in (7.8) by first computing the number of age units accumulated by an individual with phenotype α_k between times $t_{-1/2}$ and $t_{j-1/2}$ for each half node (i.e. for $j = 1, 2, \dots, w + 1$). This cumulative age, $A_{j,k}$, is computed

by numerically evaluating the integral

$$A_{j,k} = \int_{t_{-1/2}}^{t_{j-1/2}} \frac{ds}{\alpha_k \tau_i(s)},$$

using the trapezoidal rule. We find the first l such that $A_{j,k} - A_{l,k} \geq 1$, since then $g_i^{-1}(t_{j-1/2}; \alpha_k)$ is in the time interval τ_l , and use linear interpolation to approximate $g_i^{-1}(t_{j-1/2}; \alpha_k)$.

April 24, 2009

Brian Yurk
231 W 400 S
Logan, UT 84321
USA
Phone: 1-435-764-5245
Fax: 1-435-797-1822

Donna Lukiw
Springer, US

To Donna Lukiw:

I am preparing my dissertation in the Department of Mathematics and Statistics at Utah State University. I hope to complete me degree in the summer of 2009.

An article, *Modeling the Evolution of Insect Phenology*, of which I am first author, and which is published in the journal *Bulletin of Mathematical Biology*, reports an essential part of my dissertation research. I would like permission to reprint it as a chapter in my dissertation. (Reprinting the chapter may necessitate some revision.) Please note that USU sends dissertations to Bell & Howell Dissertation Services to be made available for reproduction.

I will include an acknowledgment to the article on the first page of the chapter, as shown below. Copyright and permission information will be included in a special appendix. If you would like a different acknowledgment, please so indicate.

Please indicate your approval of this request by signing in the space provided, and attach any other form necessary to confirm permission. If you charge a reprint fee for use of an article by the author, please indicate that as well. If you have any questions, please call me at the number above or send me an e-mail message at the above address. Thank you for your assistance.

Brian Yurk

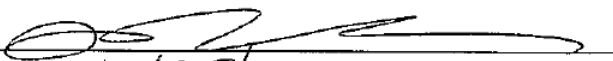
I hereby give permission to Brian Yurk to reprint the requested article in *Bulletin of Mathematical Biology*, with the following acknowledgment:

Brian Yurk and James Powell, *Modeling the evolution of insect phenology*, *Bulletin of Mathematical Biology* 71 (2009), 952-979.

Signed _____

Date _____

Fee _____


4/25/09

VITA

Brian P. Yurk

Address:

Department of Mathematics and Statistics Phone: 435-764-5245
 Lund Hall 104 Phone (department): 435-797-2809
 Utah State University e-mail: brian.yurk@aggiemail.usu.edu
 Logan, Utah
 84322-3900

Personal:

Birthdate: February 15, 1981 Birthplace: Kalamazoo, MI, USA
 Citizenship: American
 Marital status: Married (Michelle) Children: Porter (2007)

Education:

Institution	Attended	Degree Date	Degree
Utah State University	2003-2009	May 2009	Ph.D. (Math)
Hope College	1999-2003	May 2003	B.S. (Math & Geology)

Academic Experience:

Institution	Dates	Position
Utah State University	2006-Present	Graduate Instructor
Hope College	2001-2003	Teaching Assistant
Hope College	2001-2003	Mathematics Tutor
Hope College	2001-2003	Research Assistant

As a PhD student at Utah State University I taught the following courses:

- College Algebra
- Calculus I
- Calculus II
- Multivariable Calculus
- Linear Algebra and Differential Equations

I was solely responsible for all aspects of teaching and managing these classes (with the exception of college algebra); my responsibilities including lecturing and otherwise structuring classroom learning, writing syllabi, writing exams, assigning homework, grading, holding office hours, etc. In college algebra I was responsible for all aspects of the class except structuring the syllabus and writing the final exam.

Research Interests:

- Mathematical biology
- Mathematical geology
- Applied mathematics
- Mathematical modeling
- Differential equation models
- Ecology and evolution models

Publications:

1. B. Yurk and J. Powell. “The evolution of mountain pine beetle phenology in response to global warming,” In preparation.
2. B. Yurk and J. Powell. “Modeling the effects of developmental variation on insect phenology,” Submitted to *Bulletin of Mathematical Biology*.
3. B. Yurk and J. Powell. “Modeling the evolution of insect phenology,” *Bulletin of Mathematical Biology*. 71: 952-979, 2009.
4. E. Hansen, S. DeVries-Zimmerman, D. van Dijk, and B. Yurk. “Patterns of wind flow and aeolian deposition on a parabolic dune on the southeastern shore of Lake Michigan,” *Geomorphology* (In press).
doi:10.1016/j.geomorph.2007.12.012.
5. E. Hansen, A. Arbogast, D. van Dijk, and B. Yurk. “Growth and migration of parabolic dunes along the southeastern coast of Lake Michigan,” *Journal of*

Coastal Research SI 39 (Proceedings of the 8th International Coastal Symposium): 209-214.

6. A. Arbogast, E.C. Hansen, and B. Yurk. "The history of dune growth and migration along the southeastern shore of Lake Michigan: a perspective from Green Mountain Beach," *Michigan Academician*. 35(4): 455-478, Winter 2004.

Conference Talks:

1. B. Yurk and J. Powell. "Modeling the evolution of insect phenology: Can insect populations adapt to climate change?," contributed talk, 2008 Annual Meeting of the Society for Mathematical Biology. Toronto, Ontario, Canada, 2008.
2. B. Yurk and J. Powell "Evolution of insect phenology in the presence of environmental variability," contributed talk, Joint Annual Meeting of the Society for Mathematical Biology and the Japanese Society for Mathematical Biology. San Jose, CA, 2007.
3. B. Yurk and J. Powell "Predicting emergence time distributions for mountain pine beetle, an eruptive herbivore," contributed talk, Ecological Society of America, Annual Meeting. Memphis, TN, 2006.
4. B. Yurk and J. Powell "Optimal velocity profiles for the migration flights of swans," contributed talk, 3rd Annual Intermountain/Southwest Conference on Industrial and Interdisciplinary Mathematics. Tempe, AZ, 2004.
5. B. Yurk, E.C. Hansen. "Sand deposition and wind patterns on a large migrating parabolic dune, southeastern shore of Lake Michigan," contributed talk, Michigan Academy of Science, Arts, and Letters, Annual Meeting. Holland, MI, 2003.

6. B. Yurk, W. Weiss, and K. Woloszyn. "Patterns of sand transport and deposition in an actively migrating parabolic dune southwest of Holland, Michigan," contributed talk, Michigan Academy of Science, Arts, and Letters, Annual Meeting. Mount Pleasant, MI, 2002.
7. L. Kiessel and B. Yurk "Geometric characterization of graded algebras," contributed talk, Michigan Section-MAA and MichMATYC, Joint Annual Meeting. Holland, MI, 2001.

Poster Presentations:

1. B. Yurk and J. Powell. "Implications of phenotypic and environmental variability on developing insect populations," ECMTB05: European Conference for Mathematical and Theoretical Biology and Annual Meeting of the Society for Mathematical Biology. Dresden, Germany, 2005.
2. B. Yurk. "Geological history of the dune complexes along the southeastern shore of Lake Michigan," Council for Undergraduate Research Posters on the Hill. Washington, D.C., 2002.
3. B. Yurk, E.C. Hansen. "Migration history of Green Mountain Beach parabolic dune, southeastern shore of Lake Michigan," Michigan Space Grant Consortium, Annual Conference. Dearborn, MI, 2002.
4. B. Yurk, E.C. Hansen, K. Sherron, B. Johnson, A. Arbogast, D. van Dijk. "Migration history of Green Mountain Beach parabolic dune southeastern shore of Lake Michigan," Geological Society of America, Annual Meeting. Denver, CO, 2002.

5. K. Sherron, M. Hutchful, B. Johnson, B. Yurk, E.C. Hansen, D. van Dijk.
“Wind and deposition patterns on a large migrating parabolic dune,
southeastern shore of Lake Michigan,” Geological Society of America, Annual
Meeting. Denver, CO, 2002.
6. B. Johnson, B. Bodenbender, B. Yurk, E.C. Hansen. “Magnetite layers in a
massive parabolic dune, southeastern shore of Lake Michigan,” Geological
Society of America, Annual Meeting. Denver, CO, 2002.
7. B. Yurk, W. Weiss, K. Woloszyn, M. Van Oort, and E.C.
Hansen, “Development and growth of parabolic dunes along the southeastern
shore of Lake Michigan,” Geological Society of America, Annual Meeting.
Boston, MA, 2001.

Journals Reviewed For:

- *Journal of Theoretical Biology*
- *Mathematical and Computer Modeling*

Professional Memberships:

- Society for Mathematical Biology
- Ecological Society of America
- American Mathematical Society

Awards and Scholarships:

- National Merit Scholarship (1999)
- Ancient Mystic Order of the Trilobite Award (1999)
- Michigan Space Grant Consortium Undergraduate Student Fellowship (2002)
- Lampen Award in Mathematics (2002)
- Sigma Xi Research Award (2002)
- Tulip City Gem and Mineral Society Award (2003)
- Eccles Fellowship (2003)
- Remynse Scholarship (2003)
- Travel funding from the European Commission to attend the European Conference for Mathematical and Theoretical Biology and 2005 Annual Meeting of the Society for Mathematical Biology (2005)
- Departmental Teaching Award: Teaching Above and Beyond the Call of Duty (2008)
- Landahl travel grant for Society for Mathematical Biology Annual Meeting (2008)